Szakmai beszámoló a **„Tranziens receptor potenciál csatornák vaszkuláris biológiai szerepének tanulmányozása”** című 84300-as számon nyilvántartott OTKA pályázat megvalósításáról.[1]

[1] A beszámolóban a publikált eredmények kapcsán a közlemények lényegét foglalom össze és a publikációkat mellékelem a beszámoló végén. Az eddig nem publikált adatok kapcsán kissé részletesebben, a beküldés előtt álló publikációk kulcsábráinak bemutatásával igyekszem meggyőzni a bírálót az elvégzett munka sikeréről és jelentőségéről.

Rövid összefoglalás

A projekt során a TRPV1 és a TRPM4 esetében jelentős vaszkuláris simaizom-függő hatásokat azonosítottunk. A TRPA1 szerepét az értámérő endotél függő szabályozásában találtuk kimutathatónak.

A TRPV1 esetében kimutattuk, hogy (1) a különböző patkány szövetekben expressziója eltérő (Tóth et al. 2014); (2) deszenzibilizációval a neuronális TRPV1 funkció szelektíven gátolható, míg a vaszkuláris TRPV1 funkciója megtartott (Czikora et al. 2013); (3) a vaszkuláris TRPV1 farmakológiai tulajdonságai eltérnek a neuronális receptorétól (Czikora et al. 2012a); (4) a TRPV1-et aktiváló vanilloid csoportba tartozó vegyületek egy jelentős része gátló hatással van a feszültségfüggő Ca^{2+} csatornákra; (5) az anadamid vazoaktív hatásai TRPV1-től függetlenül fejlődnek ki (Czikora et al. 2012b).

A TRPM4 kapcsán kimutattuk, hogy (6) gátlása jelentősen csökkenti az agonista stimulusokra (norepinefrin, magas extracelluláris K^+ szint) bekövetkező vazokonstrikció mértékét és hogy aktiválható a calcimycinnek is hívott, A23187 számú vegyülettel.

A TRPA1 vonatkozásában kimutattuk, hogy (7) az aktivátoraiként leírt anyagok közül az allil-izotiocianát (AITC) és NaHS esetében egyaránt TRPA1-független vaszkuláris hatások jelennek meg, melyek alapján a TRPA1 vaszkuláris szerepére vonatkozó eddigi közlemények félrevezetőek lehetnek.

A fentiekben felsorolt 7 eredmény közül eddig 4-et publikáltunk, további 3 közlésre előkészített fázisban van.

A projekt finanszírozásának feltüntetésével eddig megjelent közlemények száma 10, ezek összesített impakt faktora 36,5. A közlemények közül négy a projekt munkatervében megfogalmazott célok megvalósításához kötődnek, melyeket a projekt során született eredmények publikálása várhatólag további 3 közleménnyel egészíti ki. Az egyéb megjelent közlemények közül az eredeti munkaterv megvalósítása során, annak eredményei által iniciált közlemények száma 2, a maradék 4 közlemény pedig a pályázathoz metodikájában és anyagszükségletében kapcsolódik.

A munkaterv megvalósítása kapcsán kapott eredmények

Kapszaicin (vanilloid) receptor (TRPV1)

Vaszkuláris TRPV1 expresszió és funkció (Tóth et al. 2014)

A TRPV1 vaszkuláris biológiai szerepének kapcsán sikerült további részleteket feltárnunk. Mindenekelőtt részletesen vizsgáltuk a TRPV1 vaszkuláris expresszióját és funkcióját a patkány különböző szöveteiben. Ezzel a munkával az eddig sporadikusan megjelenő funkcionális eredmények kontextusba helyezése érdekében nagy lépést tettünk. Eredményeink szerint jelentős TRPV1 expresszió figyelhető meg a vázizom-, mezentérium- és a bőr ereiben, csakúgy mint a karotiszban. Ugyanakkor a TRPV1 expresszió szorosan szabályozódik: egymástól néhány mikrométer távolságra találhatóak olyan erek, amelyek jelentős mennyiségű TRPV1-et expresszálnak és olyanok, melyekben nincs TRPV1 expresszió. Ez a jelenség a bőr és a mezenteriális szövetre különösen jellemző volt. A TRPV1 vaszkuláris biológiai hatásait is tanulmányoztuk ezen érterületeken. Az expresszálódó TRPV1 stimulációja vazokonstrikciót váltott ki a vázizomból izolált artériákban és a karotiszban. A többi érterület esetében a TRPV1 expressziója ellenére nem volt vazoaktív hatás.

Mindezen eredmények azt sugallják, hogy a vaszkuláris simaizomsejtekben történő TRPV1 expresszió és aktivitás egyaránt egy szorosan szabályozott folyamat. A TRPV1 vaszkuláris élettani jelentősége a receptor expresszió és az aktivitást reguláló folyamatok (deszenzitizáció?) folyamatok által együttesen befolyásolt. Jelentős szerepet vázizom és szívizom esetében feltételezhetünk. A vaszkuláris TRPV1 expresszió jelentőségét a neuronális TRPV1 gátlására irányuló terápiás erőfeszítések potenciális on-target mellékhatásainak szempontjából is figyelembe kell venni.

A TRPV1 deszenzibilizáció hatásai a vaszkuláris receptorra (Czikora et al. 2013)

Jelentős gyógyszergyári erőfeszítések történnek annak érdekében, hogy a TRPV1 gátlásában rejlő fájdalomcsillapító hatást kiaknázzák. Mindezideig az egyetlen elterjedten alkalmazott módszer a TRPV1 deszenzibilizációjára épül. Ennek az eredetileg Szolcsányi és Jancsó által leírt módszernek a lényege, hogy nagy dózisú kapszaicin kezelést követően a fájdalomérző neuronok válaszkészsége csökken. A módszert kiterjedten alkalmazták az érző neuronális funkciók jellemzésére és vizsgálatára is.

A kapszaicin hatásait a TRPV1-en keresztül fejti ki. Amennyiben a fenti eredményinken alapuló vaszkuláris TRPV1 hatások igazak, akkor a kapszaicin deszenzibilizáció során megfigyelt jelenségekhez a vaszkuláris TRPV1 modulációja is hozzájárulhat (árnyalva az eddig felépített képet). A kérdés tisztázása érdekében a kapszaicin deszenzibilizációt követően vizsgáltuk a vaszkuláris és neuronális TRPV1-hez köthető válaszokat. Eredményink megerősítették azon korábbi adatokat, hogy a kapszaicin deszenzibilizáció 10 héttel a kezelést követően is gátolja az érző neuronok funkcióját. Meglepő módon ugyanezen állatokban a vaszkuláris TRPV1 stimulációjára a vázizom arteriáiban bekövetkező vazokonstrikció érintetlen maradt. Ezen adatok arra utalnak, hogy a nagyobb osztódási és regenerációs kapacitással

rendelkező simaizomsejtekben expresszálódó TRPV1 nem deszenzibilizálható tartósan.

A megfigyelésnek két következménye van. Az egyik az, hogy a kapszaicin deszenzibilizáció továbbra is az érzőneuronokra specifikus módszernek tekinthető. A procedúra alkalmazásával az érző neuronok funkciója vizsgálható. A másik következmény viszont az, hogy a kapszaicin deszenzibilizációt követően megmaradó kapszaicin mediált hatások nagy valószínűséggel a vaszkuláris TRPV1 stimulációjának a következtében jelennek meg. Ezzel a módszerrel a vaszkuláris TRPV1 funkciója az érző neuronokon expresszálódó receptortól függetlenül tanulmányozható. Ez jelentheti a kulcsot a vaszkuláris TRPV1 élettani jelentőségének megértéséhez.

A vaszkuláris TRPV1 struktúra-aktivitás viszonyai (Czikora et al. 2012a)

Az érző neuronokon expresszálódó TRPV1 az elmúlt évtizedben a fájdalomcsillapításra irányuló gyógyszergyári erőfeszítések homlokterében állt. Számos klinikai tanulmányt követően sem sikerült ugyanakkor a TRPV1-et gátló antagonista hatású vegyületek klinikai bevezetése. Ennek elsődleges oka nemkívánt súlyos mellékhatások megjelenése volt, mely többnyire jelentős testhőmérséklet emelkedés formájában öltött testet. Ezen jelenség vizsgálata során talán annyit megállapíthatunk, hogy hátterében on-target (TRPV1-en ható) mellékhatás állhat. Ennek értelmében a kiküszöbölése nem látszik egyszerű feladatnak és számos gyógyszergyár fel is hagyott a TRPV1 antagonisták fejlesztésével.

Kutatásainkban vizsgáltuk a vaszkuláris TRPV1 által közvetített hatások struktúra-aktivitás viszonyait és ezeket a neuronális hatásokkal összevetettük. A kísérletek során igazoltuk, hogy az alkalmazott agonista hatású vegyületek közül a kapszaicin nincs hatással a $TRPV1^{-/-}$ knockout egér ereire és a kapszaicin hatása gátolható TRPV1 antagonistával. Ezen kísérleteket simaizom és érfalban történő intracelluláris Ca^{2+} koncentráció mérésekkel is kiegészítettük. Ezzel egyértelműen bizonyításra került, hogy a patkány vázizom artéria simaizomában funkcionális TRPV1 expresszálódik.

A struktúra-aktivitás vizsgálatok során kimutattuk, hogy a vaszkuláris TRPV1 kapszaicin és számos más TRPV1 agonista hatására egyaránt deszenzitizálódik (válaszkészség csökkenés az agonista jelenlétében). Ugyanakkor a TRPV1 mediált vazokonstrikció megjelenése jelentősen függött az alkalmazott agonista struktúrájától, mely különösen érdekes volt az érző funkcióra gyakorolt hatással (irritáció) összevetve. Az eredmények szerint a TRPV1 agonisták egy része (például a resiniferatoxin) anélkül deszenzitizálta az ereket, hogy bármiféle hatást gyakorolt volna az érátmérőre, amellett, hogy ugyanezen anyag jelentős irritációt okozott. Ezzel szemben a kapszaicin jelentős irritáló hatásával összhangban jelentős vazokonstrikciót is kiváltott.

Az eredményeink szerint a vaszkuláris simaizomban expresszálódó TRPV1 struktúra-aktivitás viszonyai eltérnek a szenzoros idegsejtek TRPV1 receptorainak struktúra-aktivitás viszonyaitól, így elvileg létrehozható olyan TRPV1 modulátor, mely célzottan tud hatni valamelyik kiválasztott TRPV1 populációra. Ennek segítségével elkerülhetőek az on-target mellékhatások, továbbá a vaszkuláris TRPV1-re szelektíven ható molekulák is fejleszthetőek.

Vanilloidok, mint feszültségfüggő Ca^{2+} csatorna ligandok

A vaszkuláris TRPV1 vizsgálata során két jelentős problémával szembesültünk. Az egyik az volt, hogy a korábbi közlemények túlnyomó többsége a kapszaicin esetében vazodilatatív hatásról számolt be, a saját kísérleteink során megfigyelt vazokonstrikcióval szemben. A másik probléma az volt, hogy az irodalomban a vazodilatatív hatást sokszor olyan ereken írták le, amelyek esetében nekünk nem sikerült TRPV1 függő vazoaktív hatást kimutatnunk, illetve amely szövetekben a TRPV1 expresszió nem bizonyult jelentősnek.

Ezen korábbi adatok kapcsán felmerült annak a lehetősége, hogy a vazodilatatív hatás egy TRPV1 független hatás eredménye. Ennek tisztázása érdekében TRPV1 antagonisták hatásait vizsgáltuk. Meglepő módon olyan szövetekből izolált erek esetében is vazodilatatív hatást kaptunk a TRPV1 antagonisták (_kapszaicin, capsazepine) használata során, amelyekben a TRPV1 stimulációja kapszaicinnel eredménytelennek bizonyult a vazokonstrikció kiváltására. Ez TRPV1 független hatásokra utalt. További kísérletekben azonban arra is fény derült, hogy a TRPV1 stimulációra használt koncentrációt meghaladó mennyiségben alkalmazott TRPV1 agonisták (kapszaicin, MSK-195) is vazodilatatív hatással bírnak olyan erek esetében, amelyekben a TRPV1 vaszkuláris expressziója alacsony, vagy az ott expresszálódó TRPV1 deszenzitizált állapotban van (1. ábra). Ezzel szemben a TRPV1 endogén agonistájaként leírt, de nem a vanilloidok közé tartozó anandamid, illetve az oldószerként használt etanol nem befolyásolta az erek kontraktilitását (1. ábra).

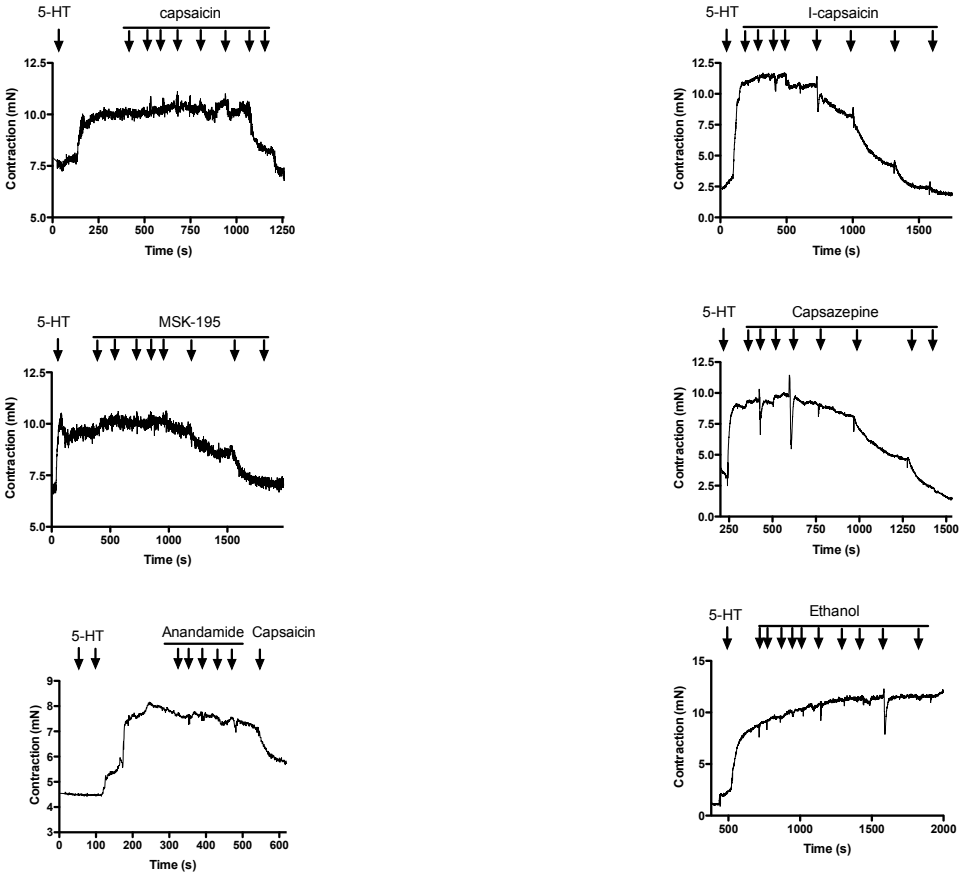

1. ábra Vanilloidok által kiváltott TRPV1 független vazorelaxáció

A kísérletek során végül igazoltuk, hogy a fenti kísérletekben használt TRPV1 ligandok egyaránt a feszültségfüggő Ca^{2+} csatornát gátolják. A kísérletekben patch clamp módszerrel vizsgáltuk a CHO sejtekben túltermelt feszültségfüggő Ca^{2+} csatorna konduktivitását. A vanilloidok (a TRPV1 agonista kapszaicin és a TRPV1 antagonista I-kapszaicin) a csatorna konduktivitását a feszültségfüggés befolyásolása nélkül csökkentették (2. ábra). Ennek alapján a feszültségfüggő Ca^{2+} csatorna eddig ismert három gátlóhelye mellett feltételezhető egy további, a vanilloidokra érzékeny gátlóhely is.

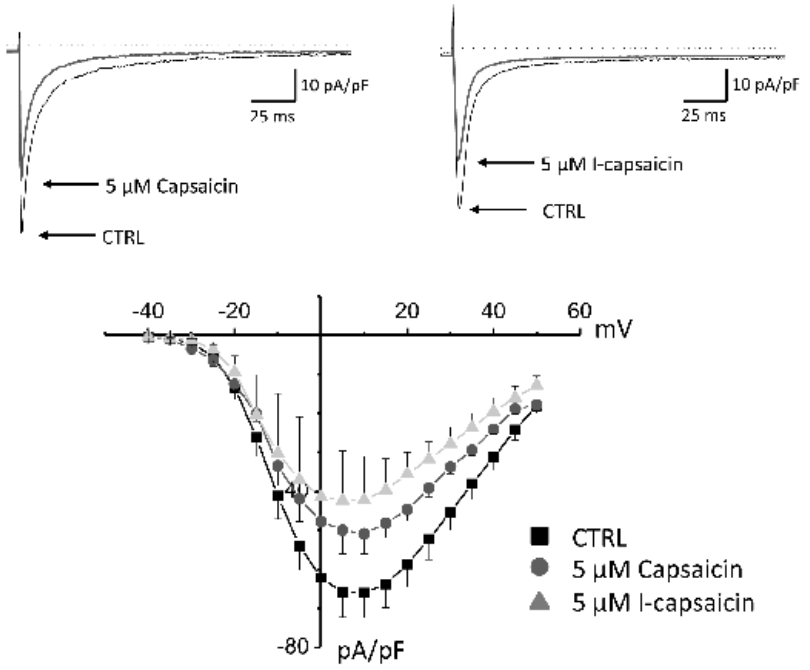

2. ábra Vanilloidok közvetlenül gátolják a feszültségfüggő Ca^{2+} csatornát

A kapott eredmények nem csak történeti jelentőségűek, miszerint a nagy dózisban/koncentrációban alkalmazott vanilloidok vazodilatatív hatásainak TRPV1 független mechanizmusa feltárásra került, hanem jelentős gyógyszerfejlesztési potenciált is hordoz. A Ca^{2+} csatorna gátlók az egyik legnagyobb mennyiségben alkalmazott gyógyszercsoportot alkotják. Mellékhatásprofiljuk ugyan kedvező, de az új támadásponton ható molekulák elvezethetnek a terápia hatékonyságának növeléséhez, illetve új betegségekben történő alkalmazásához. Végül, a feszültségfüggő Ca^{2+} csatorna egy másik típusa fontos szerepet játszik a neuronok aktiválásában, a neurotranszmitter felszabadításban is. Egy a TRPV1-et és ezt a neuronális feszültségfüggő csatornát is gátló molekula esetében jelentősebb fájdalomcsökkentő hatás várható, így ez az új hatású fájdalomcsillapítók mintapéldánya lehet.

Az anandamid vaszkuláris hatásainak mechanizmusa (Czikora et al. 2012b)

Nagy feltűnést keltett, amikor az anandamidot endogén TRPV1 agonistaként azonosították. Ennek ellenére ahogyan azt az 1. ábra is mutatja, az anandamid esetében nem sikerült jelentős vazoaktív hatást megfigyelnünk a koncentráció-érátmérő viszonyainak tanulmányozása során. Ez ellentmondott számos korábbi közleménynek. Az anandamidot korábban a TRPV1 aktiválásával hozták összefüggésbe és TRPV1 közvetített dilatatív hatást tulajdonítottak neki számos érterületen. Ennek az ellentmondásnak a feloldására számos kísérletet végeztünk el.

A kísérletek eredményeként fény derült arra, hogy az anandamidnak valóban vannak vazodilatatív hatásai. Ezen hatásokat azonban kannabinoid receptor és TRPV1 független módon fejti ki. Az anandamid ugyanis először zsírsav-amid-hidroláz (FAAH) által arachidonsavra és etanolamidra bomlik. Ezt követően az arachidonsav útvonal aktiválódik, és az érben keletkező arachidonsav metabolitoknak lesz vazodilatatív hatása. Ez az anandamid által kiváltott vazorelaxáció érinti az erek spontán miogén tónusát is.

Az eredmények kapcsán az a kép alakult ki, hogy az anandamid egy sejtek közötti információ továbbító molekula: az egyik sejttípusban (perifériás idegsejt végződés?) intracelluláris Ca^{2+} jel alakul ki. Ennek hatására anandamid termelődik, mely membrán permeabilitásánál fogva eljut a környező erekhez. Itt a fenti mechanizmus szerint lebomlik, és aktiválja ezen sejtek endogén arachidonsav útvonalát, és relaxációt vált ki. Ezen mechanizmus akár a neurovaszkuláris kapcsolatot is magyarázhatja.

A TRPM4 vaszkuláris biológiai szerepe

A kísérleteink kezdetekor a TRPM4-ről csak azt tudtuk, hogy részt vesz a spontán miogén tónus kialakításában. Ezt saját kísérleteinkben is megerősítettük. A további kísérletekben erőfeszítést tettünk arra, hogy a TRPM4 szerepét az agonista stimulusok által kiváltott vazokonstrikcióban vizsgáljuk. Nagy meglepetéssel tapasztaltuk, hogy a TRPM4 gátlása a norepinefrin és magas extracelluláris K^+ hatására kialakuló vazokonstrikciót is felfüggesztette (3. ábra).

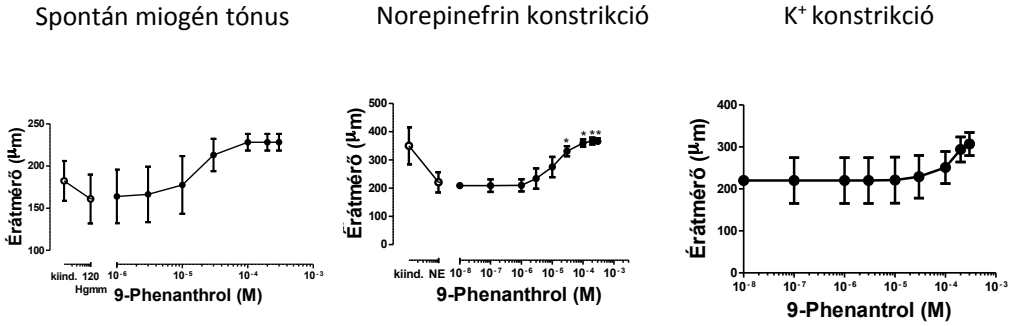

3. ábra A TRPM4 gátlás felfüggeszti a vazokonstrikciót

A TRPM4 gátlásának *in vivo* szerepét is vizsgáltuk *in vivo* vérnyomásméréssel patkányban. A kapott adatok szerint a TRPM4 gátlása jelentős vérnyomáscsökkenést vált ki (4. ábra).

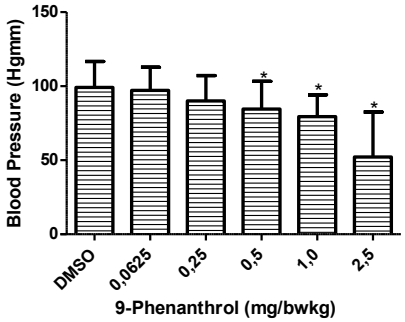

4. ábra A TRPM4 gátlása vérnyomáscsökkenést vált ki

Eredményeink kapcsán az a kép körvonalazódik, hogy a TRPM4 képes a kismértékű intracelluláris Ca^{2+} koncentráció emelkedéseket felerősíteni, azáltal, hogy aktiválódva Na^{+}-ot enged be a sejtekbe, így azokat depolarizálja és a feszültségfüggő Ca^{2+} csatornát aktiválja. Az in vivo kísérletsorozatunk azzal a reménnyel kecsegtet, hogy a vaszkuláris TRPM4 moduláció a hipertónia kezelésének új célpontja lehet.

A TRPM4 kutatásának komoly akadályát képezi, hogy midössze egy magas koncentrációban hatékony antagonistája ismert (9-fenantrol), mellyel mi is folyatattuk a kísérleteinket. Mint fentebb említettem, a TRPM4 aktiválható kismértékű intracelluláris Ca^{2+} emelkedéssel. Ez Ca^{2+} ionofórokkal is elérhető, így került figyelmünkbe a calcimycin (A23187). A calcimycin valóban képes volt izolált gracilis artériákat konstrihálni. A calcimycin konstriktív hatása kompetitívnek bizonyult a TRPM4 gátlószer 9-fenantrollal (5. ábra).

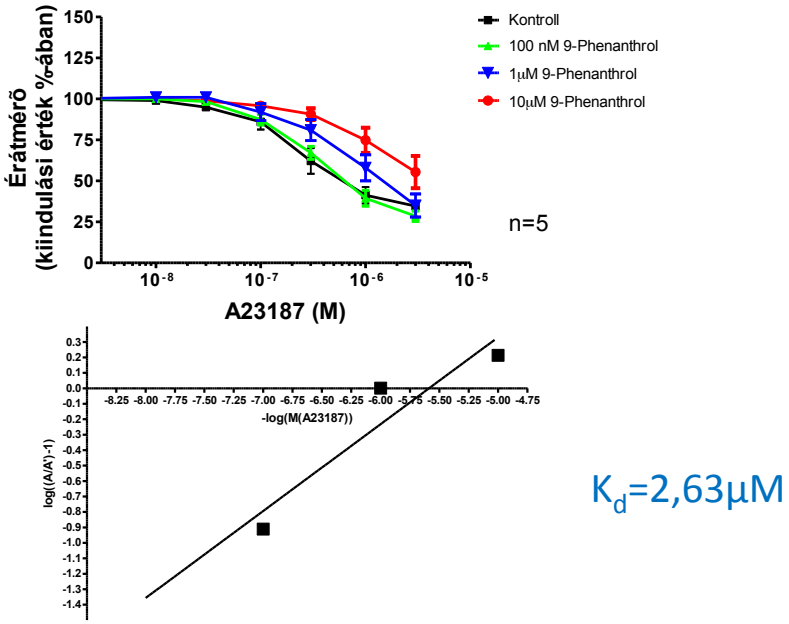

5. ábra A calcimycin egy kompetitív TRPM4 aktivátor

Ez arra utal, hogy a calcimycin közvetlenül aktiválja a TRPM4-et amelynek következménye a feszültségfüggő Ca^{2+} csatorna aktiválása és az intracelluláris Ca^{2+} koncentráció emelkedése. Ezen hipotézis ellenőrzésére patch calmp kísérleteket terveztünk. Függetlenül ezen patch clamp eredményektől a calcimycint a TRPM4 agonistájaként azonosítottuk, amely jelentős lökést adhat a TRPM4 farmakológiai kiaknázásához, élettani szerepének pontos feltárásához.

A TRPA1 vaszkuláris biológiai szerepe

A TRPA1 kapcsán a szakirodalomban ismert volt, hogy aktiválása SH reagensekkel valósítható meg és vazorelaxációt vált ki. Ezen SH regensek közül kísérleteinkben a NaHS és az allil izotiocianát (AITC) került alkalmazásra. Pintér Erikával együttműködésben sikerült ezen anyagok hatásainak specifitását is ellenőriznünk TRPA1 knockout egerek ereinek vizsgálatával. A TRPA1 válaszokat az értámérő és az érfali intracelluláris Ca^{2+} koncentráció párhuzamos mérésével vizsgáltuk (6. ábra). Meglepő eredményekre jutottunk: (1) az AITC mM-os tartományban váltott ki vazorelaxációt, mely a KO egérben nem volt megfigyelhető; (2) azonban az AITC a KO egerekben is hatással volt az intracelluláris Ca^{2+} koncentrációra 10 mM-nál; (3) A NaHS intracelluláris Ca^{2+} koncentrációra kifejtett hatásai az AITC-hez hasonlóan TRPA1 függetlennek bizonyultak ezen izolált erekben; mi több, (4) a NaHS vazodilatatív hatása megfigyelhető KO egerekben is.

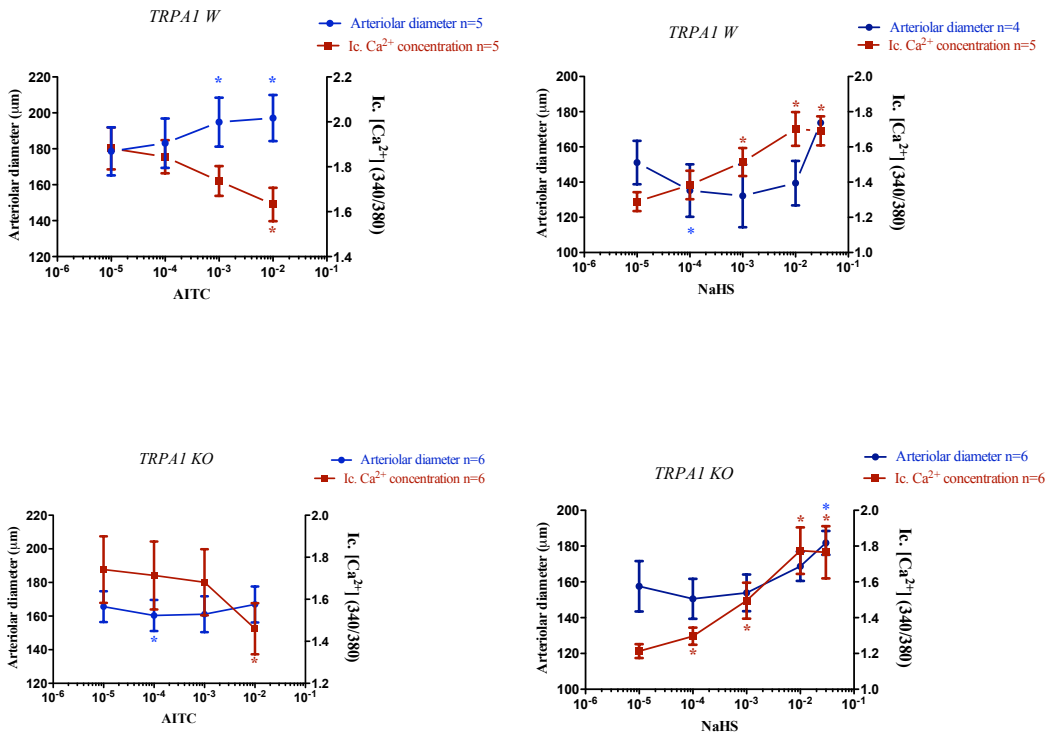

6. ábra A TRPA1 aktivációjának vaszkuláris hatásai

Az SH-reagensekkel végzett kísérleteink eredménye tehát az, hogy izolált vaszkuláris szövetekben ezen anyagok TRPA1 független intracelluláris Ca^{2+} emelkedést váltanak ki, így a TRPA1 szerepének feltárására csak részlegesen alkalmasak. Az alkalmazásukkal kapott korábbi eredmények ezért félrevezetőek lehetnek. Ezen hatások mechanizmusának feltárása a jövőben várható.

Az eredeti munkatervben nem tervezett (de a projekthez kapcsolódó) kísérleteket leíró, a projekt feltüntetésével született publikációk

Az OTKA munkatervében tervezett TRPA1-es kísérleteink eredményei által motiválva (de az eredeti munkatervben nem tervezett módon) behatóan tanulmányoztuk különböző SH reagensek vaszkuláris hatásait. Ilyen molekulák voltak a hidrogén peroxid (Csató et al. 2014) és a mieloperoxidáz enzim (Csató et al. 2015). Ezen eredmények tehát ugyan szorosan kötődnek az eredeti OTKA munkaterben foglaltakhoz, de az eredeti munkatervben ezen kísérletek tételesen nem voltak tervezve.

A projekthez szorosan nem kapcsolódó, de részben a projekt kapcsán felépített laboratóriumi háttérrel megvalósult, a pályázat feltüntetésével publikált eredmények

Egy az OTKA pályázat munkatervétől független klinikai vizsgálatsorozatban azt találtuk, hogy a keringő angiotenzin konvertáló enzim (ACE) aktivitása endogén kontroll alatt áll (Fagyas et al. 2014a), amennyiben a szerum albumin gátolja (Fagyas et al. 2014b), és így aktivitását alacsony szinten stabilizálja. Ezzel az ACE expressziójában egyéni szinten megfigyelhető különbségek kompenzálódnak (Fagyas et al. 2014c). Végül, egy közleményben az oxidatív hatású doxorubicin vaszkuláris hatásait írtuk le (Szántó et al. 2011).

Publikációs lista[2]

Csató, Viktória, Attila Pető, Ákos Koller, István Édes, Attila Tóth, and Zoltán Papp. 2014. "Hydrogen Peroxide Elicits Constriction of Skeletal Muscle Arterioles by Activating the Arachidonic Acid Pathway." PloS One 9 (8): e103858. doi:10.1371/journal.pone.0103858.

Csató, V., A. Pető, G. Á Fülöp, I. Rutkai, E. T. Pásztor, M. Fagyas, J. Kalász, I. Édes, A. Tóth, and Z. Papp. 2015. "Myeloperoxidase Evokes Substantial Vasomotor Responses in Isolated Skeletal Muscle Arterioles of the Rat." Acta Physiologica (Oxford, England) 214 (1): 109–23. doi:10.1111/apha.12488.

Czikora, Ágnes, Erzsébet Lizanecz, Judit Boczán, Andrea Daragó, Zoltán Papp, István Édes, and Attila Tóth. 2012b. "Vascular Metabolism of Anandamide to Arachidonic Acid Affects Myogenic Constriction in Response to Intraluminal Pressure Elevation." *Life Sciences* 90 (11-12): 407–15.

Czikora, Ágnes, Ibolya Rutkai, Enikő T. Pásztor, Andrea Szalai, Róbert Pórszász, Judit Boczán, István Édes, Zoltán Papp, and Attila Tóth. 2013. "Different Desensitization Patterns for Sensory and Vascular TRPV1 Populations in the Rat: Expression, Localization and Functional Consequences." *PloS One* 8 (11): e78184. doi:10.1371/journal.pone.0078184.

Czikora, A., E. Lizanecz, P. Bako, I. Rutkai, F. Ruzsnavszky, J. Magyar, R. Porszasz, et al. 2012a. "Structure-Activity Relationships of Vanilloid Receptor Agonists for Arteriolar TRPV1." *British Journal of Pharmacology* 165 (6): 1801–12.

Fagyas, Miklós, Katalin Úri, Ivetta Mányiné, Andrea Daragó, Judit Boczán, Emese Bányai, István Édes, Zoltán Papp, and Tóth Attila. 2014c. "New Perspectives in the Renin-Angiotensin-Aldosterone System (RAAS) III: Endogenous Inhibition of Angiotensin Converting Enzyme (ACE) Provides Protection against Cardiovascular Diseases." *PLoS One* 9 (4): 93719.

Fagyas, Miklós, Katalin Úri, Ivetta Mányiné, Andrea Daragó, Judit Boczán, Emese Bányai, István Édes, Zoltán Papp, and Attila Tóth. 2014a. "New Perspectives in the Renin-Angiotensin-Aldosterone System (RAAS) I: Endogenous Angiotensin Converting Enzyme (ACE) Inhibition." *PLoS One* 9 (4): 87843.

Fagyas, Miklós, Katalin Úri, Ivetta Mányiné, Áron Fülöp, Viktória Csató, Andrea Daragó, Judit Boczán, et al. 2014b. "New Perspectives in the Renin-Angiotensin-Aldosterone System (RAAS) II: Albumin Suppresses Angiotensin Converting Enzyme (ACE) Activity in Human." *PLoS One* 9 (4): 87844.

[2] A pályázat megvalósítása során eddig született közlemények, melyekben a pályázat feltüntetésre került. Vastagítással kijelölve azok, amelyek a pályázat munkatervében megjelölt feladatok elvégzésének eredményei. Dőlt betűvel szedve azok, amelyek a pályázati célok megvalósításának eredményeként szerzett, a munkaterv írásakor előre nem látható eredmények által motiválva születtek. Végül, normál betűvel szerepelnek azok a közlemények, melyek a pályázathoz csak a laboratórium metodikai- és eszköztárának felhasználásával kapcsolódtak.

Szántó, Magdolna, Ibolya Rutkai, Csaba Hegedus, Ágnes Czikora, Máté Rózsahegyi, Borbála Kiss, László Virág, Pál Gergely, Attila Tóth, and Péter Bai. 2011. "Poly(ADP-Ribose) Polymerase-2 Depletion Reduces Doxorubicin-Induced Damage through SIRT1 Induction." *Cardiovascular Research* 92 (3): 430–38. doi:10.1093/cvr/cvr246.

Tóth, Attila, Agnes Czikora, Eniko T. Pásztor, Beatrix Dienes, Péter Bai, László Csernoch, Ibolya Rutkai, et al. 2014. "Vanilloid Receptor-1 (TRPV1) Expression and Function in the Vasculature of the Rat." ***The Journal of Histochemistry and Cytochemistry: Official Journal of the Histochemistry Society*** **62 (2): 129–44. doi:10.1369/0022155413513589.**

Melléklet

A publikációs listában vastag betűvel szedett közlemények, melyek az eredetileg tervezett munkaterv megvalósítása során kapott eredmények publikálásával születtek.

Journal of Histochemistry & Cytochemistry 2014, Vol. 62(2) 129–144

DOI: 10.1369/0022155413513589
jhc.sagepub.com
SAGE

Vanilloid Receptor-1 (TRPV1) Expression and Function in the Vasculature of the Rat

Attila Tóth, Ágnes Czikora, Enikö T. Pásztor, Beatrix Dienes, Péter Bai, László Csernoch, Ibolya Rutkai, Viktória Csató, Ivetta S. Mányiné, Róbert Pórszász, István Édes, Zoltán Papp, and Judit Boczán

Division of Clinical Physiology, Institute of Cardiology (AT, AC, ETP, IR, ISM, IE, IE, ZP); Research Centre for Molecular Medicine (AT, IE, ZP); Department of Physiology (BD, LC); Department of Medical Chemistry (PB); MTA-DE Cell Biology and Signaling Research Group (PB); Department of Pharmacology and Pharmacotherapy (RP) and Department of Neurology, Faculty of Medicine, University of Debrecen, Debrecen, Hungary (JB).

Summary

Transient receptor potential (TRP) cation channels are emerging in vascular biology. In particular, the expression of the capsaicin receptor (TRPV1) was reported in vascular smooth muscle cells. This study characterized the arteriolar TRPV1 function and expression in the rat. TRPV1 mRNA was expressed in various vascular beds. Six commercially available antibodies were tested for TRPV1 specificity. Two of them were specific (immunostaining was abolished by blocking peptides) for neuronal TRPV1 and one recognized vascular TRPV1. TRPV1 was expressed in blood vessels in the skeletal muscle, mesenteric and skin tissues, as well as in the aorta and carotid arteries. TRPV1 expression was found to be regulated at the level of individual blood vessels, where some vessels expressed, while others did not express TRPV1 in the same tissue sections. Capsaicin (a TRPV1 agonist) evoked constrictions in skeletal muscle arteries and in the carotid artery, but had no effect on the femoral and mesenteric arteries or the aorta. In blood vessels, TRPV1 expression was detected in most of the large arteries, but there were striking differences at level of the small arteries. TRPV1 activity was suppressed in some isolated arteries. This tightly regulated expression and function suggests a physiological role for vascular TRPV1. (J Histochem Cytochem 62:129–144, 2014)

Keywords

dorsal root ganglia; vanilloid receptor-1 (TRPV1); resistance artery; capsaicin; arteriolar constriction; functional; vascular biology

Introduction

Capsaicin is the active component of hot chili peppers and acts as an irritant in humans (Szallasi and Blumberg 1999). The receptor that mediates the hot painful feeling upon capsaicin exposure is transient receptor potential channel vanilloid 1, TRPV1, which was first cloned and identified in sensory neurons (Tominaga et al. 1998). These physiological effects of capsaicin identified TRPV1 as a promising therapeutic target to modulate pain perception, and an extensive pharmaceutical effort was made to develop TRPV1 antagonists to relieve pain (Szallasi and Blumberg 1999). Hundreds of patents were filed and thousands of molecules developed to modulate TRPV1. However, this effort did not result in a breakthrough in pain treatment because of the physiological off-target effects of the developed TRPV1 antagonists, with subsequent work revealing that TRPV1 is involved in body temperature maintenance in addition to its other functions (Gavva 2008; Holzer 2008; Szallasi and Sheta 2012).

TRPV1 expression has been identified in various tissues in addition to sensory neurons. In particular, TRPV1 was found in the central nervous system (Toth et al. 2005) and

Received for publication May 22, 2013; accepted September 30, 2013.

Corresponding Author:
Attila Tóth, Division of Clinical Physiology, Institute of Cardiology, University of Debrecen, 22 Móricz Zs. krt., Debrecen, 4032, Hungary.
E-mail: atitoth@med.unideb.hu

in the peripheral blood vessels (Lizanecz et al. 2006). Later research on the effects of TRPV1 stimulation in blood vessels suggested both dilation and constriction effects upon TRPV1 stimulation (Kark et al. 2008). TRPV1-mediated dilation was found to be related to the perivascular sensory neuronal terminals, which were thought to release neurotransmitters (CGRP, substance P) upon stimulation and mediate vasodilation (Zygmunt et al. 1999). The vasoconstrictive properties of TRPV1, however, were much less-well characterized. Nonetheless, we (Czikora et al. 2012; Kark et al. 2008) and others (Cavanaugh et al. 2011) have recently shown that functional TRPV1 is expressed in arteriolar smooth muscle cells, where its activation results in an increase in intracellular Ca^{2+} concentration and vasoconstriction.

TRPV1-6 channels are gaining increasing attention in vascular biology. These cation channels demonstrate some selectivity to Ca^{2+} (Baylie and Brayden 2011). However, there is little consistency in the reports regarding the role of TRPV1 in vascular biology, with reports suggesting that even the same arteries can respond to capsaicin by dilation or constriction depending on the conditions (Baylie and Brayden 2011). These opposing effects on vascular diameter were explained by its localization in sensory neuronal terminals (mediating dilation) and in vascular smooth muscle cells (Kark et al. 2008).

We performed a detailed study here to reveal functional TRPV1 expression in various vascular tissues of the rat. First, antibodies that were specific for sensory neuronal TRPV1 and vascular TRPV1 expression were identified and the expression characterized. The data revealed that TRPV1 expression is not uniform in vascular beds, with some vessels expressing TRPV1 while others not in the same tissue section. Moreover, TRPV1 responses to capsaicin were different in isolated arteries where TRPV1 appears to be highly expressed, suggesting a tight regulation of TRPV1 sensitivity in arteriolar smooth muscle.

Materials & Methods

Materials and Solutions

Chemicals were from Sigma-Aldrich, unless stated otherwise. Capsaicin (8-methyl-N-vanillyl-*trans*-6-nonenamide) was dissolved in ethanol. Norepinephrine and acetylcholine were dissolved in distilled water.

Animals, Anesthesia and General Preparation for In Vivo Experiments

Male Wistar Kyoto (WKY/NCrl) rats (Charles River, Isaszeg, Hungary) were fed ad libitum (chow from Szinbad Kft, Godollo, Hungary). Rats were 250-450 g when experiments were started. Rats were anesthetized by 50 mg/kg i.p. thiopental. Animal experiments were carried out at and approved by the University of Debrecen, Medical and Health Science Center, and were in accordance with the standards established by the National Institutes of Health.

Total RNA and RT-qPCR

Tissue samples were prepared as described later for cannulated arteries. Reverse transcription-coupled quantitative PCR was performed as described previously (Bai et al. 2007). Briefly, total RNA was prepared using Trizol reagent (Life Technologies; Budapest, Hungary) according to the manufacturer's instructions. RNA was treated with DNase and 0.5 μg RNA was reverse transcribed using a High Capacity cDNA Reverse Transcription Kit (Applied Biosystems; Foster City, CA). cDNA was purified on QIAquick PCR cleanup columns (Qiagen, Valencia, CA). cDNA at 10-fold dilution was used for qPCR reactions. The quantitative PCR reactions were performed using a LightCycler 480 system (Roche Applied Science; Basel, Switzerland) and a qPCR supermix (Biocenter; Szeged, Hungary) with the following primers: TRPV1 (fwd: 5'-gaatgacaccatcgctctgc; rev: 5'- aagagggtcaccagcgtcat) and 36B4 as control (fwd: 5'- ccccgtgtgaggtcacagta; rev: 5'- atgatcagcccgaaggagaa). TRPV1 expression was normalized for 36B4 expression. Finally, the products of the PCR amplification were run on a 2% agarose gel to verify their size. To check for the amplification of primer dimers, the template was omitted from the controls and melting curve analysis was performed.

Immunohistochemistry

Tissue samples (dorsal root ganglia, gracilis muscle, mesenterium, femoral muscle, aorta, carotid artery and the ears) were dissected from the rat and embedded in Tissue-Tek O.C.T compound (Electron Microscopy Sciences; Hatfield, PA). Cryostat sections (10-μm-thick) were prepared, fixed in acetone for 10 min and blocked with normal goat sera for 20 min (1.5% in PBS, Sigma-Aldrich; St. Louis, MO). TRPV1 was stained with anti-capsaicin receptor antibodies. Antibodies were obtained from Alomone Labs (Jerusalem, Israel) (anti-TRPV1-C, 3rd loop) Calbiochem (San Diego, CA) (anti-TRPV1-N), Osenses (Keswick, Australia) (3rd loop, 4th loop) and Neuromics (Edina, MN) (N-terminal). Details and dilutions of the antibodies are shown in Table 1. Blocking peptides (synthesized based on the immunogenic TRPV1 fragment used to develop the antibodies) were also used in some cases. Binding of the TRPV1-specific antibodies was visualized using fluorescent secondary antibodies (Table 1) by a Zeiss Meta confocal microscope (Zeiss; Oberkochen, Germany). Tissue sections were also co-stained with anti-smooth muscle actin (Table 1) or with a neurofilament-specific antibody (Table 1) in the blocking

Table 1. Antibody Details.

Specificity	Region	Developed in	Working dilution	
			Western blot	Immunohistochemistry
TRPV1	C-terminal	Rabbit	1:200	1:500
TRPV1	N-terminal	Rabbit	1:200	1:750
TRPV1	3rd loop	Rabbit	1:200	1:750
TRPV1	3rd loop	Rabbit	N/A	1:100
TRPV1	4th loop	Rabbit	1:200	1:150
TRPV1	N-term	Rabbit	1:1000	1:500
Smooth muscle actin		Mouse	N/A	1:50
Neurofilament		Mouse	N/A	1:100
Anti-rabbit-biotinylated		Goat	N/A	1:200
Anti-mouse-FITC		Goat	N/A	1:200
Streptavidin-Cy3		N/A	N/A	1:500
anti-rabbit-POD			1:40000	N/A

buffer. Pictures were processed by ImageJ software (NIH; Bethesda, MD) to calculate cross-sectional areas. Cross-sectional areas were calculated by applying the AUTO mode for the dorsal root ganglia pictures in both the Threshold and the Particle analysis menus (the single manual adjustment set the maximum area to 1000).

Western Blotting

Tissue samples (20 dorsal root ganglia and two carotid arteries) were dissected from the rat, pooled, and homogenized in 200 µl of SDS sample buffer (S3401, Sigma-Aldrich) using a glass tissue homogenizer. Cultured human embryonic kidney cells (HEK293, LGC Standards; Wesel, Germany) were transfected with a human TRPV1-expression plasmid (pdEYFP-C1 construct, RZPD; Berlin, Germany). HEK293 cells were maintained in Dulbecco's modified Eagle's medium (DMEM) supplemented with 10% heat-inactivated FBS, 2 mM glutamine, 100 U/ml penicillin, and 100 µg/ml streptomycin (all from Life Technologies) at 37C, 5% CO_2. HEK293 cells (control and transfected) were collected from 100 mm diameter petri dishes and homogenized in 500 µl of SDS sample buffer. All homogenized samples were incubated at 100C for 10 min. Protein concentration was determined using a BSA standard. Protein (30 µg) was loaded onto 10% SDS-polyacrylamide gels and transferred onto nitrocellulose membranes. The membranes were then stained by a reversible protein staining dye (Ponceau S) and were cut into strips of the aforementioned samples and a prestained molecular weight standard (ProSieve QuadColor, Lonza; Rockland, MA) and probed with TRPV1-specific antibodies (Table 1). Blocking peptides (Table 1) were obtained from Alomone (ACC-030 antibody) and from EZBiolabs (Caramel, IN; PC547 antibody). Blocking peptides were used in a ratio of 1 µg peptide:1 µg antibody and were preincubated with their respective antibodies for 60 min at room temperature. All primary antibodies (Table 1) were indicated to work in western blotting, and we used dilutions suggested by the manufacturers (Table 1). Binding of the primary antibodies was detected by an anti-rabbit-POD secondary antibody (Sigma-Aldrich). Peroxidase reaction was detected by ECL (Western Lightning Plus ECL, PerkinElmer; Waltham, MA) and the signal was recorded by an imaging system (MF-Chemibis 3.2, Central European Biosystems; Budapest, Hungary). All membranes in the figures were developed together with an exposure time was 6 min. The intensity range was 0-15,984 (with recording in the range of 0-65,535).

Preparation of Cannulated Arterioles

Isolation of the skeletal (gracilis) muscle arterioles of the rat and diameter measurement of the arterioles were performed as described earlier (Lizanecz et al. 2006). Preparation of small mesenteric resistance arteries were performed likewise. The internal diameter of the arterioles was measured by video microscopy. Experiments were carried out in PSS (composition in mM: 110 NaCl, 5.0 KCl, 2.5 $CaCl_2$, 1.0 $MgSO_4$, 1.0 KH_2PO_4, 5.0 glucose and 24.0 $NaHCO_3$ equilibrated with a gas mixture of 10% O_2 and 5% CO_2, 85% N_2, at pH 7.4). After the development of spontaneous myogenic tone at 80 mmHg, arteriolar responses to acetylcholine (edothel dependent dilation, 1 nM–10 µM), to norepinephrine (vasoconstrictor, 1 nM–10 µM) and to capsaicin (TRPV1 agonist, 1 nM–10 µM) were measured. Agonists were applied in a cumulative fashion.

Measurement of Arteriolar Contractions under Isometric Conditions

Large arteries were prepared from the rat in Ca^{2+}-free PSS. Vessel Segments (4-mm long) were fixed onto a

contractile force measurement setup (DMT510A, Danish Myotechnology; Aarhus, Denmark). After fixing of the vessels on the setup in Ca^{2+}-free PSS, the buffer was changed to PSS and vessels were stretched by 10 mN. Mounted arteries were incubated in PSS for 40–60 min (until force values were stabilized) at 37C. Experiments were initiated by the addition of the smooth muscle-dependent vasoconstrictive agent norepinephrine or U-46619 in a cumulative fashion (1 nM–10 μM). After reaching the maximal response, these agents were washed away and the vessels were incubated in PSS alone, until the contractile force decreased to the baseline level before the application of the vasoconstrictive agents. Finally, capsaicin was applied (1 nM–30 μM) to investigate TRPV1-–mediated vascular effects.

Data Analysis and Statistical Procedures

Arteriolar diameter was determined by measuring the distance between the intraluminal sides of the arteriolar wall (inner diameter). Data are shown as mean diameter ± S.E.M. Student's t-tests were used to determine differences. Statistical analysis was performed using Microsoft Excel. P-values <0.05 were considered to be significant.

Results

Non-neuronal Expression of TRPV1

The expression of TRPV1 in vascular tissues was tested by RT-PCR (Fig. 1A) and qPCR (Fig. 1B) in isolated vascular preparations. TRPV1 expression was found to be the highest in dorsal root ganglia. Nonetheless, TRPV1 was also expressed in other tissues, albeit its expression was two orders of magnitude lower than that in dorsal root ganglia. TRPV1 mRNA expression was not detected in the isolated mesenteric artery (values were similar to those performed without template).

Characterization of Antibodies Developed against TRPV1

A set of six antibodies developed against TRPV1 (Table 1) were tested on dorsal root ganglia of the rat. Among the six tested, two antibodies (anti-TRPV1-N and anti-TRPV1-C) stained specifically a subset of the neurons within the dorsal root, whereas three antibodies (Alomone 3rd loop, Osenses 3rd loop and Osenses 4th loop) did not give any cell-specific staining pattern and the last (Neuromics N-terminal antibody) had a rather nonspecific neuronal staining pattern under these conditions (Fig. 2). The anti-TRPV1-N and anti-TRPV1-C antibodies were tested in detail. Both the anti-TRPV1-N (red; Fig. 3A) and anti-TRPV1-C (red; Fig. 3B) antibodies stained a subset of cell bodies within the dorsal root ganglia of the rat.

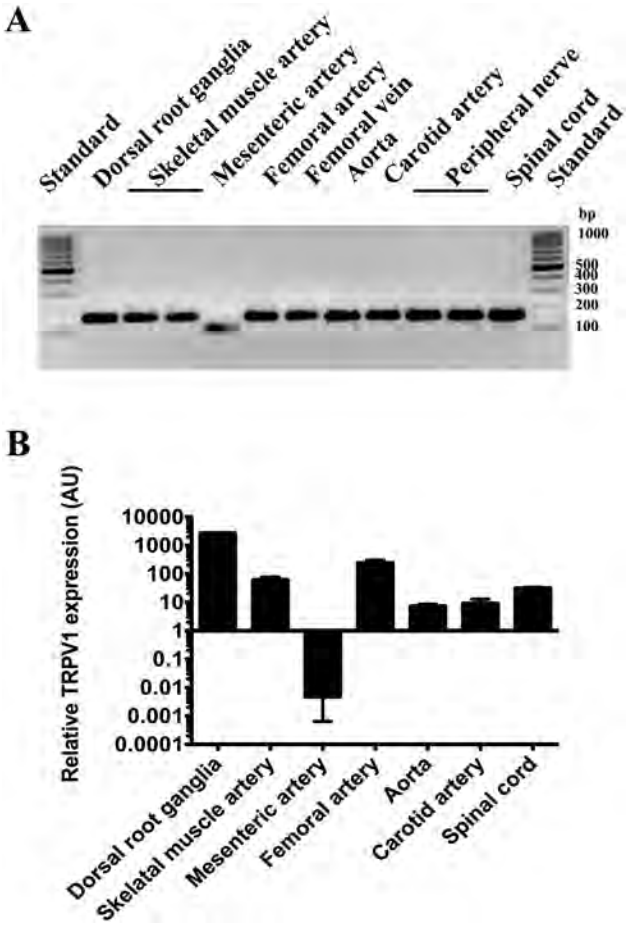

Figure 1. TRPV1 mRNA in peripheral tissues of the rat. TRPV1 expression was examined with RT-PCR (A) and qPCR (B) in peripheral tissues of the rat. Isolated mRNA (0.5 μg) from various tissue sources (isolated arteries, veins, nerves, dorsal root ganglia and spinal cord) was subjected to RT-PCR and qPCR with a primer set specific to rat TRPV1. (A) Reaction mixtures were loaded onto 2% agarose gels to separate PCR products. Bands at the apparent molecular size of 170 bp were in accordance with the expected size of the product, while the band in the mesenteric artery sample was nonspecific. (B) qPCR experiments revealed negligible expression of TRPV1 in mesenteric arteries (values were similar to those performed without template), but a reasonably high level of expression was found in other peripheral tissues (n=2–8; bars represent mean ± SEM).

TRPV1-positive cells were also stained with a neurofilament-specific antibody (green; Fig. 3), although the intensity of the signal was weaker in TRPV1-expressing cells than TRPV1-negative cells. Images taken at a higher magnification in separate experiments confirmed this observation (Fig. 4A and Fig. 4C). TRPV1-specific immunostaining was negative when the anti-TRPV1 antibodies were pre-absorbed with their respective blocking peptides (anti-TRPV1-N, Fig. 4B; anti-TRPV1-C, Fig. 4D). The company datasheets for the TRPV1 antibodies (Fig. 2, Table 1) indicate that the antibodies are suitable

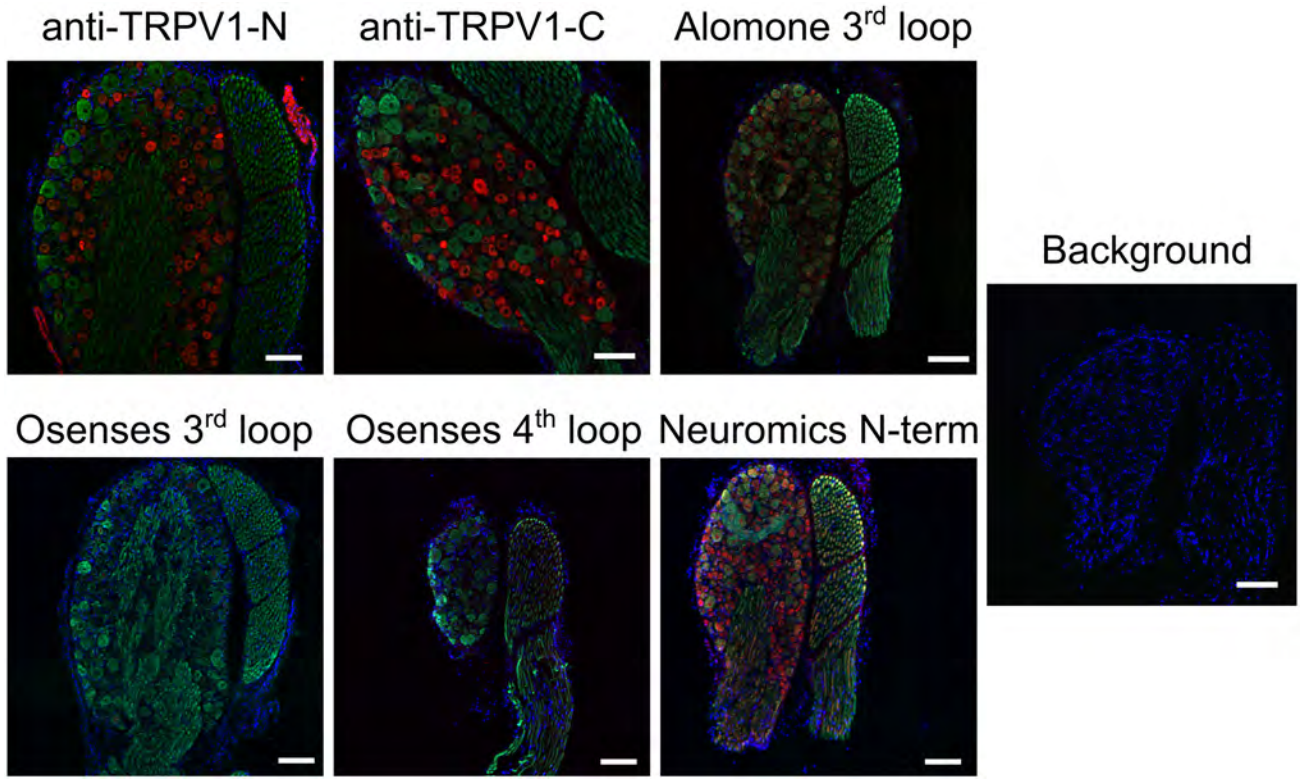

Figure 2. Specificity of TRPV1 antibodies. Six commercially available anti-TRPV1 antibodies were tested on dorsal root ganglia (cryostat sections) of the rat (red). Tissue sections were co-stained with a neurofilament-specific antibody (green, neurons). Nuclei were stained with a DAPI counterstain (blue). Background staining levels were checked by omitting the primary antibodies (and counterstaining with DAPI). Primary antibodies are indicated on the figure. Dilutions and details of the antibodies are summarized in Table 1. Bars represent 100 µm.

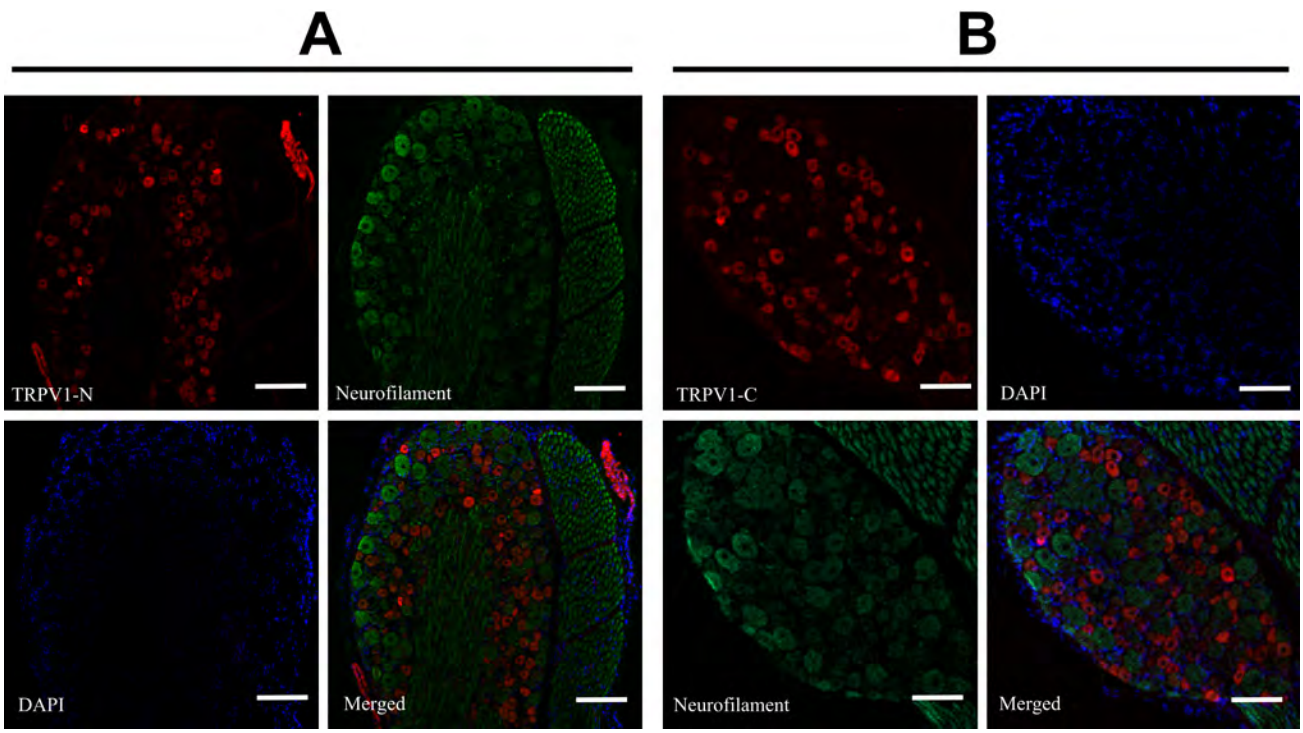

Figure 3. Colocalization of TRPV1 and neurofilament immunoreactivities. Rat dorsal root ganglia were stained with anti-TRPV1-N (A) and anti-TRPV1-C (B) antibodies (red), together with a neurofilament-specific antibody (green; neurons) and DAPI counterstain (blue; nuclei). The merged images for these three channels are shown. Bars represent 100 µm.

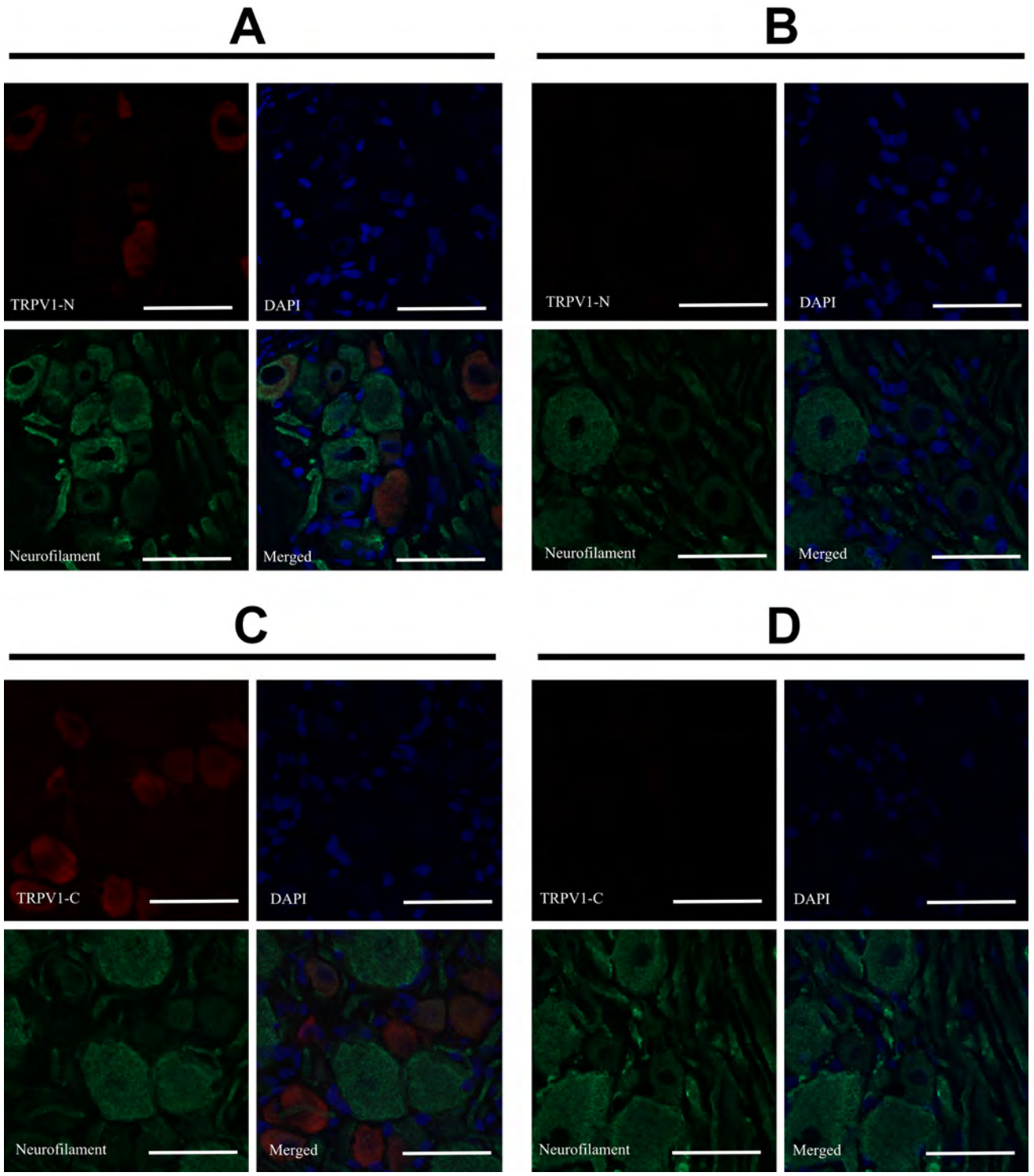

Figure 4. Specificity of neuronal TRPV1 staining. Dorsal root ganglia of the rat were stained with anti-TRPV1-N (A and B) or anti-TRPV1-C (C and D) antibodies (red); together with a neurofilament-specific antibody (green; neurons) and DAPI counterstain (blue; nuclei). Blocking peptides were synthesized according to the sequence of the immunogenic TRPV1 fragment to investigate the specificity of the TRPV1 staining. Positive staining disappeared when the antibodies were pre-incubated with the blocking peptides (B and D). Bars represent 50 μm.

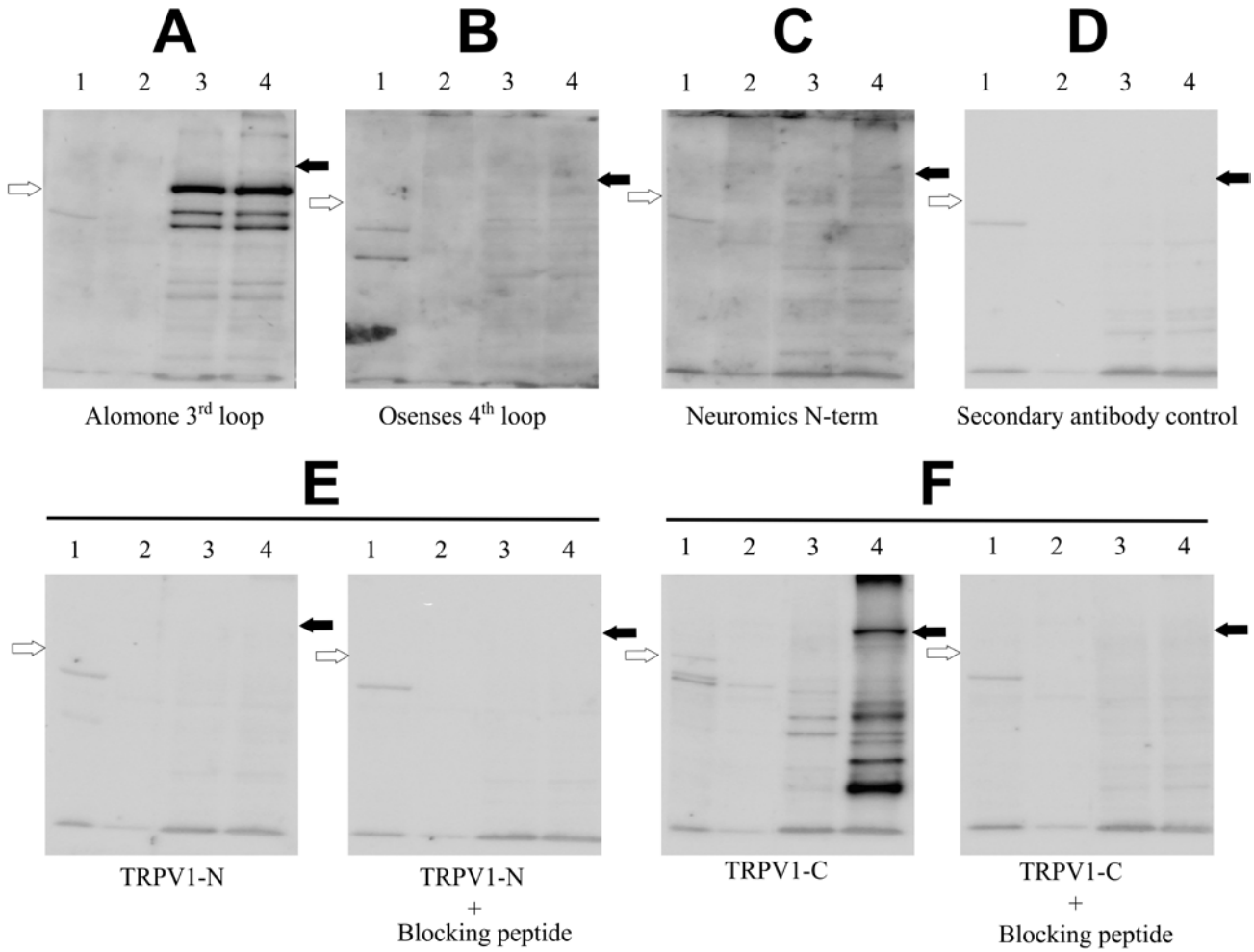

Figure 5. Specificity of TRPV1 antibodies in western blotting. Dorsal root ganglia (1) and the carotid artery (2) were harvested from the rat. HEK293 (3) and HEK293 cells transfected with GFP-TRPV1 (4) were cultured in cell culture dishes. Protein lysates from each sample were prepared in SDS sample buffer, separated on 10% polyacrylamide gels (30 µg protein/well) and transferred onto nitrocellulose membranes for TRPV1 antibody staining. Dilutions were as per the manufacturer's recommendation or 1:50 (anti-TRPV1-N antibody). (A) Alomone antibody; (B) Oseneses 4th loop, and (C) Neuromics N-terminal were assessed and compared with (D) secondary antibody alone (no primary antibody). (E, F) Blocking peptides, synthesized according to the sequence of the immunogenic TRPV1 fragment, were preincubated with the primary antibody to ascertain specificity of the staining. Membranes were incubated simultaneously with the secondary antibody (goat anti-rabbit–POD) and ECL was used for the detection. All of the membranes were developed simultaneously in a Chemibis 3.2 imager with an exposure time of 6 min. Empty arrows point to the expected position of endogenous TRPV1 (lanes 1, 2 and 3), and filled arrows to the position of GFP-TRPV1 (lane 4 only).

for western blotting. Antibodies were therefore tested in western blots of homogenates of the dorsal root ganglia, carotid artery, and in HEK293 with or without TRPV1 overexpression (Fig. 5). Some of the antibodies (Alomone 3rd loop, Osenses 4th loop and Neuromics N-terminal, Fig. 5A-5C) gave only nonspecific signals (Fig. 5). Compared with the background staining (Fig. 5D), the anti-TRPV1-N antibody did not give any signal under these conditions (Fig. 5E). The anti-TRPV1-C antibody (Fig. 5F) was found to be applicable in western blotting, detecting TRPV1 in the dorsal root ganglia and in TRPV1-overexpressing HEK293 cells but not in untransfected HEK293 cells. Moreover, this TRPV1-specific signal disappeared in the presence of the blocking peptide.

Characterization of TRPV1-positive Structures in the Dorsal Root Ganglia

The anti-TRPV1-N and anti-TRPV1-C antibodies were used to investigate TRPV1 expression in the rat. The cross-sectional area of TRPV1-positive neurons was measured in the dorsal root ganglia (anti-TRPV1-N, Fig. 6A and anti-TRPV1-C, Fig. 6B). Both antibodies stained the small-diameter neurons (Fig. 6E and 6F, respectively, cross-sectional

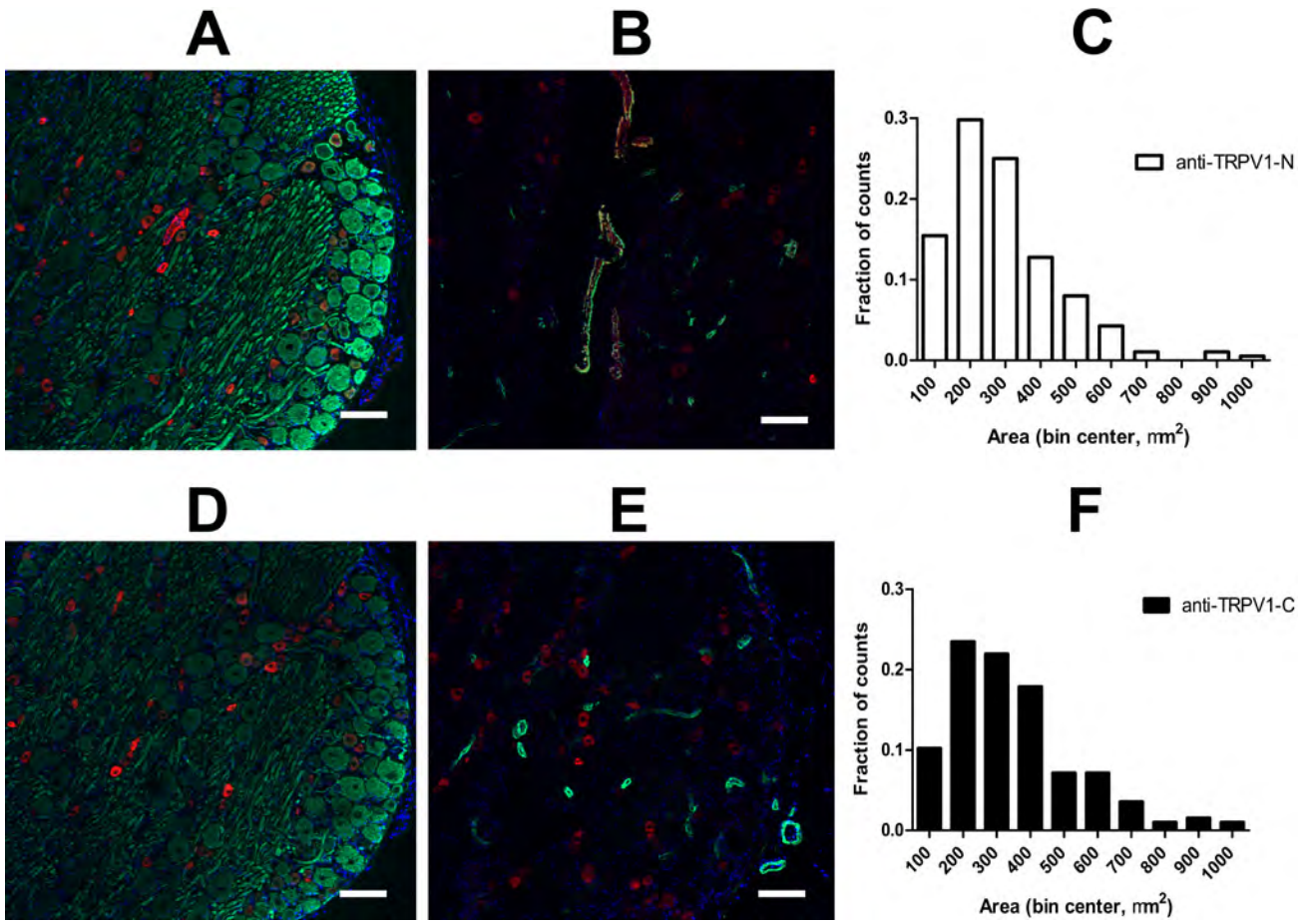

Figure 6. TRPV1 expression in sensory neurons. The selectivity of the anti-TRPV1-N (A and B) and anti-TRPV1-C (C and D) antibodies were tested in the dorsal root ganglia of the rat. Cryostat sections (10 µm) were stained using TRPV1 antibodies (red), a neurofilament-specific antibody (green; A and C) or an antibody against smooth muscle actin (green; B and D). Nuclei were stained with DAPI (blue). Cross-sectional area of the stained cells was calculated and plotted on histograms (anti-TRPV1-N, panel E, anti-TRPV1-C, panel F). Evaluations were made with ImageJ software.

diameter was 200-600 µm^2), which was in accordance with the size of the sensory neurons. Surprisingly, anti-TRPV1-N antibody also gave a TRPV1-like immunoreactivity in vascular beds within (Fig. 6A) and around (Fig. 3A) the dorsal root ganglia. We next tested the colocalization of TRPV1 with smooth muscle actin. The anti-TRPV1-N antibody stained some but not all of the smooth muscle cells (Fig. 6B), with some vessels in the section also positive for TRPV1. Anti-TRPV1-C antibody did not stain smooth muscle cells (Fig. 6D). The functional expression of TRPV1 in sensory neurons is well established, but its expression in the vasculature is a relatively novel concept. Thus, we next sought to investigate this vascular expression of TRPV1 using a combination of immunohistochemistry and functional measurements.

Characterization of Functional TRPV1 Expression in Different Vascular Tissues of the Rat

Vascular smooth muscle cells of blood vessels within the gracilis muscle of the rat were positively stained with an anti-TRPV1-N antibody (Fig. 7B), whereas anti-TRPV1-C antibody did not produce a specific staining pattern (Fig. 7D). Neither antibody stained the neurites in this tissue type (Fig. 7A and 7C, respectively). TRPV1-positive (anti-TRPV1-N antibody) arteries were isolated and the effect of the TRPV1 agonist, capsaicin, was tested. Capsaicin evoked a robust constriction in these arterioles, which was comparable to that evoked by norepinephrine (Fig. 7E).

These conflicting staining patterns of the vascular tissue by the two TRPV1 antibodies were further investigated using blocking peptides. Smooth muscle staining with anti-TRPV1-N antibody (Fig. 8A) was blocked by the immunogenic TRPV1 fragment (Fig. 8B), confirming the specificity of the TRPV1 staining. On the other hand, there was no signal above the background in the case of the anti-TRPV1-C antibody (Fig. 8C and 8D).

An inhomogeneous staining pattern was found in the mesenteric tissue with the anti-TRPV1-N antibody (Fig. 9A and 9B), while the anti-TRPV1-C antibody (Fig. 9C and 9D) again failed to show specific staining. Some of the

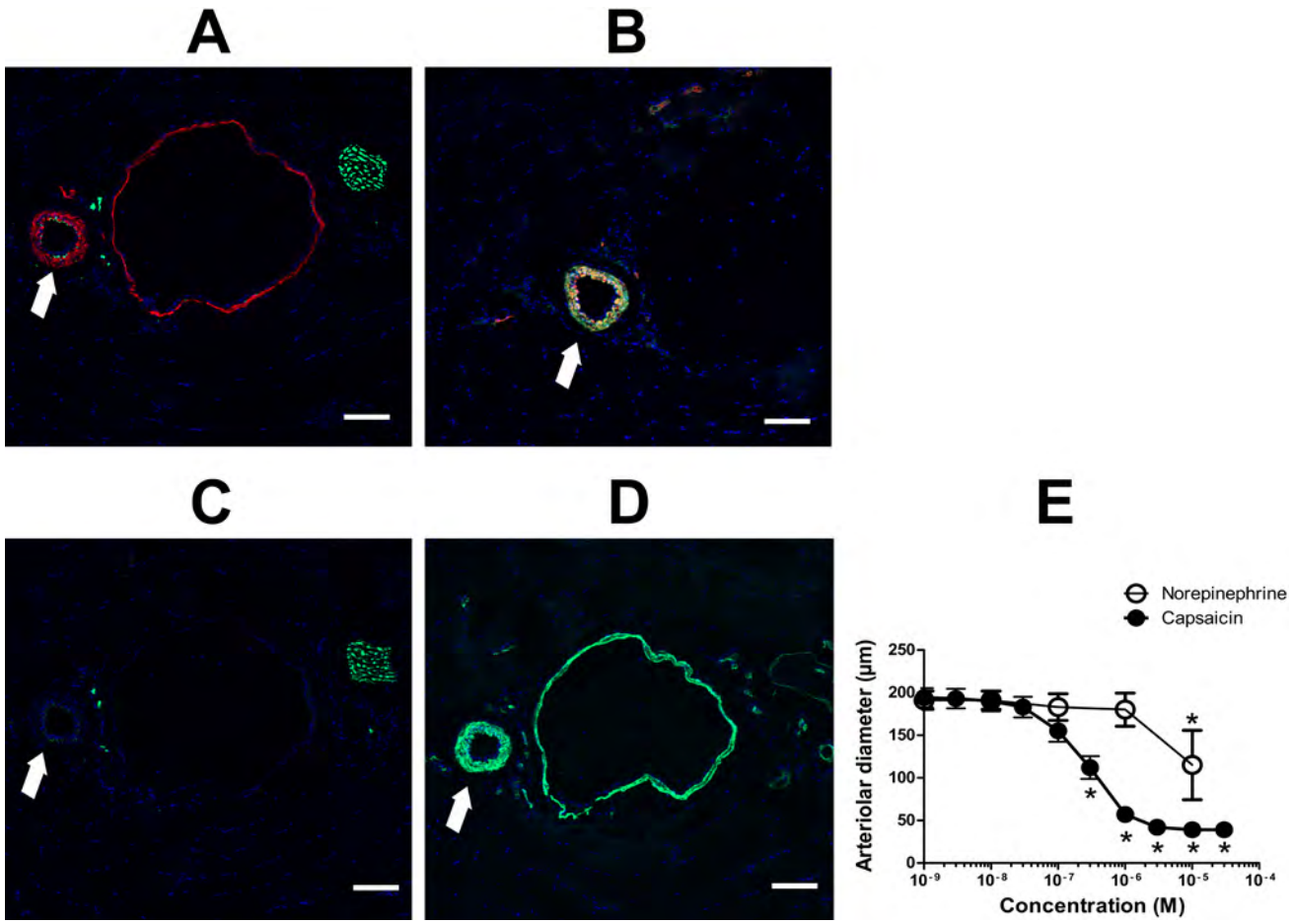

Figure 7. Functional expression of TRPV1 in skeletal muscle blood vessels. Cryostat sections were prepared from the gracilis muscle of the rat (10 µm) and were stained using anti-TRPV1-N (A and B) or anti-TRPV1-C (C and D) antibodies (red). Sections were co-stained with antibodies against neurofilament (green; A and C) or smooth muscle actin (green; B and D). The same arteries (arrows) were isolated and mounted on an isobaric (cannulated) setup. (E) Concentration-response to capsaicin (a TRPV1-specific agonist) and to norepinephrine. Data are the mean ± SEM of five independent experiments. Asterisks indicate significant differences as compared with the initial (before treatment) values.

blood vessels were positive for TRPV1, while others were not within the same tissue section (Fig. 9A and 9B). Capsaicin had no functional effect, although norepinephrine evoked substantial vasoconstriction (Fig. 9E).

The anti-TRPV1-N antibody gave a strong positive staining for sections of the femoral artery (Fig. 10B), whereas the anti-TRPV1-C antibody showed a weak background staining in skeletal muscle cells (Fig. 10D). Capsaicin had no effect in the functional measurements on these (isolated) arteries, compared with the constrictions evoked by norepinephrine (Fig. 10E). None of the peripheral neurites were stained by these antibodies (Fig. 10A and 10C).

We next examined TRPV1 staining of the aorta. The aorta was positively stained for TRPV1 using the anti-TRPV1-N antibody (Fig. 11B), but not with the anti-TRPV1-C antibody (Fig. 11D). Capsaicin had no effect on the isolated rings, whereas norepinephrine evoked substantial constrictions (Fig. 11E). There was no neuronal staining in these tissue sections (Fig. 11A and 11C).

We also tested TRPV1 staining of the carotid artery. Again, the anti-TRPV1-N antibody stained the smooth muscle layer of the tissue (Fig. 12B), whereas the anti-TRPV1-C antibody demonstrated no specific staining (Fig. 12D). Nonetheless, capsaicin evoked a partial constriction in carotid arteries, which was about 20% of the maximal constriction achieved by the thromboxane A2 agonist U-46619 (Fig. 12E). Besides vessel staining, no neuron-specific staining was found in these sections (Fig. 12A and 12C).

Finally, a tissue important in the thermoregulation was tested. Staining of the ears of the rat revealed that both the anti-TRPV1-N and anti-TRPV1-C antibodies can stain peripheral axons (Fig. 13A and 13C, respectively). The anti-TRPV1-C antibody did not stain specifically other structures (Fig. 13D). In contrast, the anti-TRPV1-N

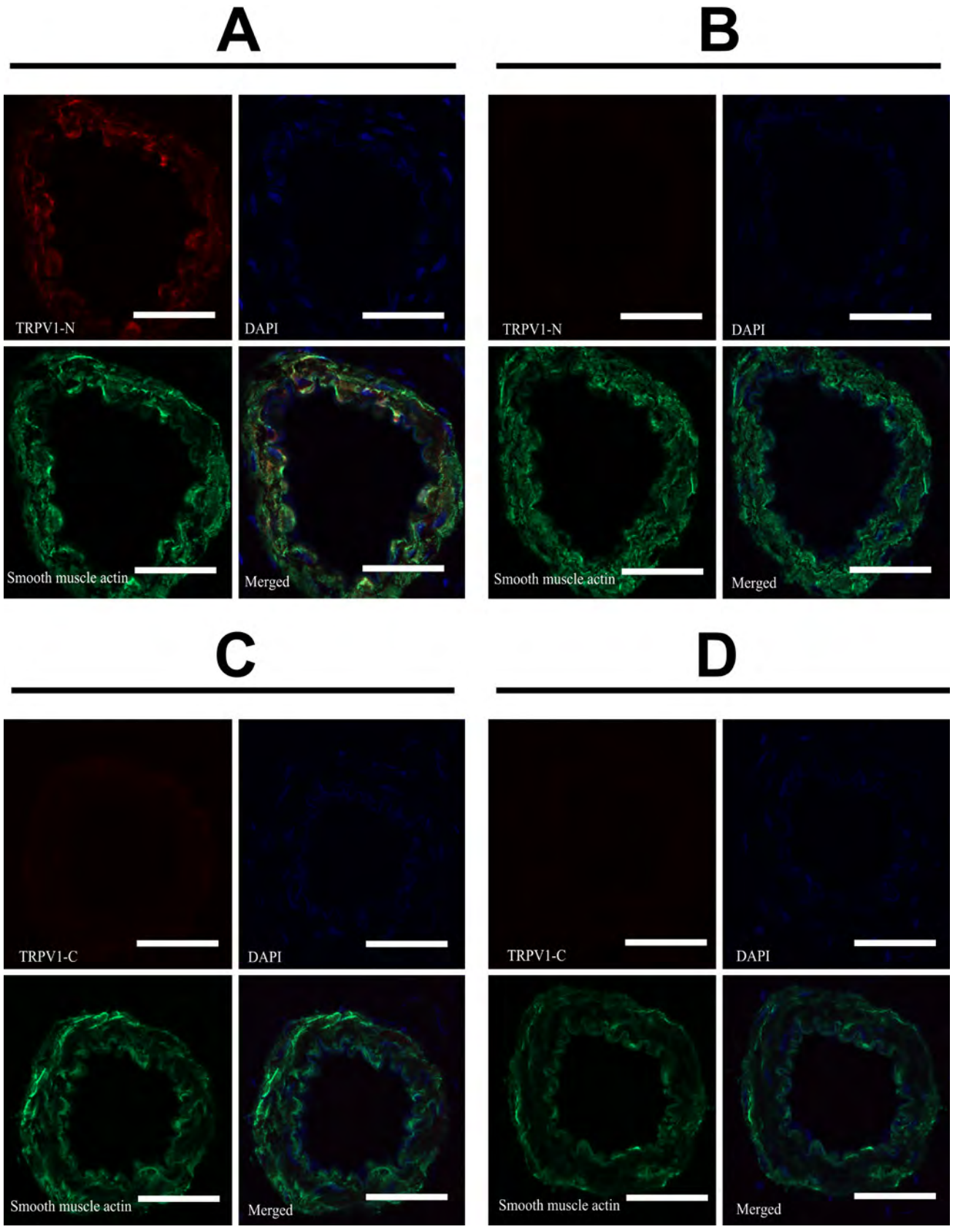

Figure 8. TRPV1 expression in smooth muscle cells. Smooth muscle expression of TRPV1 was investigated in detail. Gracilis muscle tissue sections of the rat were probed with anti-TRPV1-N (A and B; red) or anti-TRPV1-C (C and D; red) as well as anti-neurofilament (green) and DAPI (blue). Merged images are shown. (B, D) TRPV1-specific antibodies were pre-absorbed with blocking peptides to show specificity of staining (compare A with B; C with D). Bars represent 100 μm.

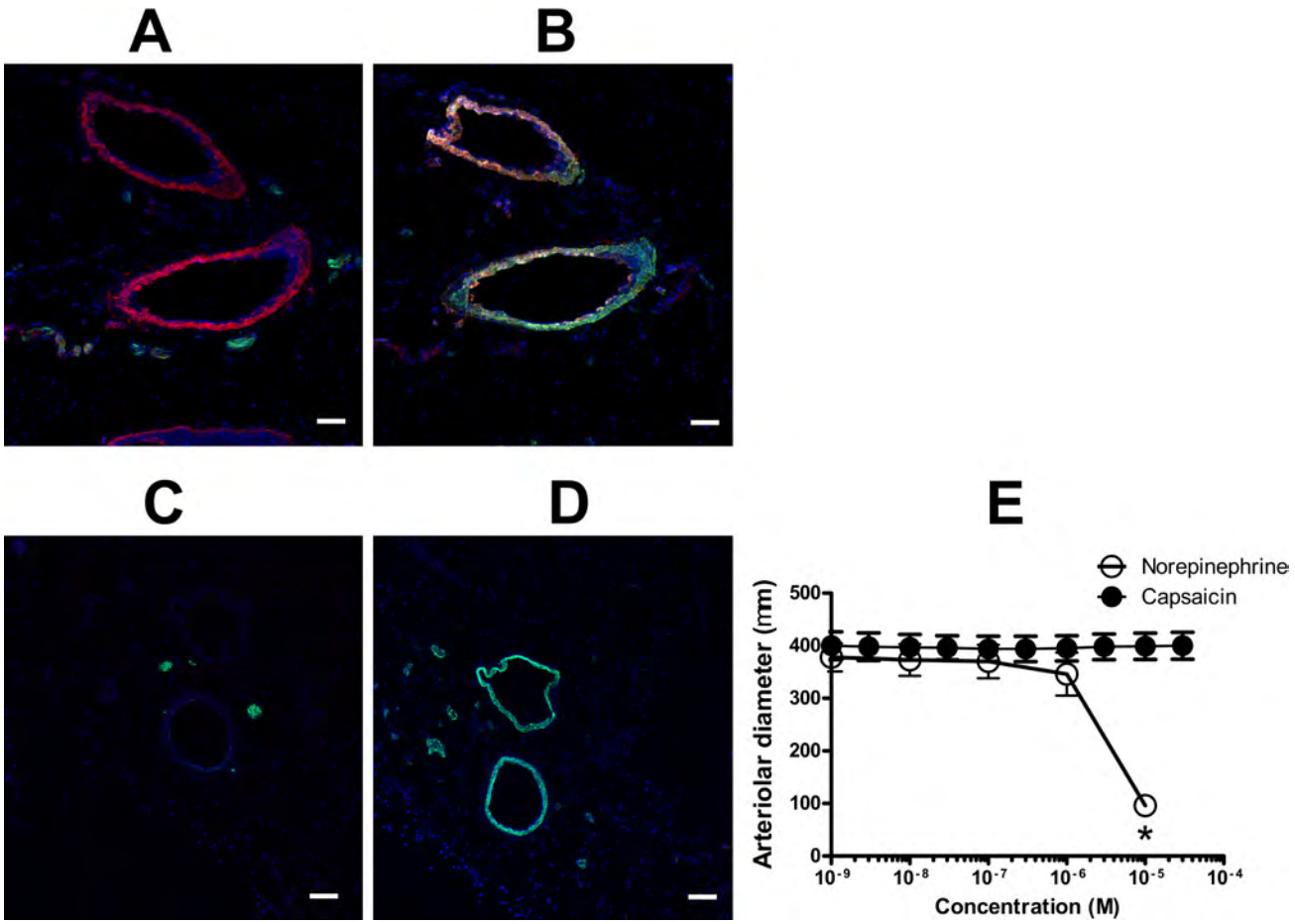

Figure 9. Expression of TRPV1 in mesenteric blood vessels. Cryostat sections were prepared from the mesenteric tissue (near the small intestine; 10 µm) and TRPV1 expression (red) was detected using anti-TRPV1-N (A and B) or anti-TRPV1-C (C and D) antibodies. Sections were co-stained with antibodies against neurofilament (green; A and C) or smooth muscle actin (green; B and D). (E) Isolated, third-order arteries from the same tissue were mounted on an isobaric vascular setup and the responses to capsaicin and norepinephrine were recorded. Data are the mean ± SEM of five independent experiments. Asterisk indicates a significant difference as compared with the initial (before treatment) value. Bars represent 100 µm.

antibody again stained some of the blood vessels (Fig. 13B). It is important to note that a very limited number of blood vessels were stained, and they appeared to have a larger diameter (Fig. 13B).

Discussion

There are numerous reports about TRPV1 expression in non-neuronal tissues. Here we made an effort to characterize these TRPV1 populations in the peripheral tissues of the rat. The presence of TRPV1 mRNA was established first. Our qPCR analysis (Fig. 1B) suggested that TRPV1 is indeed expressed in vascular preparations, although the expression level was about two orders of magnitude lower than that in the dorsal root ganglia. After establishing the presence of TRPV1 in vascular tissues, an effort was made to identify antibodies suitable for detecting TRPV1 expression. Six commercially available antibodies were tested. We found that only two of the six tested antibodies were selective for TRPV1 in dorsal root ganglia sections. These antibodies (referred as anti-TRPV1-N and anti-TRPV1-C) were then characterized in detail. We showed that one antibody (anti-TRPV1-C) was able to detect endogenous (dorsal root ganglia) and exogenous (transfected HEK293 cells) TRPV1 in western blotting. Moreover, TRPV1 staining of sensory neurons (anti-TRPV1-N and anti-TRPV1-C antibodies) and vascular smooth muscle cells (anti-TRPV1-N antibody) was blocked by the antigenic peptides, suggesting that both of these antibodies are specific for TRPV1.

We next concentrated our efforts on examining TRPV1 expression in blood vessels, with staining performed in parallel with functional measurements on the same arteries where possible. We first tested arteries present within the gracilis muscle tissue, because we have previously provided data to suggest functional TRPV1 expression in skeletal muscle arteries (Czikora et al. 2012; Kark et al. 2008;

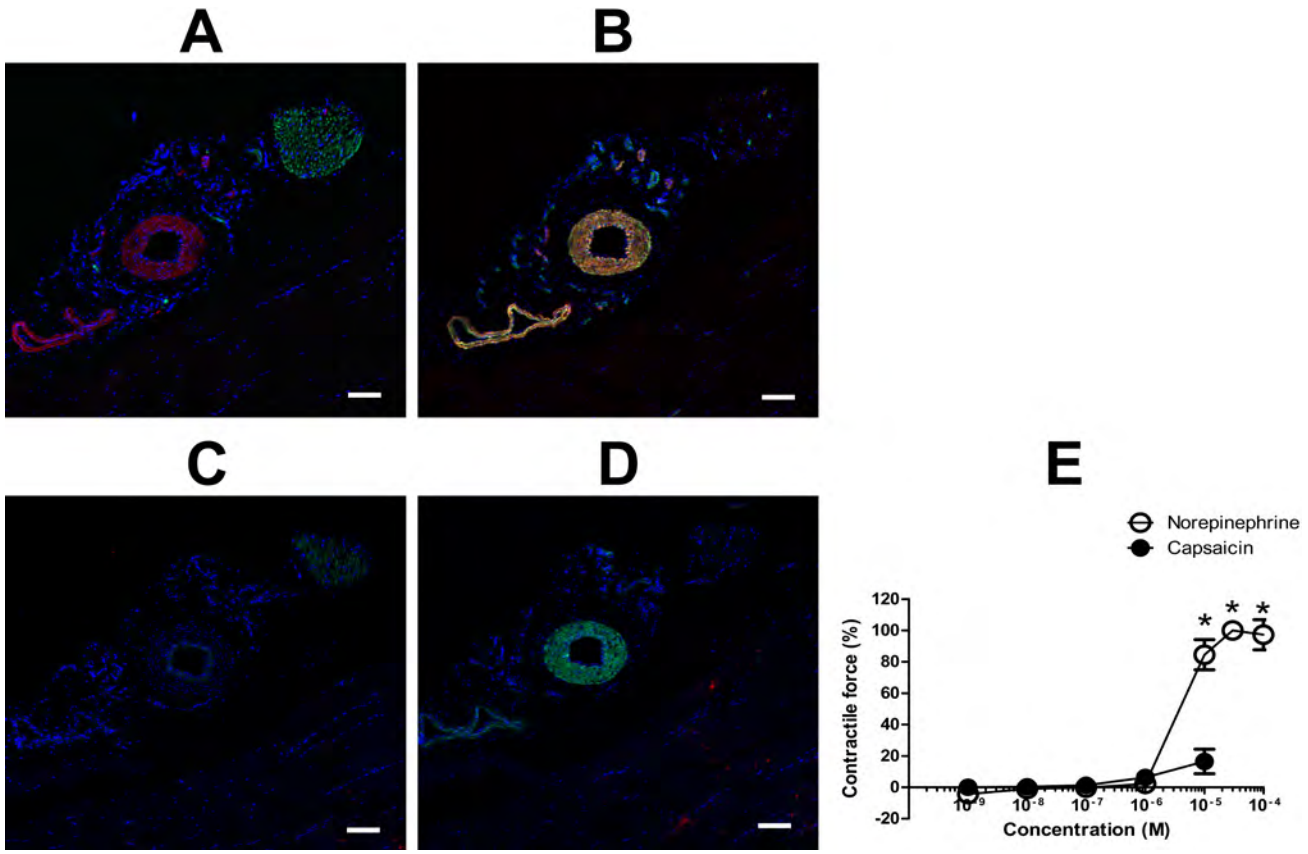

Figure 10. Expression of TRPV1 in the femoral artery. Femoral artery tissue sections were probed with anti-TRPV1-N (red; A and B) or anti-TRPV1-C (red; C and D), and anti-neurofilament (green; A and C) or anti-smooth muscle actin (green; B and D), and counterstained with DAPI (blue). (E) The same arteries were mounted on an isometric contractile force measurement system and responses to capsaicin (TRPV1-specific agonist) and norepinephrine were measured. Data are the mean ± SEM of four independent experiments. Asterisks indicate significant differences as compared with the initial (before treatment) constrictions. Bars represent 100 μm.

Lizanecz et al. 2006). Indeed, using the anti-TRPV1-N antibody, TRPV1 was found to be abundantly expressed in all blood vessels within the gracilis muscle. Interestingly, the anti-TRPV1-C antibody staining was not positive in this tissue, suggesting that the anti-TRPV1-C antibody does not recognize vascular smooth muscle-located TRPV1; however, the antibody can detect TRPV1 in sensory neurons in western blotting and immunohistochemistry. This discrepancy in staining may lead one to argue that the vascular smooth muscle staining observed with the anti-TRPV1-N antibody is artifactual; however, there are many reasons why this is unlikely: (1) Vascular TRPV1 staining was blocked by the TRPV1-specific antigenic peptide (Fig. 8); (2) Vascular TRPV1 expression is in accordance with the constrictive effect of the TRPV1 agonist capsaicin. (Capsaicin-mediated vasoconstriction is absent in TRPV1$^{-/-}$ mice (Czikora et al. 2012), which strongly suggests that a capsaicin response is specific for TRPV1); (3) TRPV1 mRNA is present in the isolated arteriolar preparations (Fig. 1); and (4) Earlier reports by an independent group also showed functional arteriolar TRPV1 expression (Cavanaugh et al. 2011).

Assuming this staining to be specific, the goal of the present work was to study TRPV1 expression and function in isolated arteries from a set of rat tissue samples, using the anti-TRPV1-C antibody as a TRPV1 expression marker in vascular tissue. There were several important observations. First, it appears that the TRPV1 is not uniformly expressed in the vascular tissue, with TRPV1 only expressed in a subset of blood vessels in some tissues (in particular, mesenteric arteries and skin). The observed differences in TRPV1 staining within the same tissue sections suggest a complex regulation of TRPV1 expression at the level of the individual vessels. Another surprising observation was the wide range of functional responses of the TRPV1-positive (anti-TRPV1-N antibody) arteries. Whereas arteries from the gracilis muscle responded to capsaicin with a robust constriction—which was

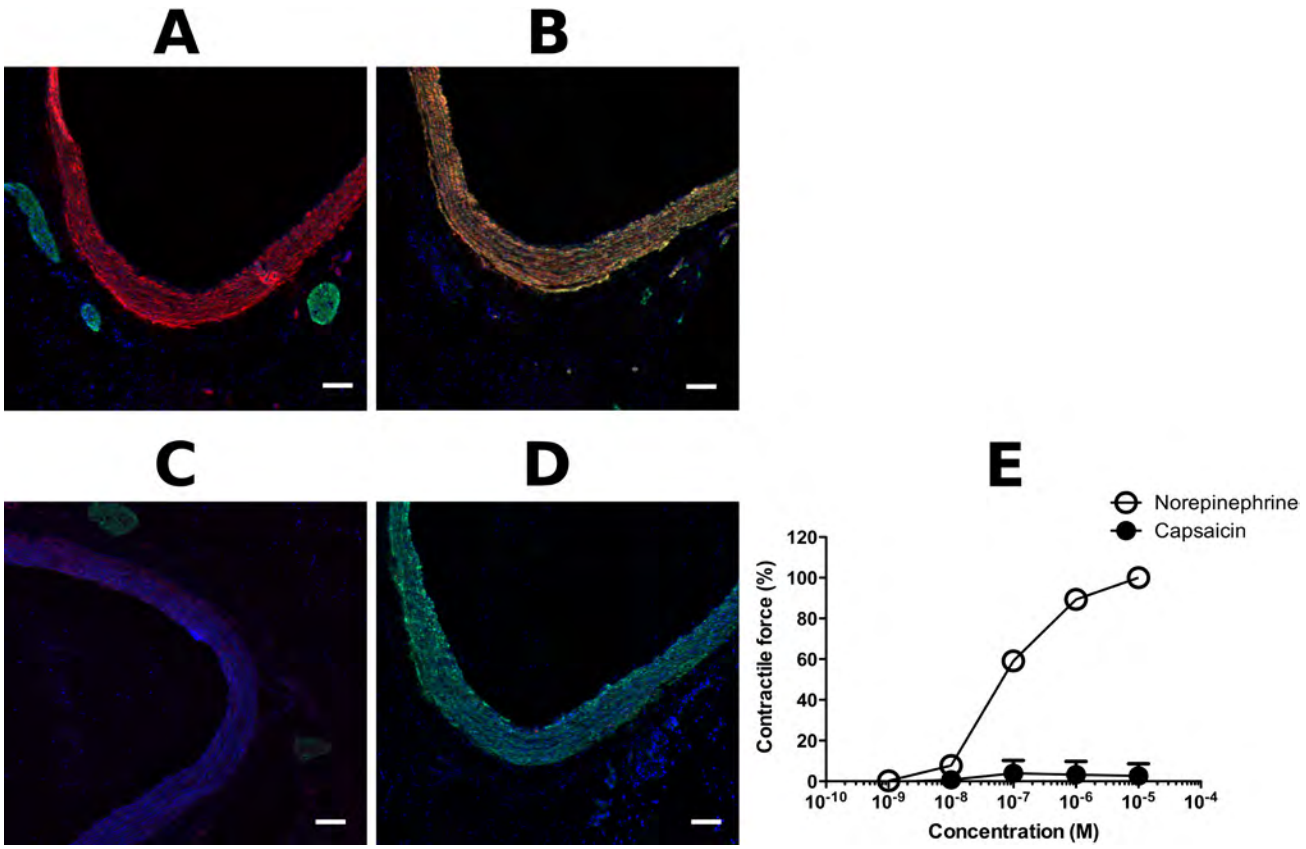

Figure 11. Expression of TRPV1 in the aorta. Rat aorta tissue sections were probed with anti-TRPV1-N (red; A and B) or anti-TRPV1-C (red; C and D), and anti-neurofilament (green; A and C) or anti-smooth muscle actin (green, B and D), and counterstained with DAPI (blue). (E) Contractions to capsaicin and norepinephrine were tested in an isometric contractile force measurement system. Data are the mean ± SEM of six independent experiments. Asterisks indicate significant differences as compared with the initial (before treatment) contractile forces. Bars represent 100 µm.

comparable to that of those evoked by norepinephrine (representing the maximal physiological vasoconstriction in this particular case)—other arteries (e.g., the carotid artery) had a limited functional TRPV1 response, even if an apparently high level of TRPV1 expression was found. Moreover, some of the arteries expressing TRPV1 did not contract upon capsaicin supplementation (femoral and mesenteric arteries and aorta).

These apparent contrasts between TRPV1 function and expression may be explained by many factors. It is possible that TRPV1 expression is regulated at the cellular level. One of the observations supporting this hypothesis is that only a portion of isolated coronary smooth muscle cells responded to capsaicin by increasing intracellular Ca^{2+} concentrations (Czikora et al. 2012). Another possibility is that TRPV1 expression is regulated at the level of the individual blood vessel (Cavanaugh et al. 2011). This is supported by the staining patterns in this study that showed uniform staining in the smooth muscle layer in a given blood vessel; although, some of the blood vessels were stained whereas others were not, even within the same tissue slice. It needs to be mentioned that this vessel-specific staining pattern has also been reported earlier with genetically engineered mice, where TRPV1 was genetically labeled with a fluorescent protein; however, the same group was not able to stain unmodified TRPV1 in the same location (Cavanaugh et al. 2011). Finally, it is also possible that the activity of vascular TRPV1 is controlled by posttranslational modifications. In this case, the physiological activity of vascular TRPV1 may be regulated by sensitization-desensitization of the receptor. Indeed, previous work demonstrates that vascular TRPV1 can be desensitized via a process involved the activation of the Ca^{2+}-dependent phosphatase, calcineurin (Lizanecz et al. 2006). An alternative explanation for the differences in the arteriolar response to capsaicin (in the case of the arteries of the gracilis muscle, as well as

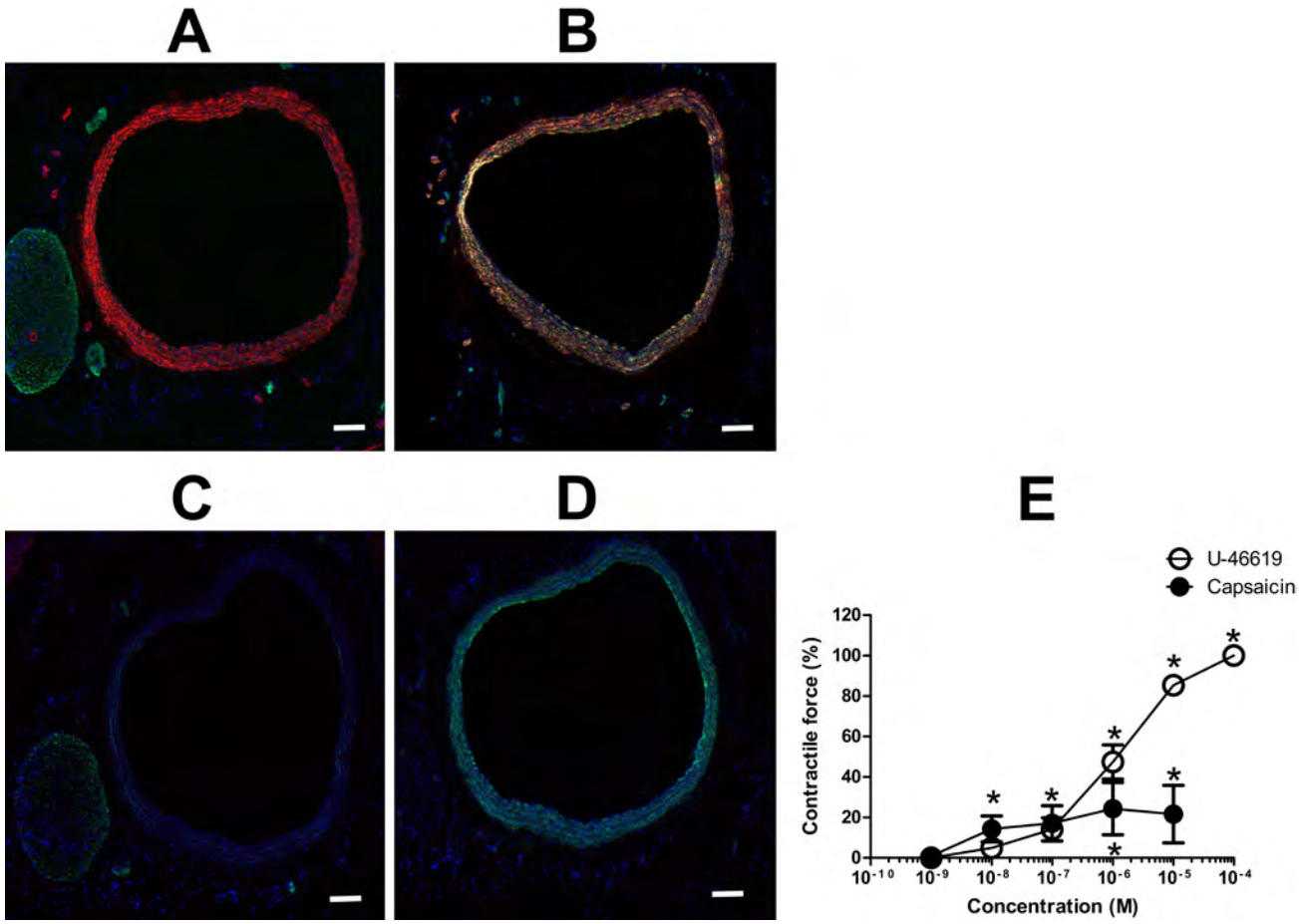

Figure 12. Expression of TRPV1 in the carotid artery. Cryostat sections were prepared from the carotid artery of the rat (10 μm) and were stained using anti-TRPV1-N (A and B) or anti-TRPV1-C (C and D) antibodies (red). Sections were also co-stained with antibodies against neurofilament (green; A and C) or smooth muscle actin (green; B and D). The same arteries were isolated and mounted on an isometric (ring) setup. (E) Concentration-responses to capsaicin and to U-46619 (a thromboxane A2 receptor agonist). Data are the mean ± SEM of eight independent experiments. Asterisks indicate significant differences as compared with the initial (before treatment) contractile forces. Bars represent 100 μm.

the femoral and carotid arteries and aorta) may be the existence of different TRPV1 isoforms. All of the preparations showed strong staining with the anti-TRPV1-N antibody. Nonetheless, at least three different TRPV1 splice variants have been suggested, which have a low sensitivity for agonists (such as the capsaicin used here) (Eilers et al. 2007; Tian et al. 2006; Vos et al. 2006; Wang et al. 2004). Moreover, these splice variants may associate with the dominant (functional) form of the TRPV1, and inhibit its activity (without affecting its apparent expression when tested by immunohistochemistry). Here, we performed a morphological study, in which we found striking differences in the TRPV1 staining pattern within arteries in close proximity (on the same tissue section) and showed that large arteries with apparently similar TRPV1 expression have strikingly different capsaicin sensitivity. Further studies are required to identify the reasons for these differences.

Regardless of the complicated regulation, the main question for this study was the functional role of TRPV1 in vascular biology. TRPV1-mediated vasoconstriction was reported three decades ago. Donnerer and Lembeck (1982) described that capsaicin evokes a three-phase response in the rat, with the second phase described as a vasoconstrictive response that was independent of sensory innervation (Donnerer and Lembeck 1982). Later, Duckles also described the direct effect of capsaicin on vascular smooth muscle cells (Duckles 1986). The presence of TRPV1 in vascular tissue was further confirmed after the identification of its gene. TRPV1 staining in the smooth muscle layer of epineurial arteries, together with a contractile response to capsaicin and resiniferatoxin, was also noted previously (Davidson et al. 2006), and recently, functional TRPV1 expression in the smooth muscle cells of intrapulmonary arteries was related to pulmonary hypertension (Martin et al. 2012). In addition to the confirming these

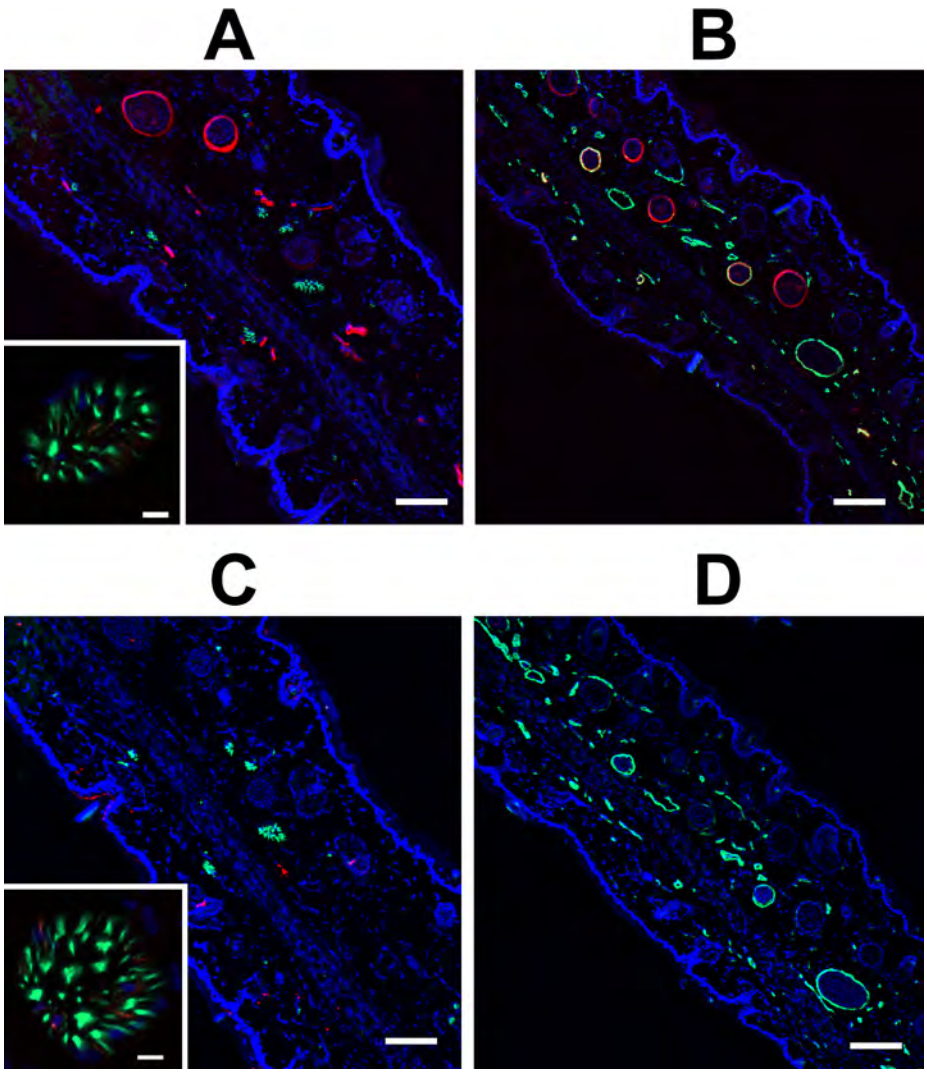

Figure 13. Expression of TRPV1 in the skin. Immunohistochemistry was performed in the skin from the hindpaw of the rat. Sections were stained with anti-TRPV1-N (red, A and B) or anti-TRPV1-C (red, C and D), and anti-neurofilament (green, A and C) or anti-smooth muscle actin (green, B and D), and counterstained with DAPI (blue). Colocalization of TRPV1-positive neurites with anti-neurofilament is shown in the insets at a higher magnification. Bars, 100 μm; inset bars,10 μm.

earlier results, our data show that arteriolar TRPV1 expression is tightly regulated (arteries within a couple of micrometers show high or undetectable level of TRPV1 expression) and that TRPV1 responses are suppressed in some cases, in spite of uniformly high TRPV1 expression.

Our data provide evidence that TRPV1 represents another significant vascular TRP channel, and suggest that TRPV1 is in its sensitized state in some skeletal muscle arteries (such as those isolated from the gracilis muscle) and in the coronary arteries (Czikora et al. 2012), but it is inhibited in other blood vessels. It is also known that TRPV1 stimulation has divergent effects in vivo: it may evoke neurogenic vasodilation (e.g., in the skin) or vascular constrictions (e.g., in the skeletal muscle) (Kark et al. 2008). These divergent effects suggest that the systemic regulation of TRPV1 may be an effective tool to regulate blood distribution between tissues. Moreover, these divergent effects are in accordance with the immunohistochemical data presented here. It is expected that arteries with sensory neuronal innervation, but without vascular TRPV1 expression (such as blood vessels in the skin; Fig. 13), respond to TRPV1 stimulation by dilation. In contrast, arteries with high smooth muscle TRPV1 expression and without apparent sensory neuronal innervation (such as the gracilis artery; Fig. 8) are expected to respond to the same TRPV1 activation by constriction. This work adds an important addition to this hypothesis in that TRPV1 expression in the arteries appears to not be necessarily functionally active. Indeed, we show that although TRPV1 is expressed in the large arteries, the activity of this receptor appears to be suppressed.

Taken together, this study made an effort to investigate the functional expression of TRPV1 in the rat. We found that TRPV1 expression in the vascular smooth muscle is regulated at the level of the individual blood vessels: some blood vessels showed intense TRPV1 immunostaining, whereas nearby vessels were negative. Moreover, the activity of the smooth muscle-expressed TRPV1 appeared to be suppressed in some cases. Nonetheless, TRPV1 was found to be widely expressed in the vasculature rat, suggesting a physiological role for these cation channels in vascular biology.

Declaration of Conflicting Interests

The author(s) declared no potential conflicts of interest with respect to the research, authorship, and/or publication of this article.

Funding

The author(s) disclosed receipt of the following financial support for the research, authorship, and/or publication of this article: The work is supported by the TAMOP-4.2.2/B-10/1-2010-0024 and TÁMOP 4.2.2.A-11/1/KONV-2012-0045 (to IÉ, ZP and AT), TÁMOP-4.2.2.A-11/1/KONV-2012-0025 (to PB) projects. These projects are implemented through the New Hungary Development Plan, co-financed by the European Social Fund. In addition, the study was supported by the Hungarian Academy of Sciences OTKA (K84300 to AT and PD83473 to PB) and Bolyai János Research Fellowship (to AT and PB), by the National Office for Research and Technology (Baross Gábor ÉletMent (to AT) and Seahorse (to PB) grants) and by the University of Debrecen (Mec-8/2011 to PB).

References

Bai P, Houten SM, Huber A, Schreiber V, Watanabe M, Kiss B, de Murcia G, Auwerx J, Ménissier-de Murcia J (2007). Poly(ADP-ribose) polymerase-2 controls adipocyte differentiation and adipose tissue function through the regulation of the activity of the retinoid X receptor/peroxisome proliferator-activated receptor-gamma heterodimer. J Biol Chem 282:37738-37746.

Baylie RL, Brayden JE (2011). TRPV channels and vascular function. Acta Physiol 203:99-116.

Cavanaugh DJ, Chesler AT, Jackson AC, Sigal YM, Yamanaka H, Grant R, O'Donnell D, Nicoll RA, Shah NM, Julius D, Basbaum AI (2011). Trpv1 reporter mice reveal highly restricted brain distribution and functional expression in arteriolar smooth muscle cells. J Neurosci 31:5067-5077.

Czikora Á, Lizanecz E, Bakó P, Rutkai I, Ruzsnavszky F, Magyar J, Pórszász R, Kark T, Facskó A, Papp Z, Edes I, Tóth A (2012). Structure-activity relationships of vanilloid receptor agonists for arteriolar TRPV1. Br J Pharmacol. 165:1801-1812.

Davidson EP, Coppey LJ, Yorek MA (2006). Activity and expression of the vanilloid receptor 1 (TRPV1) is altered by long-term diabetes in epineurial arterioles of the rat sciatic nerve. Diabetes Metab Res 22:211-219.

Donnerer J, Lembeck F (1982). Analysis of the effects of intravenously injected capsaicin in the rat. Naunyn Schmiedebergs Arch Pharmacol 320:54-57.

Duckles SP (1986). Effects of capsaicin on vascular smooth muscle. Naunyn Schmiedebergs Arch Pharmacol 333:59-64.

Eilers H, Lee S-Y, Hau CW, Logvinova A, Schumacher MA (2007). The rat vanilloid receptor splice variant VR.5'sv blocks TRPV1 activation. Neuroreport 18:969-973.

Gavva NR (2008). Body-temperature maintenance as the predominant function of the vanilloid receptor TRPV1. Trends Pharmacol Sci 29:550-557.

Holzer P (2008). The pharmacological challenge to tame the transient receptor potential vanilloid-1 (TRPV1) nocisensor. Brit J Pharmacol 155:1145-1162.

Kark T, Bagi Z, Lizanecz E, Pásztor ET, Erdei N, Czikora Á, Papp Z, Edes I, Pórszász R, Tóth A (2008). Tissue-specific regulation of microvascular diameter: opposite functional roles of neuronal and smooth muscle located vanilloid receptor-1. Mol Pharmacol 73:1405-1412.

Lizanecz E, Bagi Z, Pásztor ET, Papp Z, Edes I, Kedei N, Blumberg PM, Tóth A (2006). Phosphorylation-dependent desensitization by anandamide of vanilloid receptor-1 (TRPV1) function in rat skeletal muscle arterioles and in Chinese hamster ovary cells expressing TRPV1. Mol Pharmacol 69:1015-1023.

Martin E, Dahan D, Cardouat G, Gillibert-Duplantier J, Marthan R, Savineau J-P, Ducret T (2012). Involvement of TRPV1 and TRPV4 channels in migration of rat pulmonary arterial smooth muscle cells. Pflug Arch Eur J Phy 464:261-272.

Szallasi A, Blumberg PM (1999). Vanilloid (Capsaicin) receptors and mechanisms. Pharmacol Rev 51:159-212.

Szallasi A, Sheta M (2012). Targeting TRPV1 for pain relief: limits, losers and laurels. Expert Opin Investig Drugs 21:1351-1369.

Tian W, Fu Y, Wang DH, Cohen DM (2006). Regulation of TRPV1 by a novel renally expressed rat TRPV1 splice variant. Am J Physiol Renal 290:F117-126.

Tominaga M, Caterina MJ, Malmberg AB, Rosen TA, Gilbert H, Skinner K, Raumann BE, Basbaum AI, Julius D (1998). The cloned capsaicin receptor integrates multiple pain-producing stimuli. Neuron 21:531-543.

Toth A, Boczan J, Kedei N, Lizanecz E, Bagi Z, Papp Z, Edes I, Csiba L, Blumberg PM (2005). Expression and distribution of vanilloid receptor 1 (TRPV1) in the adult rat brain. Brain Res Mol Brain Res 135:162-168.

Vos MH, Neelands TR, McDonald HA, Choi W, Kroeger PE, Puttfarcken PS, Faltynek CR, Moreland RB, Han P (2006). TRPV1b overexpression negatively regulates TRPV1 responsiveness to capsaicin, heat and low pH in HEK293 cells. J Neurochem 99:1088-1102.

Wang C, Hu H-Z, Colton CK, Wood JD, Zhu MX (2004). An alternative splicing product of the murine trpv1 gene dominant negatively modulates the activity of TRPV1 channels. J Biol Chem 279:37423-7430.

Zygmunt PM, Petersson J, Andersson DA, Chuang H, Sørgård M, Di Marzo V, Julius D, Högestätt ED (1999). Vanilloid receptors on sensory nerves mediate the vasodilator action of anandamide. Nature 400:452-457.

OPEN ACCESS Freely available online

PLOS ONE

Different Desensitization Patterns for Sensory and Vascular TRPV1 Populations in the Rat: Expression, Localization and Functional Consequences

Ágnes Czikora[1], Ibolya Rutkai[1], Enikő T. Pásztor[1], Andrea Szalai[2], Róbert Pórszász[2], Judit Boczán[3], István Édes[1,4], Zoltán Papp[1,4], Attila Tóth[1,4]*

1 Division of Clinical Physiology, Institute of Cardiology, University of Debrecen, Debrecen, Hungary, **2** Department of Pharmacology and Pharmacotherapy, Institute of Pharmacology, University of Debrecen, Debrecen, Hungary, **3** Deparment of Neurology, University of Debrecen, Debrecen, Hungary, **4** Research Centre for Molecular Medicine, Medical and Health Science Center, University of Debrecen, Debrecen, Hungary

Abstract

Background and purpose: TRPV1 is expressed in sensory neurons and vascular smooth muscle cells, contributing to both pain perception and tissue blood distribution. Local desensitization of TRPV1 in sensory neurons by prolonged, high dose stimulation is re-engaged in clinical practice to achieve analgesia, but the effects of such treatments on the vascular TRPV1 are not known.

Experimental approach: Newborn rats were injected with capsaicin for five days. Sensory activation was measured by eye wiping tests and plasma extravasation. Isolated, pressurized skeletal muscle arterioles were used to characterize TRPV1 mediated vascular responses, while expression of TRPV1 was detected by immunohistochemistry.

Key results: Capsaicin evoked sensory responses, such as eye wiping (3.6 ± 2.5 versus 15.5 ± 1.4 wipes, $p<0.01$) or plasma extravasation (evans blue accumulation 10 ± 3 versus 33 ± 7 μg/g, $p<0.05$) were reduced in desensitized rats. In accordance, the number of TRPV1 positive sensory neurons in the dorsal root ganglia was also decreased. However, TRPV1 expression in smooth muscle cells was not affected by the treatment. There were no differences in the diameter (192 ± 27 versus 194 ± 8 μm), endothelium mediated dilations (evoked by acetylcholine), norepinephrine mediated constrictions, myogenic response and in the capsaicin evoked constrictions of arterioles isolated from skeletal muscle.

Conclusion and implications: Systemic capsaicin treatment of juvenile rats evokes anatomical and functional disappearance of the TRPV1-expressing neuronal cells but does not affect the TRPV1-expressing cells of the arterioles, implicating different effects of TRPV1 stimulation on the viability of these cell types.

Citation: Czikora Á, Rutkai I, Pásztor ET, Szalai A, Pórszász R, et al. (2013) Different Desensitization Patterns for Sensory and Vascular TRPV1 Populations in the Rat: Expression, Localization and Functional Consequences. PLoS ONE 8(11): e78184. doi:10.1371/journal.pone.0078184

Editor: Alexander G. Obukhov, Indiana University School of Medicine, United States of America

Received June 5, 2013; **Accepted** September 9, 2013; **Published** November 8, 2013

Funding: The work is supported by the TÁMOP 4.2.2.A-11/1/KONV-2012-0045 project (to IÉ, ZP and AT, National Development Agency, http://www.nfu.hu/?lang=en). This project is implemented through the New Hungary Development Plan, co-financed by the European Social Fund. In addition, the study was supported by the Hungarian Academy of Sciences OTKA (K84300 to AT, RP, http://www.otka.hu/en) and Bolyai János Research Fellowship (to AT, http://mta.hu/english/) and by Baross Gábor ÉletMent grant by the National Office for Research and Technology, Hungary (http://www.nih.gov.hu/english). The funders had no role in study design, data collection and analysis, decision to publish, or preparation of the manuscript.

Competing Interests: The authors have declared that no competing interests exist.

* E-mail: atitoth@med.unideb.hu

Introduction

The therapeutic potential of TRPV1 modulation in various painful states has been recognized in a series of publications some 40 years ago [1–4]. In these early works capsaicin specific responses were related to a specific receptor, which could be desensitized by the application of high dose of capsaicin at an early phase of the life of the rat. These robust changes in sensory function led to the recognition of pharmacological approach to manipulate nociceptors [5]. Capsaicin desensitization therefore become a powerful approach to characterize peripheral nociceptors and to achieve topical analgesia. Although molecular identification of the receptor responsible for capsaicin mediated responses [6] resulted in a rise in therapeutic interest in systemic TRPV1 modulation to inhibit the pain pathway, no successful antagonists were introduced to the market [7], probably due to the unfavorable side effects of the systemic treatment [8]. On the other hand, local capsaicin desensitization recently re-emerged as a therapeutic method to selectively defunctionalize capsaicin expressing sensory neurons and to achieve local analgesia [9,10].

TRPV1 regulates cellular Ca^{2+} levels via direct permeation ($P_{Ca}/P_{Na}\sim10$) [6], which concomitantly down-regulates its own activity. Among the Ca^{2+}-activated enzymes that are believed to play pivotal roles in this TRPV1 acute desensitization process is the Ca^{2+}/calmodulin-dependent Ser/Thr phosphatase 2B, calcineurin [11–13], which dephosphorylates TRPV1 receptors. Conversely, phosphorylations at several consensus sites for protein kinase C (PKC) [14–16] and cAMP-dependent protein kinase A

(PKA) [17,18] can reduce the Ca^{2+}- mediated desensitization of TRPV1. Thus, the dynamic balance between the Ca^{2+}-dependent phosphorylation and dephosphorylation of the TRPV1 protein appears to play a critical role in the acute desensitization of TRPV1 [12].

In contrast with the acute desensitization, neonatal capsaicin treatment results in the deletion of TRPV1 expressing peripheral sensory neurons [19,20]. Capsaicin evoked sensory neuronal cell death may be mediated by Ca^{2+} overload of the TRPV1 expressing cells [21].

Activation of TRPV1 leads to central (pain) and to local "sensory-efferent" effects [22]. These include the release of vasoactive agents (such as calcitonin gene-related peptide) from sensory neurons and subsequent vasorelaxation [23]. In recent years, TRPV1 expression has been identified in many cells types in addition to sensory neurons as referenced by Keeble et al in recent reviews [24,25]. In particular, TRPV1 expression was detected in various cell types in the brain [26], and in arteriolar smooth muscle [27]. In accordance with this latter non-neuronal localization, activation of TRPV1 resulted in a substantial vasoconstriction *in vivo* and *in vitro* [27,28] through direct activation of endogenous TRPV1 in vascular smooth muscle cells [29].

The effects of capsaicin desensitization were investigated here. Capsaicin desensitization is the only clinically available, approved and effective treatment option to regulate TRPV1 mediated sensory functions. Since functional TRPV1 expression has been identified in non-neuronal cells, these receptors may have physiological functions which may also be modulated by therapeutic capsaicin applications. Morphological and functional studies were performed to reveal differences between desensitization of sensory neurons and vascular smooth muscle cells. Our data suggest that capsaicin desensitization has only a transient effect on the vascular TRPV1. Therefore, vascular TRPV1 function is maintained even if the same treatment depletes sensory neurons.

Methods

Animals, anaesthesia and general preparation in the *in vivo* experiments

Male Wistar Kyoto (WKY/NCrl) rats obtained from Charles River (Isaszeg, Hungary) were fed by CRLT/N chow (Szinbad Kft, Godollo, Hungary). Experiments were performed on male Wistar rats weighing about 250 g at the beginning of the experiments raised on a standard laboratory food and water *ad libitum*. Anaesthesia was performed with 50 mg/kg i.p. thiopental. Animal experiments were carried out and approved by the Hungarian Ministry of Rural Development and by the University of Debrecen, Medical and Health Science Center (Registration number: 31/2007/DE MÁB), and were in accordance with the standards established by the National Institutes of Health.

Capsaicin pretreatment of rats

Newborn rats (at day 14 of life) were pretreated with Diaphyllin (Richter, Hungary), Bricanyl (Astra Zeneca, Hungary), and atropine (Egis, Hungary, 100 g/0,1 ml i.p.). Ten minutes later animals were injected with capsaicin (subcutaneously). The procedure was repeated for a total of five consecutive days. The total dose of capsaicin was 300 mg/kg, administered on a dose schedule of 10 mg/kg, 20 mg/kg; 50 mg/kg; 100 mg/kg; and 120 mg/kg on days 1 through 5, respectively. Rats were then kept in the animal facility for 10 weeks when experiments were performed. The weight of the rats was in the range of 360–492 g at this time.

Measurement of capsaicin evoked sensory irritation

One drop (10 μl) of capsaicin solution (50 μg/ml in physiological saline) was put into the right or left conjunctiva of the rat, in a random order. The number of eye wipes was counted during 60 s. Rats were scarified after capsaicin treatments.

Measurement of capsaicin evoked involuntary sensory neuronal functions

Plasma extravasation was measured according to Pinter et al. [30]. Rats were anesthetised and a tail vein was cannulated for the injection of Evans blue dye (30 mg/kg). One min after Evans blue administration capsaicin was injected (1 mg/kg, i.v.). Rats was sacrificed by transcardiac perfusion with 50 ml of 0.9% w/v saline, at 37°C, through the left cardiac ventricle 10 min after injection of Evans blue. The urinary bladder was removed and weighed, and the Evans blue was extracted in 1 ml of formamide for 24 h. Evans blue content was determined by spectrophotometry (at 620 nm). Plasma extravasation was expressed as the content of Evans blue dye in micrograms per gram of wet tissue.

Preparation of cannulated skeletal muscle arterioles

Isolation of the skeletal (gracilis) muscle arterioles of the rat and diameter measurement of the arterioles were performed as described earlier [12]. The internal diameters of the cannulated skeletal muscle (m. gracilis) arterioles were determined at the midpoint of the arteriolar segment by videomicroscopy. Cannulated arterioles were incubated in a physiological solution (PSS, composition in mM: 110 NaCl, 5.0 KCl, 2.5 $CaCl_2$, 1.0 $MgSO_4$, 1.0 KH_2PO_4, 5.0 glucose and 24.0 $NaHCO_3$ equilibrated with a gas mixture of 10% O_2 and 5% CO_2, 85% N_2, at pH 7.4.). Experiments were started after the development of a spontaneous tone in response to intraluminal pressure of 80 mmHg. First, acetylcholine (1 nM–10 μM) was used to determine dilatative capacity (acetylcholine causes endothelium dependent vasodilatation), and then norepinephrine (1 nM–10 μM) was applied to measure maximal constrictive response (norepinephrine causes smooth muscle dependent constriction). Vascular autoregulation (myogenic response) were also determined. Intraluminal pressure was increased from 20 to 120 mmHg in 20 mmHg increments and arteriolar diameter was measured after 4 min incubations at each intraluminal pressures. These measurements were performed in PSS to assess the active myogenic response. Passive diameter was determined in Ca^{2+} free PSS at the end of the experiments. Changes in diameter in response to a TRPV1 agonist was tested with cumulative dose (capsaicin, 1 nM–30 μM).

Immunohistochemical procedures

Tissue sections were prepared as detailed earlier [27]. In short, rat skeletal muscle (m. gracilis), dorsal root ganglions (thoracic) were dissected from Wistar rats and were embedded in Tissue-Tek O.C.T compound (Electron Microscopy Sciences, Hatfield, PA, USA). Cryostat sections (thickness 10 μm) were placed on adhesive slides and fixed in acetone for 10 min. The slices were blocked with normal goat sera (1.5% in PBS, Sigma, St. Louis, MO, USA) for 20 min and stained with an anti-capsaicin receptor antibody (PC 547 (rabbit), Calbiochem, San Diego, CA) at a 1:500 (for gracilis muscle) and 1:200 dilution (for dorsal root ganglia), and co-stained with smooth muscle actin antibody (NCL-SMA, dilution, 1:50; Novocastra Laboratories, New Castle, UK) or with a neurofilament-specific antibody (dilution, 1:50; Sigma) in the blocking buffer. Then, the slices were incubated with biotinylated anti-rabbit (Jackson, Suffolk, England, 1:200) and FITC conjugated anti-mouse antibodies (Jackson, Suffolk, England, 1:100).

Biotinylated antiobody was detected by Cy3 conjugated streptavidine (Jackson, Suffolk, England, 1:500). The pictures were captured by a Scion Corporation (Frederick, MA) digital camera attached to a Nikon Eclipse 80i fluorescent microscope (Nikon, Tokyo, Japan) further processed by ImageJ (freeware from www.nih.gov) software.

Materials and solutions

Chemicals were from Sigma-Aldrich (St. Louis, MO, USA). Capsaicin (8-Methyl-N-vanillyl-*trans*-6-nonenamide) was dissolved in ethanol. Norepinephrine and acetylcholine were dissolved in distilled water. Evans Blue concentration was measured by using a NOVOstar plate reader.

Data analysis and statistical procedures

Arteriolar diameter was determined by measuring the distances between the intraluminal sides of the arteriolar wall (inner diameter). Data are shown as average diameter ± S.E.M. Statistical analysis was made by Microsoft Excel using Student's t-tests. P-values$<$0.05 were considered to be significant.

Results

Effects of desensitization on capsaicin-evoked eye-wiping movements

Sensory irritation was assessed by eye wiping assays. Capsaicin evoked a high number of wiping movements in control rats (15.5±1.4 wiping movements, n = 10), while desensitized rats (neonatal capsaicin application) were almost insensitive to the same treatment (3.6±2.5 wipes, n = 10; p$<$0,001, Fig. 1A).

Effects of desensitization on capsaicin – induced plasma extravasation

Systemic activation of TRPV1 expressing sensory neurons by capsaicin resulted in an increase in Evans blue accumulation in the urinary bladder of control rats (33±7 μg/g wet tissue; n = 9, Fig. 1B). Neonatal capsaicin desensitization significantly attenuated this response (Evans blue accumulation decreased to 10±3 μg/g wet tissue; n = 5, p = 0,03 versus control, Fig. 1B).

Immunochemistry of TRPV1

Dorsal root ganglia (DRG) were isolated from control and desensitized rats and TRPV1 expression was evaluated by immunohistochemistry. TRPV1 expression was found in a subset of neurons (neurons were visualized by neurofilament specific staining) in control rats but was missing in desensitized rats (Fig. 2). However, TRPV1 like immunostaining was also found in blood vessels associated with the DRGs, irrespective to the desensitization procedure. The localization of that TRPV1 expression to vascular smooth muscle cells was tested by the co-application of antisera against TRPV1 and vascular smooth muscle actin (Fig. 3). Indeed, some of the TRPV1 immunoreactivity overlapped with vascular smooth muscle specific staining. We thus find that, that while neonatal capsaicin treatment was found to be effective to eliminate TRPV1 immunoreactivity in sensory neurons, it was without effects on the vascular smooth muscle cell located TRPV1 immunoreactivity (Fig. 3). Similarly, TRPV1 expression was not affected by neonatal capsaicin treatment in the gracilis muscle of the rat (Fig. 4).

Physiological effects of neonatal capsaicin desensitization on isolated skeletal muscle arterioles

There were no significant differences between control and desensitized rats in acetylcholine mediated dilation (Fig. 5A), norepinephrine mediated constriction (Fig. 5B) and vascular

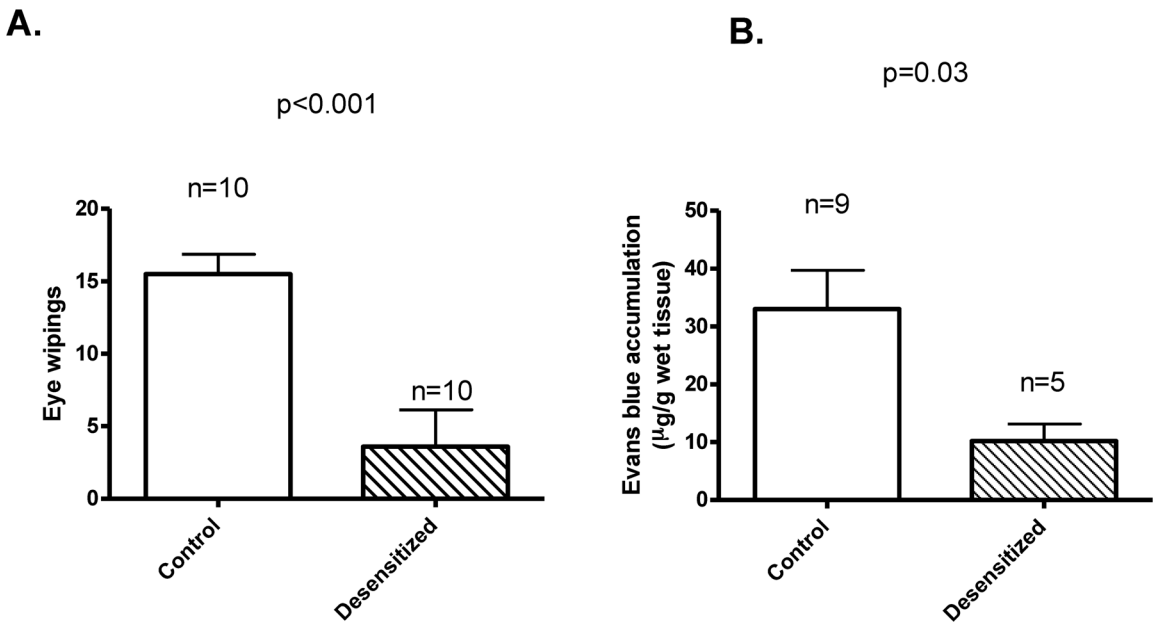

Figure 1. Effects of neonatal capsaicin desensitization on sensory functions. Rats were treated with saline (Control) or with capsaicin (Desensitized) at 14 days of life. Sensory functions were measured 10 weeks after capsaicin treatment. (A) Eye wiping (a measure of capsaicin evoked sensory irritation) was reduced in desensitized rats (n = 10 in both groups, p$<$0.001). (B) Plasma extravasation was similarly reduced (Evans blue accumulation, a measure of capsaicin mediated neurogenic inflammation) (n = 9 for Control and n = 5 for Desensitized, p = 0.03).
doi:10.1371/journal.pone.0078184.g001

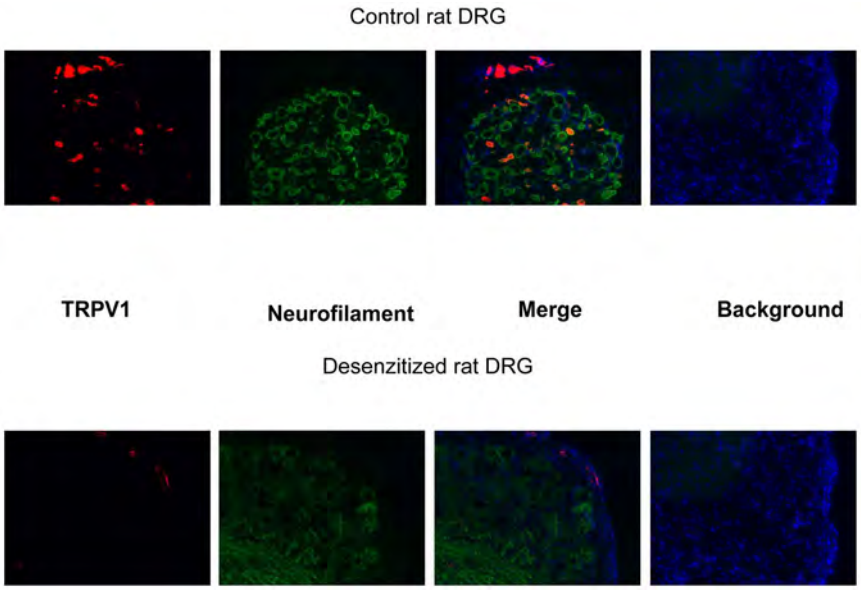

Figure 2. Effects of neonatal capsaicin desensitization on sensory TRPV1 expression. TRPV1 expression was examined in the dorsal root ganglia of control and capsaicin desensitized (neonatal capsaicin treatment) adult rats. Tissue sections were probed with antibodies specific to TRPV1 (red) and neurofilament (green). TRPV1 expression was present in a subset of sensory neurons in control rats, which was missing in desensitized rats within the dorsal root ganglia. However, TRPV1 immunoreactivity was also found in non-neuronal cell types, located at the outer regions of ganglia (regions occupied by sensory neurons are indicated by the freehand drawing). Images are representative of at least 10 sections.
doi:10.1371/journal.pone.0078184.g002

autoregulation (spontaneous myogenic response, Fig. 5C) in isolated skeletal muscle resistance arteries. Moreover, capsaicin mediated arteriolar constrictions were also unaffected in both groups of rats (Fig. 5D), which was in contrast with the capsaicin mediated sensory functions (Fig. 1).

Direct application of capsaicin (1 μmol/L) resulted in a transient constriction (maximal decrease of arteriolar diameter was 70±3% at 105 s) followed by a dilation in the continuous presence of capsaicin (constriction at the end of the 20 min long incubation was only 8±6%) (Fig. 6A). Besides to the acute desensitization (desensitization in the presence of the agonist) tachyphylaxis (desensitization to the repeated application of the agonist) was also determined. Although tachyphylaxis was apparent upon the second capsaicin challenge (first versus second treatment on Fig. 6A), capsaicin treatment did not eliminate capsaicin responsiveness completely (maximal constriction upon

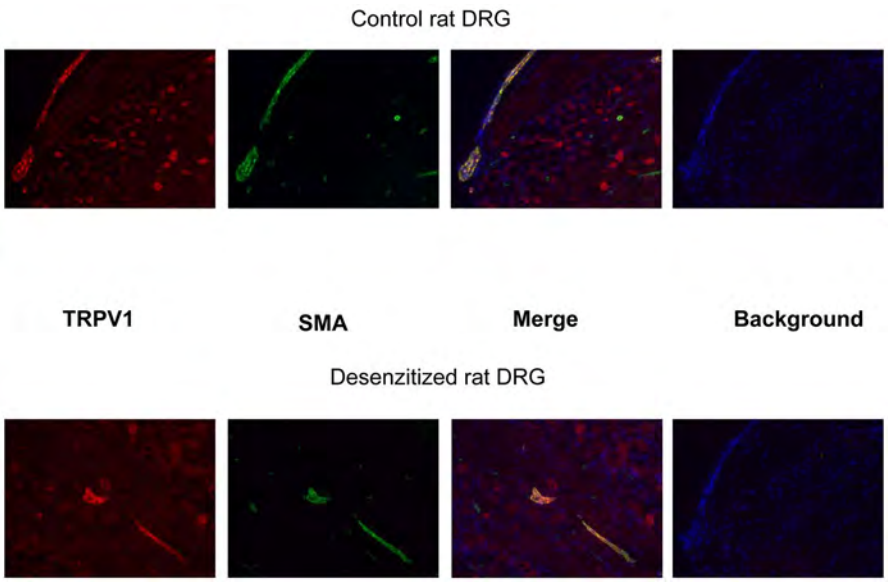

Figure 3. TRPV1 immunoreactivity in vascular smooth muscle cells. Rat dorsal root ganglia sections were co-stained by anti TRPV1 (red) and anti vascular smooth muscle actin (SMA, green) antibodies. Some of the TRPV1 positive cells were co-stained by the antibody specific to vascular smooth muscle actin, suggesting TRPV1 expression in this cell type. Moreover, vascular TRPV1 expression was not affected by neonatal capsaicin treatment (note similar TRPV1 staining in SMA positive regions of control and desensitized rats). Images are representative of at least 6 sections.
doi:10.1371/journal.pone.0078184.g003

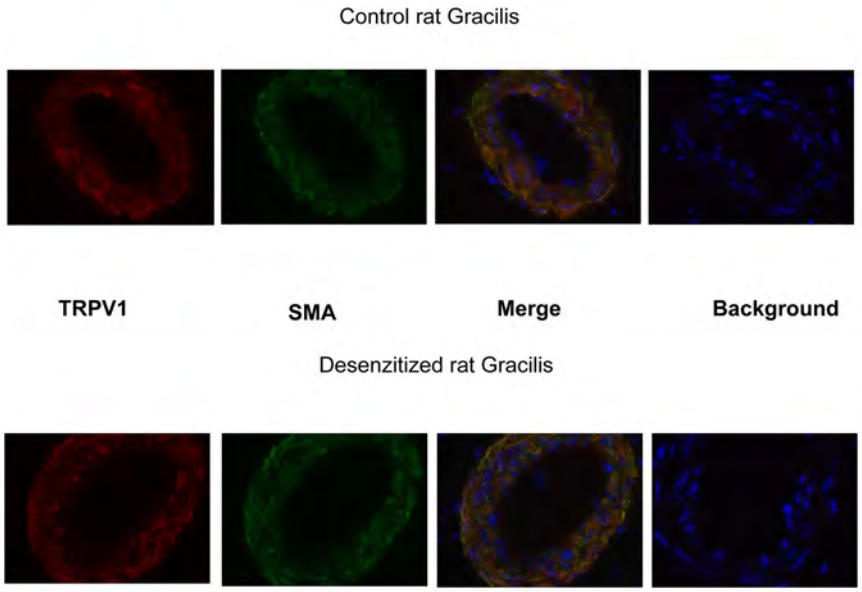

Figure 4. Effects of neonatal capsaicin desensitization on vascular TRPV1 expression. Skeletal muscle (gracilis muscle of the rat) tissue sections were stained with anti-TRPV1 (red) and anti-vascular smooth muscle actin (SMA, green) antibodies. There appeared a complete overlap of the staining patterns (merged images). Arteriolar TRPV1 expression was not affected by neonatal capsaicin desensitization, similarly to the vascular TRPV1 in the dorsal root ganglia. Images are representative of at least 10 sections.
doi:10.1371/journal.pone.0078184.g004

second capsaicin treatment was 26±9% at 270 s, while constriction was only 10±4% at the end of the 20 min long treatment, Fig. 6A). To test if capsaicin mediated desensitization may affect the viability of the different vascular cell types, smooth muscle (norepinephrine, Fig. 6B) and endothelium (acetylcholine, Fig. 6C) mediated responses were also tested. Norepinephrine mediated responses were almost identical (Fig. 6B), while the limited shift in acetylcholine responses (Fig. 6C) did not reach the level of significance ($p>0.05$), suggesting that acute *in vitro* TRPV1 desensitization did not have a significant effect of TRPV1 independent functions of skeletal muscle arterioles.

Discussion

Capsaicin containing herbs were used from the prehistoric era in the medicinal efforts to relieve pain and inflammation [31]. Capsaicin treatment was introduced to eliminate sensory responses about fifty years ago [3] and these experiments lead to the identification of primary nociceptors [5]. Cloning of the receptor (named as TRPV1) and the development of knock out models confirmed its role in inflammatory hyperalgesia [32]. It was even proposed that there are endogenous ligands (endovanilloids) binding to the capsaicin binding site of TRPV1 [23], although the physiological relevance of these proposed endovanilloids to modulate TRPV1 are still under debate, especially in skeletal muscle arterioles [33].

TRPV1 appeared to be a sensory neuronal specific receptor, which has a role in nociception and can be selectively targeted by small molecules. Not surprisingly, TRPV1 become a pharmaceutical target to develop a new generation of painkillers as well as to treat other therapeutic conditions [7]. Although almost all of the major pharmaceutical companies initiated a TRPV1 research program, these efforts have not yet produced approved drugs [34].

The apparent failure of introduction of TRPV1 antagonists into the clinical practice is probably not the result of insufficient potency of the developed antagonists [34]. Nonetheless, clinical application of the TRPV1 agonists capsaicin and resiniferatoxin offer an alternative to TRPV1 antagonists for treating challenging painful conditions such as neuropathic pain [10,35]. It is important to note that therapy to achieve desensitization is different from that based on the application of antagonists in terms of the potential side effects. Antagonists may cause side effects if their receptors play a significant physiological role, while desensitizing agonists may activate receptors which are expressed, but without much physiological role. Interestingly, while recent data suggested that TRPV1 may be expressed in other cell types than sensory neurons (see Keeble et al [24,25] for references and [36]), the potential side effects of capsaicin desensitization had not been tested on these receptors.

Selective elimination of TRPV1 positive sensory neurons and attenuation of capsaicin evoked sensory neuron mediated effects were found following systemic neonatal capsaicin treatment confirming earlier data [37,38]. Effects of this treatment on the vascular smooth muscle located TRPV1 was addressed here for the first time. It was found that neonatal capsaicin treatment does not affect arteriolar TRPV1 function and expression. It is in accordance with the limited if any permanent vascular effects of neonatal capsaicin desensitization.

It has been suggested that capsaicin has biphasic effects on the vasculature: at lower concentrations, capsaicin (up to 10 nM) evokes vasodilation in skin due to sensory nerve activation, while higher concentrations (0.1–1 μM) lead to substantial constrictions in skeletal muscle arterioles due to non-neuronal TRPV1 stimulation [27]. This apparent difference in sensitivity may be due to (i) receptor sensitivity or (ii) a difference in TRPV1 receptor density in skin and skeletal muscle arterioles as been concluded by Fernandes et al [25]. As the matter of the first hypothesis a recent study designed to detect pharmacological differences between TRPV1 populations in the sensory nerves and in the arteriolar smooth muscle proved that these TRPV1 populations are pharmacologically different: some TRPV1 agonists were irritative (a measure of sensory neuronal TRPV1 activation), but without

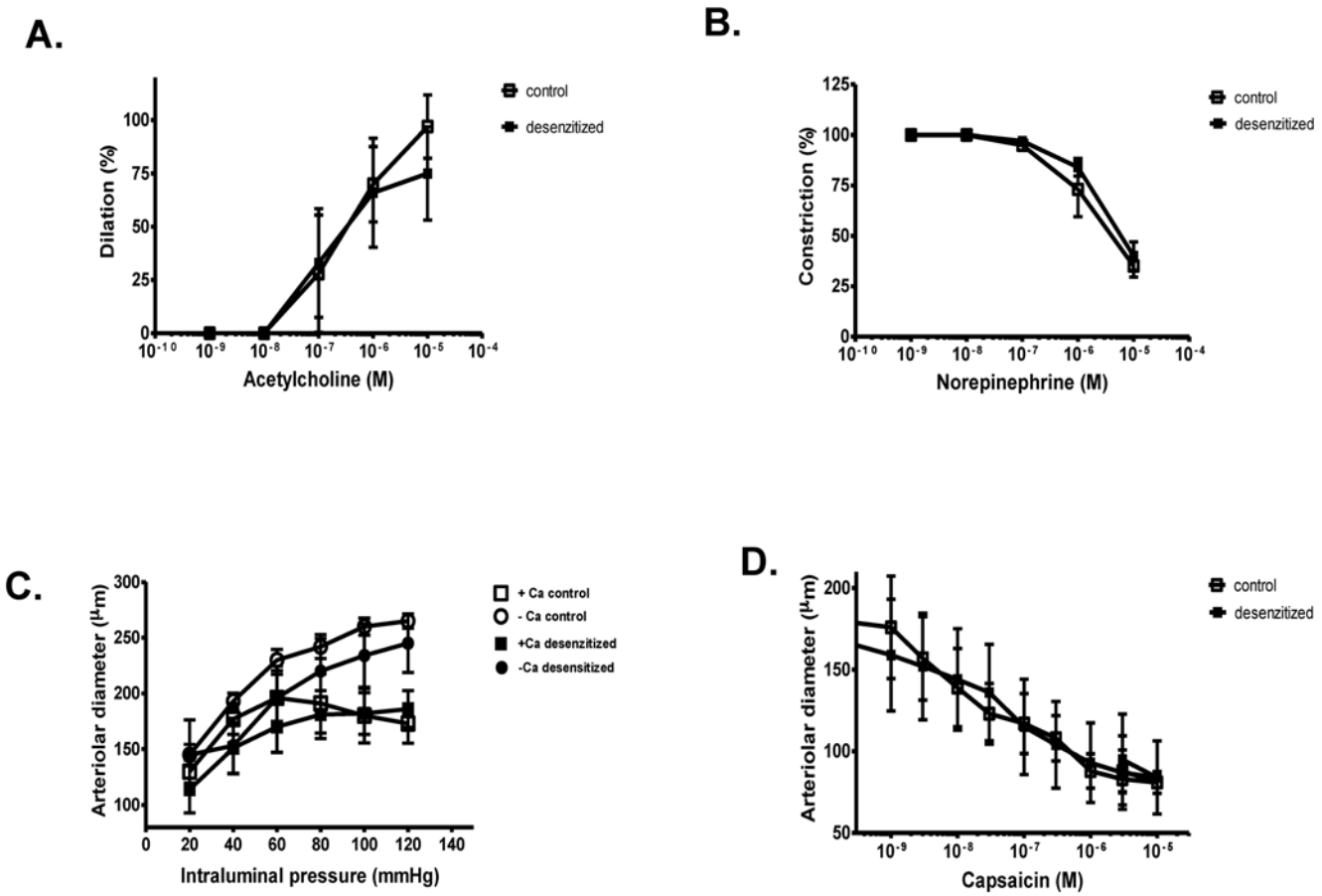

Figure 5. Functional effects of neonatal capsaicin desensitization on arteriolar TRPV1. Effects of neonatal capsaicin desensitization were characterized on the functional properties of isolated, cannulated skeletal muscle arterioles. Endothelial responses were tested by the application of acetylcholine (Panel A, values normalized to the maximal acetylcholine mediated dilations, symbols represent the mean ± SEM, n = 4 for the control and n = 4 for the desensitized). Smooth muscle functions were assessed by norepinephrine (Panel B, symbols represent the mean ± SEM of n = 4 determinations in both cases). The spontaneous myogenic tone (Panel C, symbols represent the mean ± SEM of n = 4 determinations for all groups) was tested by the contractile response developing in response to increasing intraluminal pressure (from 20 mmHg to 120 mmHg in 20 mmHg increments). Finally, capsaicin mediated responses were also tested by the cumulative application of the drug. Capsaicin evoked a dose-dependent constriction, supporting a physiological role for this receptor in vascular smooth muscle cells, which was not affected by the desensitization protocol (Panel D, symbols represent the mean ± SEM of n = 4 determinations for both groups).
doi:10.1371/journal.pone.0078184.g005

vasoconstrictive effects [29]. Capsaicin evoked vasoconstriction was mediated by direct activation of arteriolar smooth muscle located TRPV1 and was missing in TRPV1 knock out mice, suggesting that both the irritation (sensory neuronal response) and vasoconstriction (smooth muscle response) are mediated by TRPV1 [29]. As the matter of the second hypothesis (different expression of TRPV1 in perivascular nerves) a clear tissue specific difference was described. Arteries in the skin were densely innervated by TRPV1 positive fibers, in contrast with arteries in the skeletal muscle [27]. This fact suggests that sensory neuron mediated dilation plays a dominant role in the skin upon TRPV1 stimulation, but may have a limited effect in the skeletal muscle.

TRPV1 was found to be important in inflammation affecting arteriolar diameter. The most prominent contribution of TRPV1 stimulation to the neurogenic inflammation is the local release of neuropeptides (such as CGRP and substance P) from the sensory neurons [23], which is missing in capsaicin desensitized rats [5]. However, it was found recently, that TRPV1 stimulation also increases the plasma concentration of PACAP-38, an anti-inflammatory peptide [39], and somatostatin [40] suggesting a complex regulation of neurogenic inflammatory response, as summarized by Alawi and Keeble in an exemplary review [24]. These observations suggest that TRPV1 has a role in vascular inflammation. Chronic physiological activation of TRPV1 expressing sensory neurons may contribute to the inflammatory response and to painful effects such as hyperalgesia and allodynia [24]. In particular, diabetic rats showed increased TRPV1 function (while TRPV1 expression decreased) in the dorsal root ganglia [41], a feature which is similarly present in human diabetic patients [42]. This represents a local feedback regulating TRPV1 activity: TRPV1 activation causes a desensitization of the TRPV1 itself (limiting hyperalgesia and allodynia), which is mediated by decreased expression of TRPV1 in the tissues. This suggests that TRPV1 desensitization has an effect on tissue perfusion. In particular, diabetic or other kind of neuropathies result in a decrease in TRPV1 expressing sensory neurons, mediating vasodilation. As a result, patients with diabetes may have an impaired regulation of blood flow leading to the dominance of smooth muscle TRPV1 mediated vasoconstrictions over the physiological sensory neuronal TRPV1 mediated vasodilations. This altered vascular response may contribute to the progression of the disease in the skin.

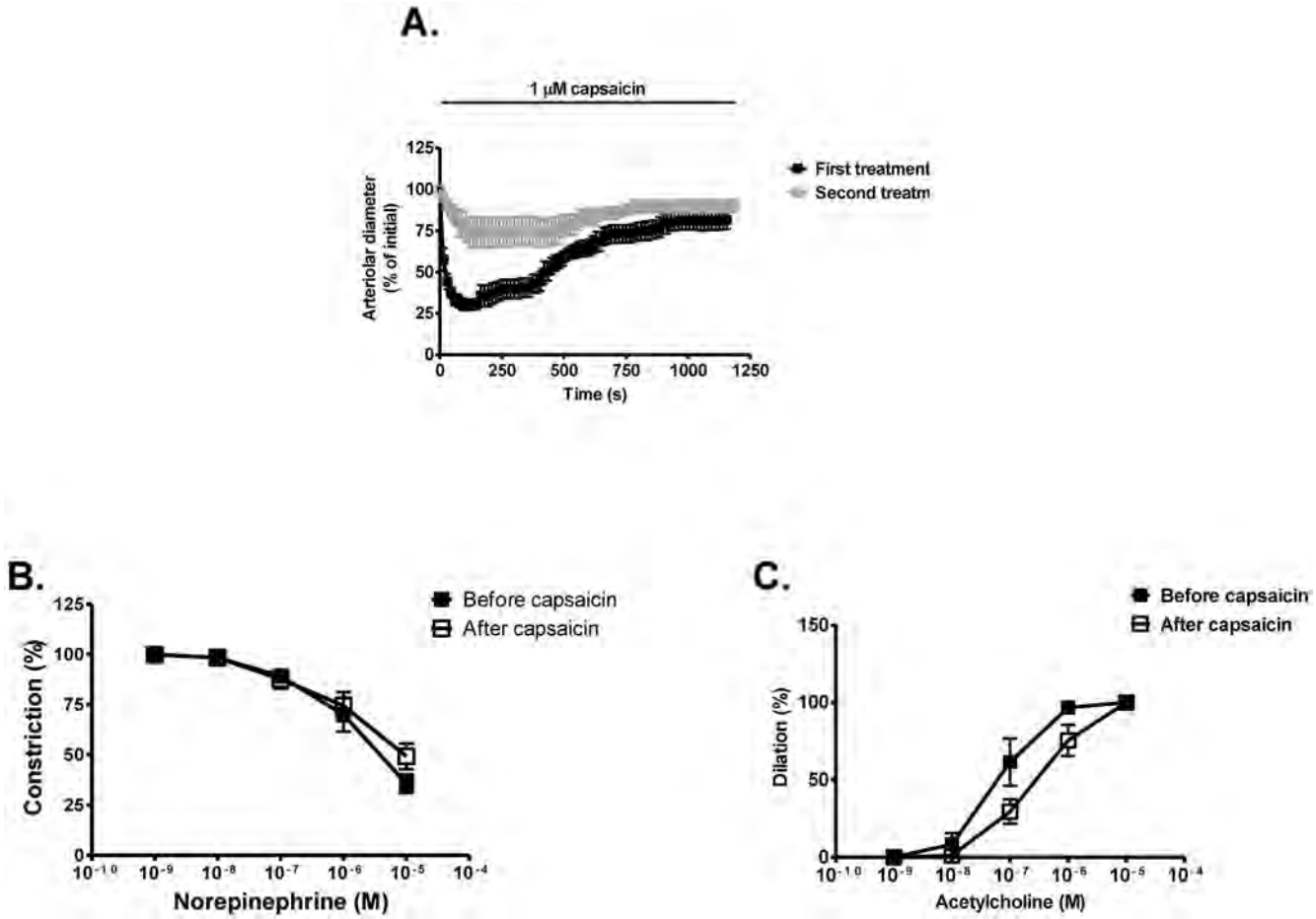

Figure 6. Functional effects of acute capsaicin desensitization on vascular TRPV1. The short-term effects of capsaicin were tested here. Arterioles were isolated from control rats and were treated with capsaicin (1 μM, First treatment). Capsaicin was washed away after the 20 min long treatment and the arterioles were incubated in the physiological buffer alone for 40 min (regeneration). Then capsaicin effects we re-tested (Second treatment) to estimate the level of tachyphylaxis (n = 6 arteries were tested, symbols represent the mean ± SEM of time-matched arteriolar diameter). Acute desensitization to capsaicin was apparent upon the first treatment (decrease and then increase in arteriolar diameter in the continuous presence of capsaicin, maximal decrease was 70±3% at 95 s after capsaicin application, Panel A). The magnitude of the response was decreased upon the second capsaicin treatment on the same arterioles (tachyphylaxis, decreased response to repeated capsaicin stimuli, maximal decrease was 27±9% at 125 s after capsaicin application, Panel A). This acute capsaicin desensitization (20 min treatment) did not affect norepinephrine mediated constrictions (symbols represent the mean ± SEM of n = 6 determinations, Panel B) or acetylcholine mediated dilations (symbols represent the mean ± SEM, n = 6, Panel C).
doi:10.1371/journal.pone.0078184.g006

The apparent difference between sensory neurons and vascular smooth muscle cells in response to high capsaicin stimulation (desensitization) described in this work may be explained by at least two mechanisms. First, vascular smooth muscle cells are able to proliferate, therefore the seriously damaged TRPV1 expressing cells may be replaced. Alternatively, capsaicin damage is less severe in vascular smooth muscle cells compared to sensory neurons. To test this latter possibility, isolated arteries were treated with capsaicin *in vitro*. Arteriolar TRPV1 was rapidly (within minutes) desensitized to capsaicin and capsaicin treatment did not affect TRPV1 independent functions, suggesting that capsaicin mediated Ca^{2+} toxicity did not occur in these cells.

We propose that vascular smooth muscle cells can be activated by the application of high doses of capsaicin, but the Ca^{2+} toxicity is limited by fast desensitization, in accordance with previous findings [12]. Vascular smooth muscle cells are therefore protected from prolonged capsaicin treatments and maintain their viability. These cells then are able to regenerate and regain capsaicin responsiveness (and probably their physiological role) within a short period of time. In contrast, sensory neurons seem to be eliminated and not replaced upon neonatal capsaicin treatment. Taken together, our data suggest that capsaicin desensitization is an effective method to specifically regulate sensory functions, in contrast with TRPV1 antagonists, which may affect vascular TRPV1 mediated processes in addition to sensory functions.

Acknowledgments

We thank Peter M. Blumberg for his invaluable comments and corrections.

Author Contributions

Conceived and designed the experiments: RP JB IÉ ZP AT. Performed the experiments: ÁC IR ETP AS AT. Analyzed the data: ÁC ETP JB AT. Wrote the paper: ÁC AT.

References

1. Jancso-Gabor A, Szolcsanyi J, Jancso N (1970) Stimulation and desensitization of the hypothalamic heat-sensitive structures by capsaicin in rats. J Physiol 208: 449–459.
2. Jancso-Gabor A, Szolcsanyi J, Jancso N (1970) Irreversible impairment of thermoregulation induced by capsaicin and similar pungent substances in rats and guinea-pigs. J Physiol 206: 495–507.
3. Jancso N, Jancso-Gabor A, Szolcsanyi J (1967) Direct evidence for neurogenic inflammation and its prevention by denervation and by pretreatment with capsaicin. Br J Pharmacol Chemother 31: 138–151.
4. Jancso N, Jancso-Gabor A, Szolcsanyi J (1968) The role of sensory nerve endings in neurogenic inflammation induced in human skin and in the eye and paw of the rat. Br J Pharmacol Chemother 33: 32–41.
5. Szolcsanyi J (1977) A pharmacological approach to elucidation of the role of different nerve fibres and receptor endings in mediation of pain. J Physiol (Paris) 73: 251–259.
6. Caterina MJ, Schumacher MA, Tominaga M, Rosen TA, Levine JD, et al. (1997) The capsaicin receptor: a heat-activated ion channel in the pain pathway. Nature 389: 816–824.
7. Wong GY, Gavva NR (2009) Therapeutic potential of vanilloid receptor TRPV1 agonists and antagonists as analgesics: Recent advances and setbacks. Brain Res Rev 60: 267–277.
8. Gavva NR, Treanor JJ, Garami A, Fang L, Surapaneni S, et al. (2008) Pharmacological blockade of the vanilloid receptor TRPV1 elicits marked hyperthermia in humans. Pain 136: 202–210.
9. Backonja M, Wallace MS, Blonsky ER, Cutler BJ, Malan P Jr, et al. (2008) NGX-4010, a high-concentration capsaicin patch, for the treatment of postherpetic neuralgia: a randomised, double-blind study. Lancet Neurol 7: 1106–1112.
10. Noto C, Pappagallo M, Szallasi A (2009) NGX-4010, a high-concentration capsaicin dermal patch for lasting relief of peripheral neuropathic pain. Curr Opin Investig Drugs 10: 702–710.
11. Docherty RJ, Yeats JC, Bevan S, Boddeke HW (1996) Inhibition of calcineurin inhibits the desensitization of capsaicin-evoked currents in cultured dorsal root ganglion neurones from adult rats. Pflugers Archiv European journal of physiology 431: 828–837.
12. Lizanecz E, Bagi Z, Pásztor ET, Papp Z, Edes I, et al. (2006) Phosphorylation-dependent desensitization by anandamide of vanilloid receptor-1 (TRPV1) function in rat skeletal muscle arterioles and in Chinese hamster ovary cells expressing TRPV1. Molecular pharmacology 69: 1015–1023.
13. Mohapatra DP, Nau C (2005) Regulation of Ca2+-dependent desensitization in the vanilloid receptor TRPV1 by calcineurin and cAMP-dependent protein kinase. The Journal of Biological Chemistry 280: 13424–13432.
14. Bhave G, Hu HJ, Glauner KS, Zhu W, Wang H, et al. (2003) Protein kinase C phosphorylation sensitizes but does not activate the capsaicin receptor transient receptor potential vanilloid 1 (TRPV1). Proc Natl Acad Sci U S A 100: 12480–12485.
15. Mandadi S, Numazaki M, Tominaga M, Bhat MB, Armati PJ, et al. (2004) Activation of protein kinase C reverses capsaicin-induced calcium-dependent desensitization of TRPV1 ion channels. Cell Calcium 35: 471–478.
16. Numazaki M, Tominaga T, Toyooka H, Tominaga M (2002) Direct phosphorylation of capsaicin receptor VR1 by protein kinase Cepsilon and identification of two target serine residues. J Biol Chem 277: 13375–13378.
17. Bhave G, Zhu W, Wang H, Brasier DJ, Oxford GS, et al. (2002) cAMP-dependent protein kinase regulates desensitization of the capsaicin receptor (VR1) by direct phosphorylation. Neuron 35: 721–731.
18. Mohapatra DP, Nau C (2003) Desensitization of capsaicin-activated currents in the vanilloid receptor TRPV1 is decreased by the cyclic AMP-dependent protein kinase pathway. The Journal of Biological Chemistry 278: 50080–50090.
19. Ralevic V, Karoon P, Burnstock G (1995) Long-term sensory denervation by neonatal capsaicin treatment augments sympathetic neurotransmission in rat mesenteric arteries by increasing levels of norepinephrine and selectively enhancing postjunctional actions. J Pharmacol Exp Ther 274: 64–71.
20. Scadding JW (1980) The permanent anatomical effects of neonatal capsaicin on somatosensory nerves. J Anat 131: 471–482.
21. Cortright DN, Szallasi A (2004) Biochemical pharmacology of the vanilloid receptor TRPV1. An update. Eur J Biochem 271: 1814–1819.
22. Szolcsanyi J (1983) Tetrodotoxin-resistant non-cholinergic neurogenic contraction evoked by capsaicinoids and piperine on the guinea-pig trachea. Neurosci Lett 42: 83–88.
23. Zygmunt PM, Petersson J, Andersson DA, Chuang H, Sørgård M, et al. (1999) Vanilloid receptors on sensory nerves mediate the vasodilator action of anandamide. Nature 400: 452–457.
24. Alawi K, Keeble J (2010) The paradoxical role of the transient receptor potential vanilloid 1 receptor in inflammation. Pharmacology & Therapeutics 125: 181–195.
25. Fernandes ES, Fernandes MA, Keeble JE (2012) The functions of TRPA1 and TRPV1: moving away from sensory nerves. British Journal of Pharmacology 166: 510–521.
26. Toth A, Boczan J, Kedei N, Lizanecz E, Bagi Z, et al. (2005) Expression and distribution of vanilloid receptor 1 (TRPV1) in the adult rat brain. Molecular Brain Research 135: 162–168.
27. Kark T, Bagi Z, Lizanecz E, Pásztor ET, Erdei N, et al. (2008) Tissue-specific regulation of microvascular diameter: opposite functional roles of neuronal and smooth muscle located vanilloid receptor-1. Molecular Pharmacology 73: 1405–1412.
28. Cavanaugh DJ, Chesler AT, Jackson AC, Sigal YM, Yamanaka H, et al. (2011) Trpv1 reporter mice reveal highly restricted brain distribution and functional expression in arteriolar smooth muscle cells. J Neurosci 31: 5067–5077.
29. Czikora Á, Lizanecz E, Bakó P, Rutkai I, Ruzsnavszky F, et al. (2012) Structure-activity relationships of vanilloid receptor agonists for arteriolar TRPV1. British Journal of Pharmacology 165: 1801–1812.
30. Pinter E, Szolcsanyi J (1995) Plasma extravasation in the skin and pelvic organs evoked by antidromic stimulation of the lumbosacral dorsal roots of the rat. Neuroscience 68: 603–614.
31. Szallasi Á, Blumberg PM (1999) Vanilloid (capsaicin) receptors and mechanisms. Pharmacological Reviews 51: 159–212.
32. Caterina MJ, Leffler A, Malmberg A, Martin W, Trafton J, et al. (2000) Impaired nociception and pain sensation in mice lacking the capsaicin receptor. Science 288: 306–313.
33. Czikora Á, Lizanecz E, Boczán J, Daragó A, Papp Z, et al. (2012) Vascular metabolism of anandamide to arachidonic acid affects myogenic constriction in response to intraluminal pressure elevation. Life Sciences 90: 407–415.
34. Khairatkar-Joshi N, Szallasi Á (2009) TRPV1 antagonists: the challenges for therapeutic targeting. Trends in Molecular Medicine 15: 14–22.
35. Kissin I, Szallasi A (2011) Therapeutic targeting of TRPV1 by resiniferatoxin, from preclinical studies to clinical trials. Curr Top Med Chem 11: 2159–2170.
36. Mezey E, Toth ZE, Cortright DN, Arzubi MK, Krause JE, et al. (2000) Distribution of mRNA for vanilloid receptor subtype 1 (VR1), and VR1-like immunoreactivity, in the central nervous system of the rat and human. Proc Natl Acad Sci U S A 97: 3655–3660.
37. Jancso G, Hokfelt T, Lundberg JM, Kiraly E, Halasz N, et al. (1981) Immunohistochemical studies on the effect of capsaicin on spinal and medullary peptide and monoamine neurons using antisera to substance P, gastrin/CCK, somatostatin, VIP, enkephalin, neurotensin and 5-hydroxytryptamine. J Neurocytol 10: 963–980.
38. Nagy JI, Vincent SR, Staines WA, Fibiger HC, Reisine TD, et al. (1980) Neurotoxic action of capsaicin on spinal substance P neurons. Brain Res 186: 435–444.
39. Helyes Z, Pozsgai G, Börzsei R, Németh J, Bagoly T, et al. (2007) Inhibitory effect of PACAP-38 on acute neurogenic and non-neurogenic inflammatory processes in the rat. Peptides 28: 1847–1855.
40. Helyes Z, Thán M, Oroszi G, Pintér E, Németh J, et al. (2000) Anti-nociceptive effect induced by somatostatin released from sensory nerve terminals and by synthetic somatostatin analogues in the rat. Neuroscience Letters 278: 185–188.
41. Hong S, Wiley JW (2005) Early painful diabetic neuropathy is associated with differential changes in the expression and function of vanilloid receptor 1. The Journal of Biological Chemistry 280: 618–627.
42. Facer P, Casula MA, Smith GD, Benham CD, Chessell IP, et al. (2007) Differential expression of the capsaicin receptor TRPV1 and related novel receptors TRPV3, TRPV4 and TRPM8 in normal human tissues and changes in traumatic and diabetic neuropathy. BMC Neurology 7: 11.

BJP British Journal of Pharmacology

DOI:10.1111/j.1476-5381.2011.01645.x
www.brjpharmacol.org

RESEARCH PAPER

Structure-activity relationships of vanilloid receptor agonists for arteriolar TRPV1

Á Czikora[1], E Lizanecz[1], P Bakó[1], I Rutkai[1], F Ruzsnavszky[2], J Magyar[2], R Pórszász[3], T Kark[3], A Facskó[4], Z Papp[1,5], I Édes[1,5] and A Tóth[1,5]

[1]*Division of Clinical Physiology, Institute of Cardiology;* [2]*Department of Physiology,* [3]*Department of Pharmacology and Pharmacotherapy, Institute of Pharmacology,* [4]*Department of Ophthalmology, and* [5]*Research Centre for Molecular Medicine, Medical and Health Science Center, University of Debrecen, Debrecen, Hungary*

Correspondence
Attila Tóth, Institute of Cardiology, Division of Clinical Physiology, University of Debrecen, 22 Moricz Zs krt, Debrecen, 4032,Hungary. E-mail: atitoth@dote.hu

Keywords
vanilloid receptor (TRPV1); resistance artery; vascular autoregulation

Received
21 January 2011
Revised
12 July 2011
Accepted
09 August 2011

BACKGROUND AND PURPOSE

The transient receptor potential vanilloid 1 (TRPV1) plays a role in the activation of sensory neurons by various painful stimuli and is a therapeutic target. However, functional TRPV1 that affect microvascular diameter are also expressed in peripheral arteries and we attempted to characterize this receptor.

EXPERIMENTAL APPROACH

Sensory TRPV1 activation was measured in rats by use of an eye wiping assay. Arteriolar TRPV1-mediated smooth muscle specific responses (arteriolar diameter, changes in intracellular Ca^{2+}) were determined in isolated, pressurized skeletal muscle arterioles obtained from the rat and wild-type or $TRPV1^{-/-}$ mice and in canine isolated smooth muscle cells. The vascular pharmacology of the TRPV1 agonists (potency, efficacy, kinetics of action and receptor desensitization) was determined in rat isolated skeletal muscle arteries.

KEY RESULTS

Capsaicin evoked a constrictor response in isolated arteries similar to that mediated by noradrenaline, this was absent in arteries from TRPV1 knockout mice and competitively inhibited by TRPV1 antagonist AMG9810. Capsaicin increased intracellular Ca^{2+} in the arteriolar wall and in isolated smooth muscle cells. The TRPV1 agonists evoked similar vascular constrictions (MSK-195 and JYL-79) or were without effect (resiniferatoxin and JYL-273), although all increased the number of responses (sensory activation) in the eye wiping assay. Maximal doses of all agonists induced complete desensitization (tachyphylaxis) of arteriolar TRPV1 (with the exception of capsaicin). Responses to the partial agonist JYL-1511 suggested 10% TRPV1 activation is sufficient to evoke vascular tachyphylaxis without sensory activation.

CONCLUSIONS AND IMPLICATIONS

Arteriolar TRPV1 have different pharmacological properties from those located on sensory neurons in the rat.

Abbreviations

AMG9810, (E)-3-(4-t-butylphenyl)-N-(2,3-dihydrobenzo[b][1,4] dioxin-6-yl)acrylamide; CHO-TRPV1, CHO cells overexpressing rat TRPV1; DRG, dorsal root ganglion; JYL-1511, *N*-(4-*tert*-butylbenzyl)-*N*′-[3-methoxy-4-(methyl-sulphonylamino)benzyl]thiourea; JYL-273, 2-(4-t-butylbenzyl)-3-{[(4-hydroxy-3-methoxybenzyl)ami- no]carbothioyl} propyl pivalate; JYL-79, 2-(3,4-dimethylbenzyl)-3-{[(4-hydroxy-3-methoxy-benzyl)amino]carbothioyl}propyl pivalate; MSK-195, *N*-[2-(3,4-dimethylbenzyl)-3-(pivalyloxy)propyl]-2-[4-(2-aminoethoxy)-3 methoxyphenyl]acetamide; TRPV1, transient receptor potential vanilloid 1; TRPV1-/-, B6.129X1-*Trpv1tm1Jul*/J mice

Introduction

The transient receptor potential vanilloid 1 (TRPV1) is a non-selective cation channel, originally found in sensory C and Aδ fibres (Caterina *et al.*, 1997). It functions as a ligand-, proton- and heat-activated molecular integrator of nociceptive stimuli (Szallasi and Blumberg, 1999; Di Marzo *et al.*, 2002; Ross, 2003) and hence represents a promising drug

target for analgesia (Szallasi *et al.*, 2007; Gunthorpe and Szallasi, 2008).

However, TRPV1 expression has recently been identified in many cells in addition to sensory neurons. In particular, TRPV1 expression was detected in various cell types in the brain (Toth *et al.*, 2005a), and in the periphery, including arteriolar receptors responsible for vasoconstriction (Kark *et al.*, 2008). Moreover, while functional expression of TRPV1 in the CNS remained elusive, activation of vascular TRPV1 has been shown to result in substantial vasoconstriction both *in vivo* and *in vitro* (Kark *et al.*, 2008). TRPV1 antagonists are in clinical trials for various conditions including dental pain, osteoarthritis, neuropathic pain, overactive bladder, chronic cough, rectal hypersensitivity, migraine, lower back pain and interstitial cystitis (Khairatkar-Joshi and Szallasi, 2009). Although some results of these trials are promising, they also revealed that TRPV1 antagonists can evoke serious hyperthermia (Gavva *et al.*, 2008). This hyperthermia is probably related to the involvement of TRPV1 in temperature regulation *in vivo* (Gavva *et al.*, 2007). However, the mechanism of this effect is not clear. Although some antagonists cause hyperthermia (Gavva *et al.*, 2008), others are without thermoregulatory effects in humans (Khairatkar-Joshi and Szallasi, 2009). This suggests that the TRPV1 responsible for analgesia is pharmacologically different from that involved in thermoregulation. The nature and identity of these TRPV1-dependent responses have not been identified yet, but it is plausible that a separate pool of receptors exists (Steiner *et al.*, 2007).

Capsaicin evokes vasoconstriction in skeletal muscle arteries presumably by activating TRPV1 located in smooth muscle (Kark *et al.*, 2008). Here we attempted to characterize this receptor pharmacologically. To achieve this, we chose a series of commercially available TRPV1 agonists and tested them in assays that measured not only their potency and efficacy, but also their kinetics of action and ability to induce desensitization (Toth *et al.*, 2005b). Our experiments revealed different pharmacological profiles for vascular TRPV1 when compared with that of TRPV1 responsible for sensory activation. These findings indicate that sensory neuronal and arterial receptor populations of TRPV1 can be selectively targeted.

Methods

The applied drug/molecular target nomenclature (e.g. receptors, ion channels) conforms to the *British Journal of Pharmacology*'s Guide to Receptors and Channels (Alexander *et al.*, 2011).

Animals, anaesthesia and general preparation in the in vivo *experiments*

The experiments were performed on male Wistar rats ($n = 119$ rats) weighing 250–450 g and on male mice (six control C57BL/6J and five TRPV1$^{-/-}$ knockout mice). Rats (WKY/NCrl) were obtained from Charles River (Isaszeg, Hungary), while mice was obtained from Jackson Laboratories (Bar Harbor, ME, USA) and maintained on a standard laboratory food (CRLT/N chow from Szinbad Kft, Godollo, Hungary) and water *ad libitum*. Anaesthesia was induced by administration of pentobarbital sodium (100 mg·kg^{-1} i.p.). All animal care and experimental procedures complied with NIH guidelines and were approved by the Ethical and Experimental Animal Research Committee of the University of Debrecen.

Isolation of arterioles and measurement of vascular diameter

The isolation of skeletal muscle (m. gracilis) arterioles of the rat and measurement of the diameter of arterioles were performed as described previously (Lizanecz *et al.*, 2006). Briefly, arterioles were kept in a physiological saline solution (PSS; composition in mM: 110 NaCl, 5.0 KCl, 2.5 $CaCl_2$, 1.0 $MgSO_4$, 1.0 KH_2PO_4, 5.0 glucose and 24.0 $NaHCO_3$ equilibrated with a gas mixture of 10% O_2, 5% CO_2 and 85% N_2, at pH 7.4.) at an intraluminal pressure of 80 mmHg until the development of spontaneous myogenic response (constriction to intraluminal pressure). Changes in intraluminal arteriolar diameter were measured after the various treatments. First ACh was used to determine dilator capacity and endothelium function, and then noradrenaline (NA) was applied to measure maximal constrictor response and smooth muscle function. Changes in diameter to TRPV1 agonists were tested next with cumulative doses of the agonists (capsaicin, 0.1 nM–1 μM; resiniferatoxin, 1 pM–10 nM; JYL-273, 0.1 nM–1 μM; MSK-195, 0.1 nM–3 μM; JYL-79, 3 pM–10 μM; JYL-1511, 1 nM–1 μM). The specificity of the capsaicin responses was tested by the application of the TRPV1 antagonist AMG9810. Cumulative dose-response curves for capsaicin were obtained in the absence and presence of 100, 300 and 1000 nM AMG9810 (obtained from Tocris Bioscience, Ellisville, MO, USA). Desensitization of arteriolar TRPV1 was tested in separate experiments. Acute desensitization (decrease in response in the continuous presence of agonist) was determined by measurement of arteriolar diameter during 20 min incubations with a high concentration of the drugs. This was followed by 40 min regeneration (in PSS solution) and tachyphylaxis (decrease of response upon re-administration of the agonist) was assessed by measuring the response to 1 μM capsaicin. Arterioles were isolated from wild-type and TRPV1 knockout mice as detailed for the rat. Experiments were also performed similarly; ACh was used to determine endothelial function, and NA was applied to estimate smooth muscle function. Changes in diameter to TRPV1 agonists were tested by measuring responses to cumulative doses of capsaicin (0.1 nM–30 μM).

Determination of antagonist equilibrium dissociation constant

A conventional Schild plot (Arunlakshana and Schild, 1959) was constructed based on the measured values. EC_{50} of capsaicin was calculated in the absence (designated as A) or in the presence of AMG9810 (designated as A'), then log((A/A')-1) values were plotted as a function of the logarithm of AMG9810 concentration (Figure 2B). Data were fitted by linear regression, and the antagonist equilibrium dissociation constant was obtained from the *x*-intercept.

Parallel measurement of vascular diameter and intracellular Ca^{2+} concentrations

Skeletal muscle arterioles were isolated and cannulated from the gracilis muscle of the rat, as mentioned above. After the

arteries had been mounted in the tissue chamber, the physiological buffer was supplemented with 1% BSA and 5 μM Fura-2AM fluorescent Ca^{2+} indicator dye for 60–120 min until a spontaneous myogenic tone developed. Then, the tissue chamber was placed on the stage of a Nikon TS100 (Tokyo, Japan) inverted microscope to measure intracellular Ca^{2+} concentrations by an IncyteIm2 instrument (Intracellular Imaging Inc, Cincinnati, OH, USA) by recording images (cut-off >510 nM) excited alternatively by 340 and 380 nm light. Images were recorded every 2–5 s and evaluated offline. Outer diameter of the arteries was determined on each recorded image and arteriolar Ca^{2+} concentrations were detected by calculating ratios between averaged signal intensity at 340 and 380 nm excitation in the whole arteriolar segment (representing a minimum of 200 pixels). A movie representative of the full experiment has been uploaded as a supplementary video file, and additional movies can also be seen at our website (http://www.debkard.hu/upload/file/klinfiz/kkk/Vascularsystem/Vascularsystem.html).

Isolation of smooth muscle cells from canine coronary arteries

Adult beagle dogs (10–14 kg) were anaesthetized with an i.v. injection containing 10 $mg \cdot kg^{-1}$ ketamine hydrochloride (Calypsol, Richter Gedeon, Hungary) and 1 $mg \cdot kg^{-1}$ xylazine hydrochloride (Sedaxylan, Eurovet Animal Health BV, Bladel, the Netherlands). After the chest had been opened, the heart was rapidly removed and the right coronary artery was perfused with Ca^{2+}-free minimum essential Eagle's medium, Joklik modification solution, supplemented with taurine (2.5 $g \cdot L^{-1}$), pyruvic acid (175 $mg \cdot L^{-1}$), ribose (750 $mg \cdot L^{-1}$), allopurinol (13.5 $mg \cdot L^{-1}$) and NaH_2PO_4 (200 $mg \cdot L^{-1}$) equilibrated with a mixture of 95% O_2 and 5% CO_2 (similar to all further solutions) for 5 min to remove the blood. Then the solution was changed to Dulbecco's modified Eagle's medium (DMEM), and an approximately 2.5 cm long right coronary artery segment was isolated and cannulated at both ends. The cannulae were connected to a peristaltic pump, and the solution was pumped from the tissue chamber into the arteriolar lumen (from which it leaked back to the tissue chamber). Then DMEM was supplemented with 3 $mg \cdot mL^{-1}$ collagenase type I (Worthington, Lakewood, NJ, USA) for 30 min and with 1 $mg \cdot mL^{-1}$ elastase (Worthington) at 60 min. The vessel fell apart after about 90 min under these conditions; the cell-rich solution was then transferred into 24-well plates. After the adherence of the cells to the glass coverslips placed in the wells (about 10 min), the solution was replaced with DMEM to remove the digesting enzymes, and the cells were incubated for 60 min in a CO_2 thermostate. Then, the media was changed to DMEM containing 1 $mg \cdot mL^{-1}$ BSA and 5 μM fura2-acetoxymethyl ester (Molecular Probes, Eugene, OR, USA) for 2 h at room temperature. The cover slips were then placed in a suitable chamber for intracellular Ca^{2+} concentration measurements. These measurements were started by washing the cells with Dulbecco's PBS (DPBS) three times, and the measurements were performed in DPBS. The fluorescence of individual cells was measured with an InCyt Im2 fluorescence imaging system (Intracellular Imaging Inc., Cincinnati, OH, USA). The cells within a field were illuminated alternately at 340 and 380 nm. Emitted light at >510 nm was measured. The cells were treated with 1 μM capsaicin and then with 100 mM KCl. Data were analysed with the InCyt 4.5 software and further processed with Excel (Microsoft Corp, Redmond, WA, USA) and Prism 5.0 (GraphPad Software, Inc., San Diego, CA, USA) software.

Measurement of eye wiping

The eye wiping assay was performed as described previously (Jakab *et al.*, 2005). In short, one drop (10 μL) of agonists (capsaicin, 1 μM; resiniferatoxin, 10 nM; JYL-273, 1 μM; MSK-195, 1 μM; JYL-79, 1 μM; JYL-1511, 1 μM) was put into the right or left conjunctiva of the rat (single treatment for each rat). The number of eye wipes was counted for 60 s. In the control group, the same volume of solvent was administered in a similar manner.

Materials and solutions

Chemicals were from Sigma-Aldrich (St. Louis, MO, USA) if not stated otherwise. Resiniferatoxin, JYL-273, MSK-195, JYL-79 and JYL-1511 were from Alexis (Enzo Life Sciences AG, Lausen, Switzerland). TRPV1 agonists were dissolved in ethanol.

Statistical analysis

Arteriolar diameter was measured in μm, determined at 80 mmHg intraluminal pressure. Results are shown as mean ± SEM. Statistical differences were evaluated by Student's *t*-test by comparing values before and after treatments (paired) or comparing eye wipes of vehicle-treated rats with those of TRPV1 agonist-treated rats (unpaired).

Results

Application of the TRPV1-specific agonist capsaicin (1 μM) resulted in a substantial constriction (decrease of arteriolar diameter from 210 ± 11 μm to 91 ± 17 μm, $n = 7$, $P < 0.01$) of skeletal muscle (m. gracilis) arterioles (Figure 1) similar to NA (10 μM, decrease of arteriolar diameter to 68 ± 9 μm, $n = 7$, Figure 1). In contrast, the endothelium-dependent vasodilator ACh evoked dilatation (increase in arteriolar diameter to 240 ± 20 μm, $n = 7$, $P = 0.028$, Figure 1).

The vast majority of published data suggest that vascular TRPV1 stimulation produces a dilatation. It was therefore necessary to test the TRPV1 specificity of these capsaicin-mediated contractile responses. First, a competitive antagonist of TRPV1 was applied. AMG9810 antagonized capsaicin-mediated contractions in a dose-dependent manner (Figure 2A). Moreover, the potency of AMG9810 determined in these assays (177 nM, Figure 2B) was in agreement with its potency determined in other TRPV1-specific systems (Gavva *et al.*, 2005). Nonetheless, the TRPV1 selectivity of these capsaicin-mediated contractile responses was also tested in TRPV1 knockout ($TRPV1^{-/-}$) mice. The potency of capsaicin (EC_{50}) was 137 nM (Figure 2C) and efficacy was 73% (decrease in diameter from 69 ± 8 μm to 24 ± 3 μm, $n = 6$, Figure 2C) in arteries from wild-type mice, while the same capsaicin treatments were without effect in $TRPV1^{-/-}$ mice (Figure 2C, $n = 5$).

Next, the potential mechanism of TRPV1-mediated constrictions was evaluated. Activation of TRPV1 results in an

increase in intracellular Ca^{2+} concentrations in many TRPV1-expressing cell types and this contributes to the physiological effects. To detect capsaicin-mediated changes in intracellular Ca^{2+} concentrations, a Ca^{2+} imaging system was applied. Simultaneous measurement of intracellular Ca^{2+} concentration and vascular diameter (outer diameter in this case) of cannulated rat arterioles isolated from the gracilis muscle of the rat was performed (Figure 3). The capsaicin-evoked vasoconstriction was parallelled by an increase in intracellular Ca^{2+} concentration (supplementary video file and Figure 3A). Moreover, both vascular diameter and intracellular Ca^{2+} concentration increased in a dose-dependent manner, with potency in the nanomolar range (note maximal responses at 1 μM, Figure 3B). To identify the TRPV1-expressing cell type, arteriolar smooth muscle cells were isolated from canine coronary arteries (these arteries also responded to capsaicin treatment with a dose-dependent constriction; data not shown) and changes in intracellular Ca^{2+} concentrations to capsaicin (1 μM) and KCl (100 mM) treatments were tested (Figure 4). The capsaicin-mediated increase in intracellular Ca^{2+} concentrations in the cells responding to capsaicin (10 out of 28 cells, representative data in Figure 4A and B) was similar (increase in 340/380 ratio from 0.69 ± 0.10 to 0.93 ± 0.17, Figure 4C) to the increase evoked by depolarization (100 mM KCl, 340/380 ratio was 1.04 ± 0.20, Figure 4C).

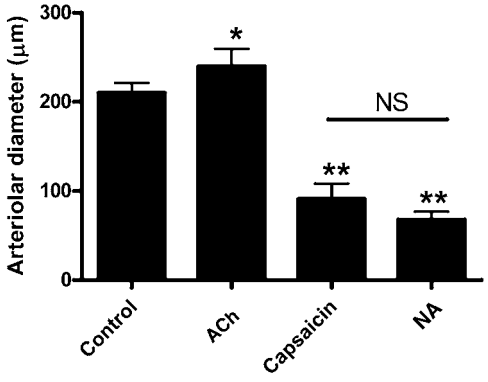

Figure 1

Functional effects of TRPV1 stimulation in skeletal muscle arteries. Internal diameter of cannulated gracilis arteries were measured at 80 mmHg intraluminal pressure before treatments (control). The existence of spontaneous myogenic tone and viability of endothelium was determined by ACh (10 μM)-evoked dilatations. The constrictor response to TRPV1 agonist capsaicin (1 μM) was compared with the effect of NA (10 μM). Experiments were performed on the same ($n = 7$) arteries. Values are mean ± SEM. Significant differences are represented by asterisks (*$P < 0.05$ or **$P < 0.01$).

Having established the TRPV1 specificity of capsaicin-evoked vasoconstriction, the pharmacological properties of these receptors on skeletal muscle arteries of the rat were characterized in detail. The potency of capsaicin on this receptor (EC_{50}) was 221 nM (Figure 5A), efficacy was 58 ± 7% constriction ($n = 7$), which was not significantly different from the efficacy of NA (69 ± 3% constriction, $n = 6$, $P < 0.01$ vs. control, $P = 0.08$ vs. capsaicin). The kinetics of the vasoconstrictor response was determined by continuous application of capsaicin (1 μM) for 20 min. Maximal constriction (decrease of arteriolar diameter from 160 ± 11 μm to 76 ± 16 μm, $n = 9$) was achieved at 90 s (Figure 5B). After that, an acute desensitization (decrease of response in the presence of agonist) was observed. Arteriolar diameter was similar to the control at the end of the 20 min treatment (gradual increase to 150 ± 13 μm, $n = 9$, Figure 5B). Finally, tachyphylaxis (decrease of response upon repeated application of the agonist) was measured by the re-application of capsaicin (1 μM) after a 40 min regeneration period. Arteriolar diameter decreased from 161 ± 17 μm to 109 ± 18 μm ($n = 6$), suggesting significant resensitization of the receptor (Figure 5C).

Resiniferatoxin was tested under the same conditions (Figure 6). Surprisingly no vascular effects were detected upon

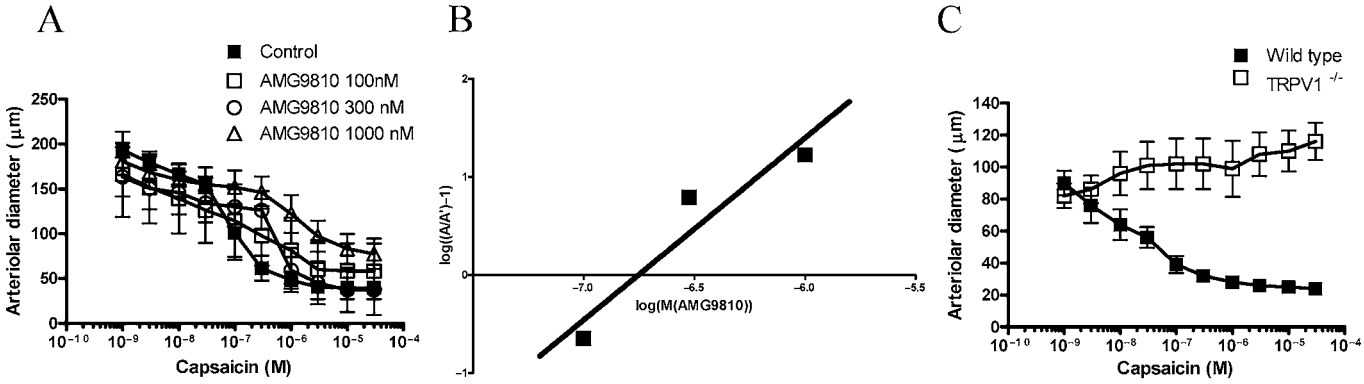

Figure 2

TRPV1 specificity of capsaicin-evoked vasoconstriction. Internal diameter of cannulated gracilis arteries was measured at 80 mmHg intraluminal pressure upon addition of different doses of capsaicin (cumulative dose-response curve) in the absence (control) and presence of the TRPV1 antagonist AMG9810 (100, 300 and 1000 nM, A). Symbols are means ± SEM of five to nine independent determinations. The equilibration dissociation constant of AMG9810 was determined by the conventional Schild plot (*x*-intercept, B). Finally, gracilis arterioles isolated from control (wild-type) and TRPV1 knockout ($TRPV1^{-/-}$) mice were also tested for capsaicin-mediated vasoconstriction (C). Symbols are mean ± SEM of five to six independent determinations.

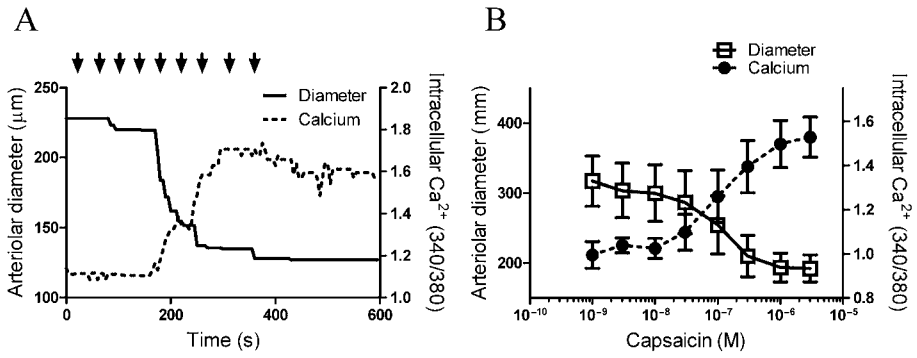

Figure 3

Mechanism of capsaicin-mediated vasoconstriction: skelatal muscle arteries. Capsaicin-evoked changes in arteriolar diameter were recorded in parallel with changes in intracellular Ca^{2+} concentrations of the vascular wall. An individual experiment is shown in (A) (the full recorded experiment also available in the supplementary movie). Solid line represents the arteriolar diameter (please note that in this specific case, the outer diameter is plotted), while dotted line shows intracellular Ca^{2+} concentrations expressed as 340/380 ratio. Capsaicin was administered in a cumulative fashion (indicated by the arrows, the applied capsaicin doses were: 3×10^{-10}, 10^{-9}, 3×10^{-9}, 10^{-8}, 3×10^{-8}, 10^{-7}, 3×10^{-7}, 10^{-6}, 3×10^{-6} M). (B)The mean responses ±SEM of $n = 5$ single determinations.

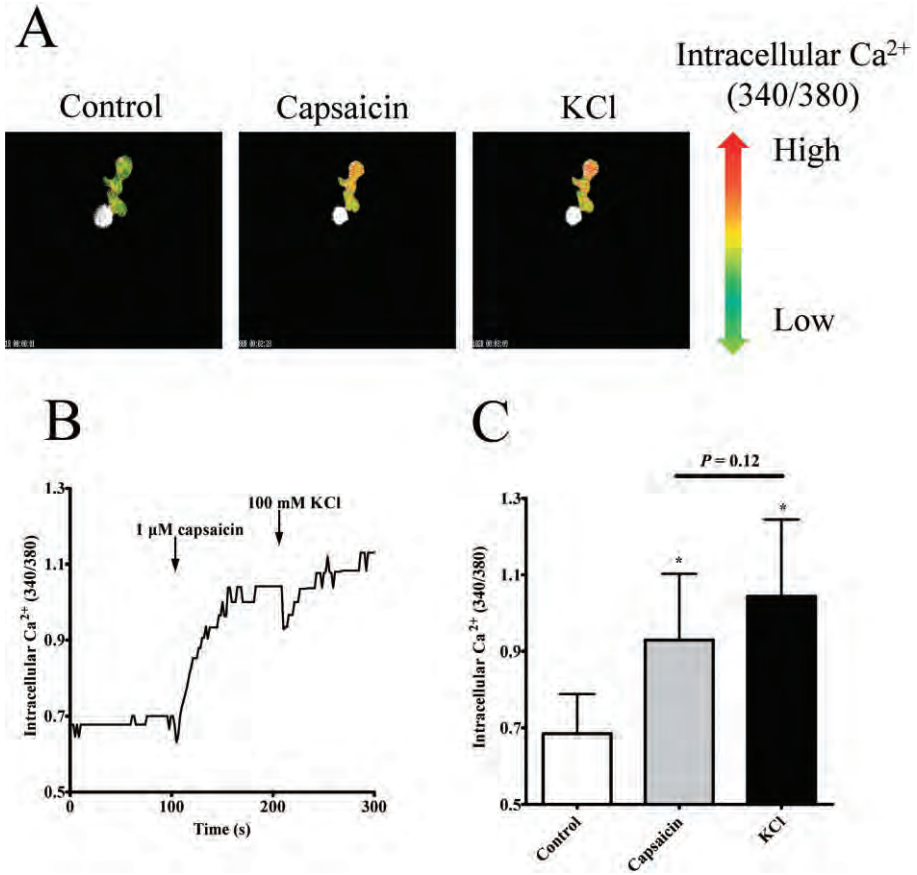

Figure 4

Mechanism of capsaicin-mediated vasoconstriction: isolated arteriolar smooth muscle cells. Canine, freshly isolated coronary arteriolar smooth muscle cells were loaded with fura-2 fluorescent Ca^{2+}-sensitive dye and treated with capsaicin (1 µM) and KCl (100 mM). Changes in intracellular Ca^{2+} concentrations were detected as changes in the 340/380 fluorescence ratio (a representative experiment is shown in A, where green pixels represent low values and red represent high values). Capsaicin evoked a fast increase in the intracellular Ca^{2+} concentrations in some cells, which was not increased further upon the addition of KCl (B). These observations were confirmed when responses of the capsaicin-sensitive cells (10 out of 28 viable cells) were evaluated (C). Columns represent mean ± SEM.

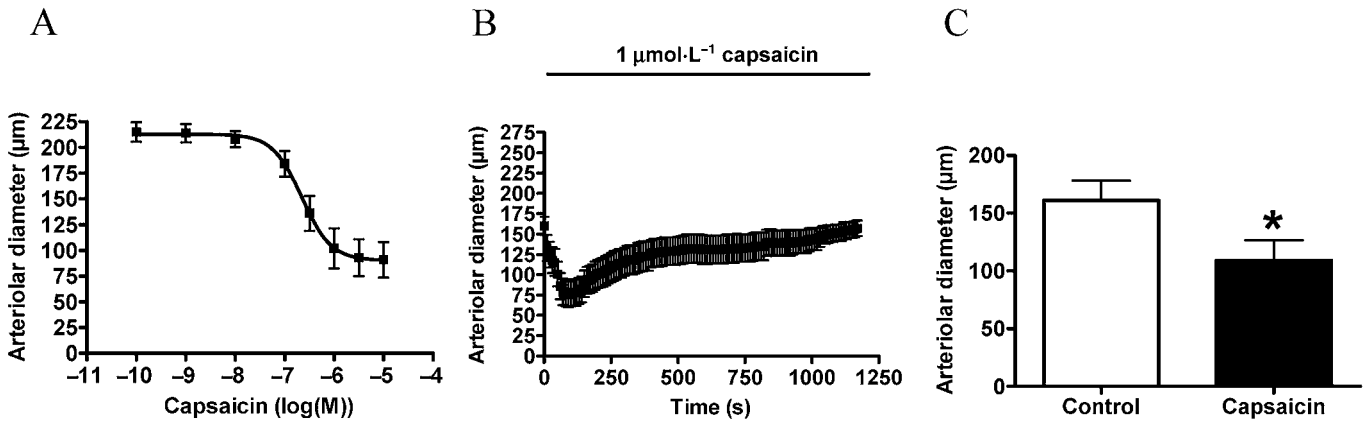

Figure 5

Pharmacological characterization of vascular responses to capsaicin. Experiments were performed on cannulated arteries as mentioned above. First, a cumulative dose-response curve was obtained (A, $n = 7$). Next on a separate set of arteries, the kinetics of response were measured by the application of 1 µM capsaicin for 20 min. Arteriolar diameter was measured at 10 s intervals (B, $n = 9$). After this 20 min treatment, the arteries were washed and were incubated in PSS solution for 40 min (regeneration). At the end of regeneration, vasoconstriction to the same dose of capsaicin (1 µM) was measured to determine tachyphylaxis (C, $n = 7$). Values are mean ± SEM, significant difference ($P < 0.05$) is represented by an asterisk.

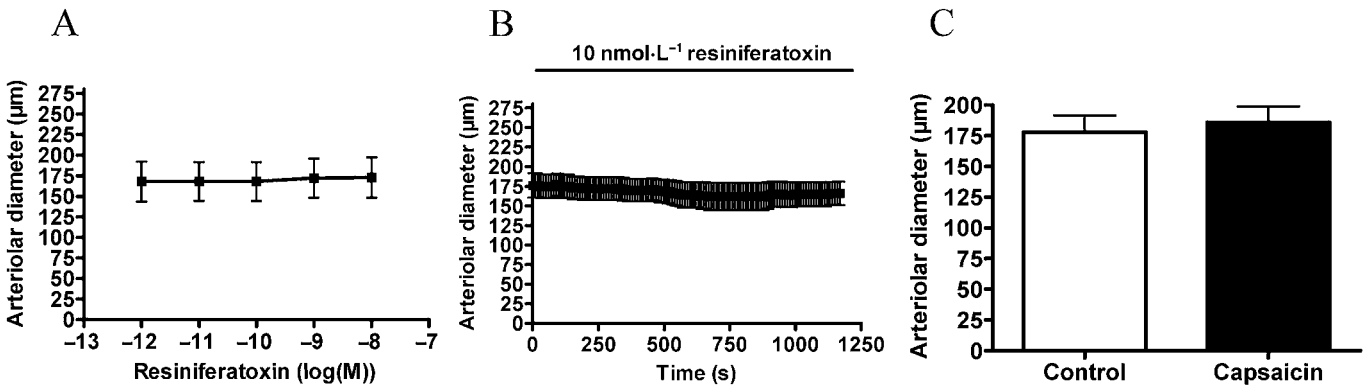

Figure 6

Arteriolar response to resiniferatoxin. Experiments were performed as mentioned in Figure 4 with resiniferatoxin. Responses to cumulative doses are shown in (A) ($n = 3$). No functional response was detected after 20 min of resiniferatoxin (B, 10 nM, $n = 5$). However, this treatment desensitized the receptors to capsaicin (1 µM) measured after regeneration (C, $n = 5$).

application in a concentration range from 1 pM to 10 nM (Figure 6A). Moreover, no effects were detected upon application of 10 nM for 20 min (Figure 6B). However, capsaicin (1 µM) was without effect after 40 min regeneration (Figure 6C), suggesting complete desensitization of arterial TRPV1 upon the otherwise ineffective resiniferatoxin treatments.

JYL-273 was ineffective at evoking arteriolar vasoconstriction in the concentration range 0.1 nM to 1 µM ($n = 7$, Figure 7A), nor did 1 µM JYL-273 applied for 20 min have any effect ($n = 5$, Figure 7B). However, similar to resiniferatoxin, this 20 min incubation resulted in complete desensitization of TRPV1 as evidenced by the lack of a response to capsaicin ($n = 4$, Figure 7C).

MSK-195 had a potency of 120 nM and an efficacy of 71 ± 11% ($n = 5$, Figure 8A). Application of 1 µM MSK-195 for 20 min resulted in a transient decrease in arterial diameter (decrease from 235 ± 19 µm to 155 ± 25 µm at 90 s, $n = 6$, Figure 8B). However, the kinetics of this acute desensitization were slower than that for capsaicin, since the original arteriolar diameter was not restored during the 20 min incubation (arterial diameter after 20 min incubation was 193 ± 25, $P = 0.03$ vs. before treatment, $n = 6$, Figure 8B). Similar to all the agonists mentioned above, MSK195 also evoked a complete desensitization of capsaicin-sensitive vascular TRPV1 (Figure 8C).

JYL-79 was found to be more potent on vascular TRPV1 (EC_{50} = 3.9 nM, $n = 8$, Figure 9A) than capsaicin. Its efficacy was 36 ± 8% ($n = 8$, Figure 9A). It also evoked a transient vasoconstriction when applied at a concentration of 1 µM (decrease of vascular diameter from 228 ± 13 µm to 127 ± 12 µm at 100 s, $n = 5$, Figure 9B). The desensitization of the receptor was not complete at the end of the 20 min incuba-

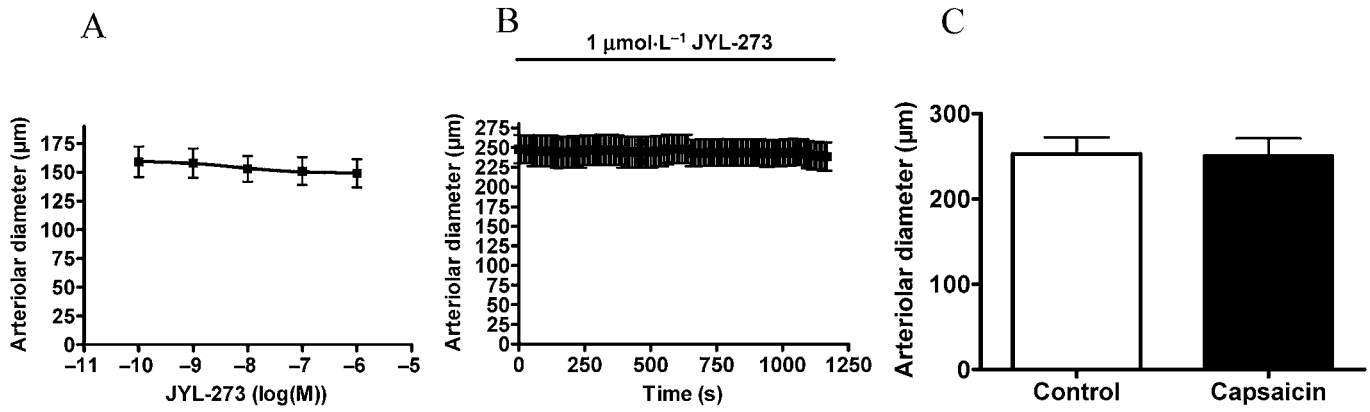

Figure 7

Arteriolar response to JYL-273. Experiments were performed as mentioned in Figure 4 with JYL-273. Responses to cumulative doses are shown in (A) ($n = 7$). No functional response was detected after 20 min of JYL-273 (B, 1 μM, $n = 5$). However, this treatment desensitized the receptors to capsaicin (1 μM) measured after regeneration (C, $n = 4$).

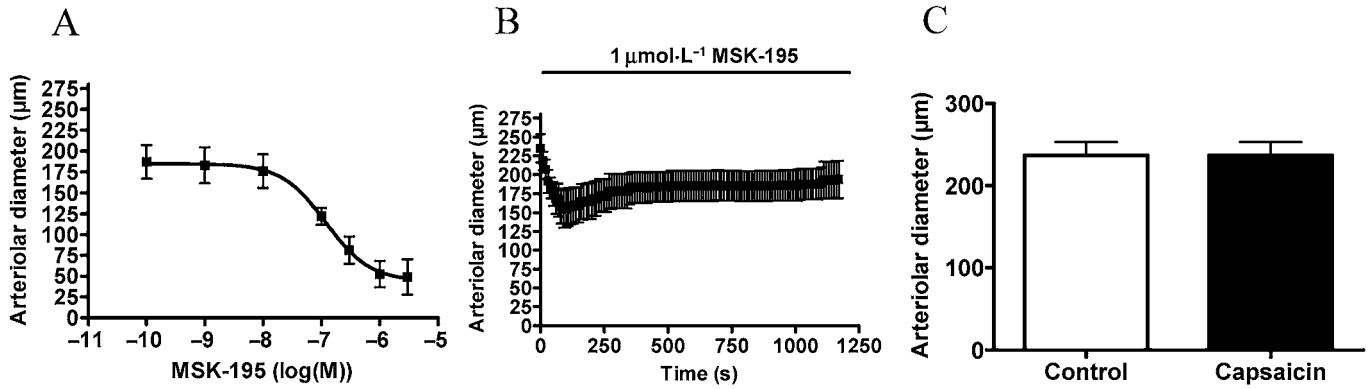

Figure 8

Arteriolar response to MSK-195. Experiments were performed as mentioned in Figure 4 with MSK-195. Responses to cumulative doses are shown in (A) ($n = 5$). A transient vasoconstriction was observed upon MSK-195 stimulation for 20 min (B, 1 μM, $n = 6$). In addition, this treatment desensitized the receptors to capsaicin (1 μM) measured after regeneration (C, $n = 6$).

tion (vascular diameter at 20 min was 204 ± 13 μm, $P = 0.046$ vs. before treatment, $n = 5$, Figure 9B). Moreover, no response to capsaicin (1 μM) was observed after 40 min regeneration ($n = 5$, Figure 9C).

To estimate the threshold of TRPV1 stimulation, which causes complete desensitization of vascular TRPV1, a partial agonist (JYL-1511) was applied. Its efficacy as an agonist was about 17%, and its potency was 3 nM in a CHO cells overexpressing rat TRPV1 (CHO-TRPV1) cell line (Wang *et al.*, 2003). JYL-1511 was without effect on the vascular diameter in the concentration range 1 nM–1 μM ($n = 6$, Figure 10A). Application of 1 μM for 20 min was also without effect (Figure 10B). A partial inhibition (tachyphylaxis) of the capsaicin response (1 μM) was noted after 40 min regeneration (decrease of vascular diameter from 244 ± 14 μm to 209 ± 17 μm, $P = 0.02$, $n = 6$, Figure 10C). The level of partial agonism/antagonism was also determined (Figure 11). Application of JYL-1511 (1 μM) resulted in a decrease in the arteriolar diameter (arterial diameter decreased to 94 ± 3%, $n = 6$) and immediate capsaicin treatment (1 μM) resulted in a decrease in diameter to 83 ± 6% ($P = 0.04$, $n = 6$). In contrast, the same capsaicin treatment alone evoked a decrease in diameter to 43 ± 7% ($P < 0.01$, $n = 7$) in separate experiments. According to these data, the agonism of JYL-1511 is 10 ± 5% and antagonism is 70 ± 11% at the vascular TRPV1.

The aim of this study was to detect differences between TRPV1 populations responsible for sensory neuronal activation and vasoconstriction. A weakness in the previous characterization of the applied agonists is that their effects were tested only *in vitro*, many times only on TRPV1 receptors expressed exogenously (Table 1). Sensory neuronal activation was also tested here by use of the eye wiping assay. JYL-1511 did not evoke significant effects, while all of the other agonists increased the number of eye wipes (Figure 12). Note, that although these data were in complete agreement with previous *in vitro* results (Table 1), differences between sensory neuronal and vascular effects were also noted. In particular, resiniferatoxin and JYL-273 were both ineffective at evoking

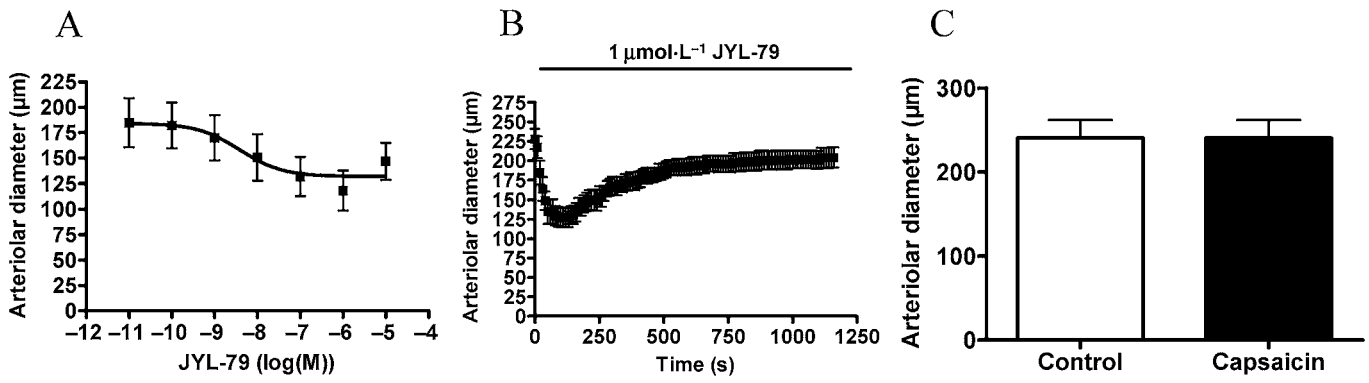

Figure 9

Arteriolar response to JYL-79. Experiments were performed as mentioned in Figure 4 with JYL-79. Responses to cumulative doses are shown in (A) (n = 8). A transient vasoconstriction was observed upon JYL-79 stimulation for 20 min (B, 1 µM, n = 5). In addition, this treatment desensitized the receptors to capsaicin (1 µM) measured after regeneration (C, n = 5).

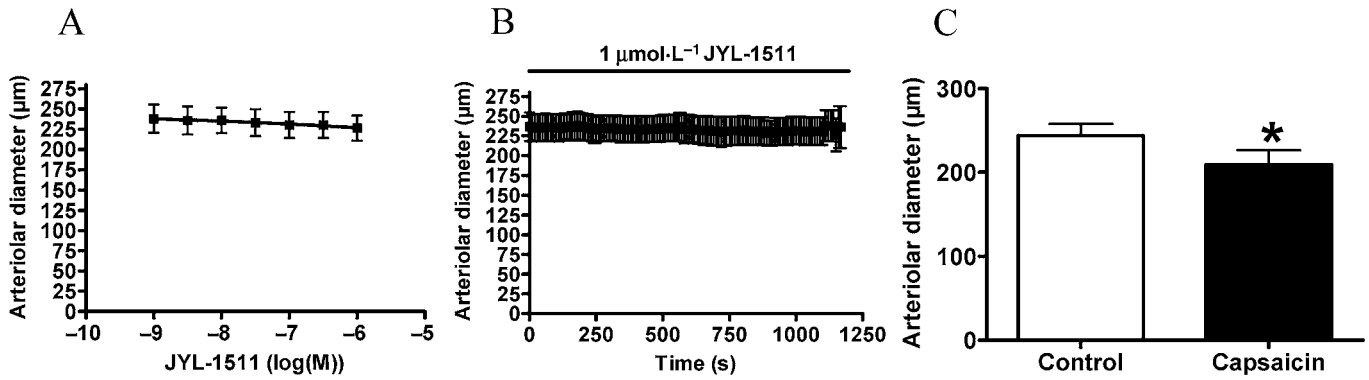

Figure 10

Arteriolar response to JYL-1511. Experiments were performed as mentioned in Figure 4 with JYL-1511. Responses to cumulative doses are shown in (A) (n = 6). No functional response was detected after 20 min of JYL-1511 (B, 1 µM, n = 6). However, this treatment desensitized the receptors to capsaicin (1 µM) measured after regeneration (C, n = 6).

acute activation of vascular TRPV1 receptors (Figures 6 and 7, respectively).

Discussion and conclusions

Here we report an analysis of the pharmacological properties of a vasoconstrictor population of TRPV1. Changes in vascular diameter in response to various agonists and partial agonist/antagonists of the receptor were measured. Our data suggest that significant differences in the pharmacological properties of endogenous TRPV1 pools exist. There are at least two important consequences of this observation. Firstly, TRPV1 antagonists being developed as analgesic agents should be tested for side effects on the circulation. Secondly, selective modulation of vascular TRPV1 may also be a therapeutic target. Pharmacological exploitation of vascular TRPV1 seems to be a reasonable aim with the substantial chemical libraries constructed to develop successful TRPV1 antagonists.

Vascular TRPV1 was characterized here by measuring the vasoconstriction upon TRPV1 stimulation. Previously, TRPV1 was shown to be expressed in vascular smooth muscle cells and it was suggested that activation of TRPV1 is directly linked to intracellular Ca^{2+} elevations in smooth muscle (Kark *et al.*, 2008). Indeed, in the present study we found that a decrease in arteriolar diameter was paralleled by an increase in intracellular Ca^{2+} concentrations in the vascular wall (Figure 3); moreover, direct intracellular Ca^{2+} concentration measurements revealed, for the first time, the presence of functional TRPV1 in isolated arteriolar smooth muscle cells (Figure 4).

Vasoconstriction in response to TRPV1 stimulation was reported decades ago (Molnar and Gyorgy, 1967; Toda *et al.*, 1972; Donnerer and Lembeck, 1982; Duckles, 1986; Edvinsson *et al.*, 1990) and this effect was confirmed later (Szolcsanyi *et al.*, 2001; Dux *et al.*, 2003; Scotland *et al.*, 2004; Keeble and Brain, 2006; Lizanecz *et al.*, 2006). Nonetheless, these responses were not thought to be of interest. One of the reasons for this was that pharmaceutical research had

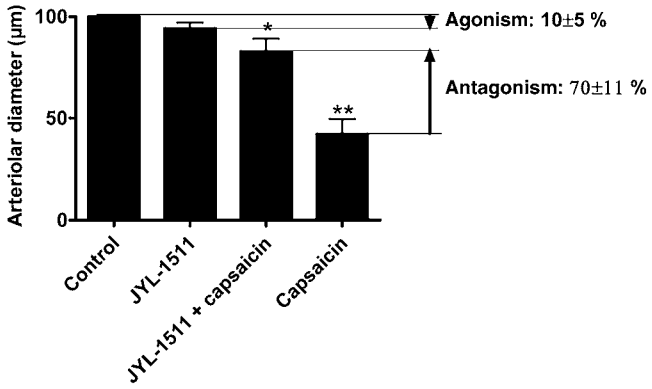

Figure 11

Partial agonism/antagonism of JYL-1511 on TRPV1 located in vascular smooth muscle. Changes in internal diameter of the arteries were measured before treatments (control, $n = 6$) and after addition of 1 µM JYL-1511 (JYL-1511, $n = 6$). Capsaicin responses were also determined in the presence of 1 µM JYL-1511 (JYL-1511 + capsaicin, $n = 6$). Finally, capsaicin responses alone (1 µM, without any pretreatment) were also measured on a different set of arteries (capsaicin, $n = 7$). The efficacy of JYL-1511 as a partial agonist was expressed as the percentage of decrease in arteriolar diameter evoked by the application of capsaicin alone (100%, capsaicin). Its efficacy as a partial antagonist was expressed as the percentage of decrease in capsaicin constriction (100%, capsaicin) in the presence of JYL-1511 (1 µM, JYL-1511 + capsaicin).

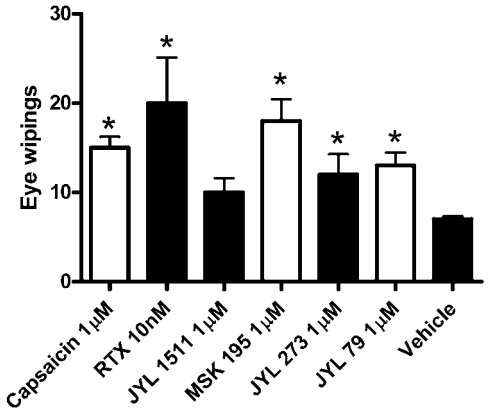

Figure 12

Sensory neuronal irritation evoked by application of the TRPV1 ligands. TRPV1 agonists or vehicle were applied in the eye of rats to determine their ability to evoke sensory neuronal irritation. Number of eye wipes was counted for 60 s after application of 10 µL of the drugs onto the conjunctiva of the rats. Concentrations of the drugs were chosen to represent the highest dose used in the vascular experiments (indicated in the figure). Columns represent mean ± SEM ($n = 5$), significant differences ($P < 0.05$) from the control (wipes upon administration of the vehicle alone) are represented by asterisks.

Table 1

Pharmacological properties of TRPV1 agonists

Agonist	Dorsal root ganglion/CHO-TRPV1 K_i (binding)	Dorsal root ganglion/CHO-TRPV1 EC_{50} ($^{45}Ca^{2+}$ uptake)	CHO-TRPV1 EC_{50} (intracellular Ca^{2+})	Acute desensitization	Arteriolar TRPV1 (vasoconstriction) Potency	Arteriolar TRPV1 (vasoconstriction) Efficacy	Arteriolar TRPV1 (vasoconstriction) Acute desensitization	Tachyphylaxis
Capsaicin	1.8 ± 0.3 µM (Wang *et al.*, 2003)	95 ± 8 nM (Pearce *et al.*, 2008)	35 ± 11 nM (Toth *et al.*, 2005b)	+ (Toth *et al.*, 2005b)	221 nM	58 ± 7%	+	–
Resiniferatoxin	23 pM (Lee *et al.*, 2001)	1.5 ± 0.3 nM (Pearce *et al.*, 2008)	81 ± 20 pM (Toth *et al.*, 2005b)	– (Toth *et al.*, 2005b)	>10 nM	No effect at 10 nM	N/A	+
JYL-273	11 ± 4 nM (Lee *et al.*, 2001)	361 ± 54 nM (Lee *et al.*, 2002)	No data	No data	>3 µM	No effect at 1 µM	N/A	+
MSK-195	No data	162 ± 33 nM (Lee *et al.*, 2002)	52 ± 12 nM (Toth *et al.*, 2005b)	– (Toth *et al.*, 2005b)	120 nM	71 ± 11%	+	+
JYL-79	19 ± 4 nM (Lee *et al.*, 2001)	58 ± 8 nM (Lee *et al.*, 2002)	2.4 ± 1.0 nM (Toth *et al.*, 2005b)	– (Toth *et al.*, 2005b)	3.9 nM	36 ± 8%	+	+
JYL-1511	50 ± 17 nM (Wang *et al.*, 2003)	3.4 ± 0.5 µM (Wang *et al.*, 2003)	No data	+ (Wang *et al.*, 2003)	N/A	No effect at 1 µM	N/A	+/–

concentrated on the exploitation of the obvious potential of sensory neuronal TRPV1 as an analgesic target. Another reason was that stimulation of sensory neuronal TRPV1 in the perivascular nerves evokes vasodilatation (Zygmunt *et al.*, 1999), probably obscuring the vasoconstrictor response in many cases. In accordance with this latter mechanism, earlier reports showed concentration-dependent biphasic effects of TRPV1 stimulation; low dose capsaicin evoked dilatation, while higher concentrations resulted in constriction (Edvinsson *et al.*, 1990; Dux *et al.*, 2003). This suggested the involvement of different receptors or different pharmacology for TRPV1-mediating vascular dilatation and constriction.

Although the mechanism of the vasoconstrictor effects of TRPV1 agonists were generally not investigated in detail (Porszasz *et al.*, 2002; Dux *et al.*, 2003; Keeble and Brain, 2006), it was suggested that TRPV1-induced vasoconstriction is probably mediated by endothelin-1 (Szolcsanyi *et al.*, 2001) or substance P (Scotland *et al.*, 2004) release from sensory neurons.

We have recently shown that stimulation of TRPV1 in skeletal muscle arterioles results in a substantial vasoconstriction (Lizanecz *et al.*, 2006). Moreover, intra-arterial injection of capsaicin into the hind limb evoked a dose-dependent increase in blood flow in the skin (probably representing vasodilatation in this organ) and simultaneously, a decrease of blood flow in skeletal muscle (representing vasoconstriction) (Kark *et al.*, 2008). These data suggested that vascular TRPV1 have sensory neuron-independent physiological effects.

The TRPV1 specificity of capsaicin-mediated arteriolar vasoconstriction was ultimately proven here. Most importantly, capsaicin-mediated responses were absent in TRPV1 knockout mice (Figure 2C). Moreover, an effort was also made to investigate the potential mechanisms. The intracellular Ca^{2+} concentration measurements we obtained showed that capsaicin increased the diameter of the arterial wall of skeletal muscle arteries (Figure 3), as well as in isolated arteriolar smooth muscle cells (Figure 4). Although only 10 out of 28 isolated smooth muscle cells responded to capsaicin, these data strongly suggest that functional TRPV1 is expressed in arterial smooth muscle cells and that the activation of these receptors leads to an increase in smooth muscle intracellular Ca^{2+} concentrations and to vasoconstriction. Next, the effects of pharmacological TRPV1 inhibition on this response were tested. The TRPV1 antagonist AMG9810 (previously tested on exogenous and sensory neuronal TRPV1) inhibited this capsaicin-evoked arteriolar constriction in a competitive fashion. These findings suggest that TRPV1 antagonists developed as analgesic agents may also interfere with skeletal muscle blood perfusion by inhibiting vascular TRPV1.

Nonetheless, the major goal of this present work was to investigate the structure-activity relationship of TRPV1 agonists for the vascular TRPV1 in functional assays. Our results confirmed that TRPV1 stimulation by capsaicin evokes a substantial constriction in isolated cannulated skeletal muscle arteries (Lizanecz *et al.*, 2006; Kark *et al.*, 2008). Here, a series of commercially available agonists were also tested in addition to capsaicin. Significant differences in potency, efficacy and desensitization were found (Table 1). It was observed that some of the TRPV1 agonists (such as resiniferatoxin, JYL-273) were able to desensitize vascular TRPV1 without any apparent vascular effects. This behaviour of resiniferatoxin in the vascular diameter assay is not unprecedented; a very similar action ('desensitization' to capsaicin without prior activation) has been demonstrated for pulmonary chemoreflex (Szolcsanyi *et al.*, 1990). One hypothesis for this desensitization is that low level activation of TRPV1 with certain structures may be sufficient to evoke complete tachyphylaxis, without increasing the intracellular Ca^{2+} concentrations to those levels needed to induce vasoconstriction. Alternatively, tachyphylaxis may be the reason for the irreversible activation of TRPV1 by resiniferatoxin (Jeffry *et al.*, 2009) leading to a sustained Ca influx. To measure the level of activation needed to evoke tachyphylaxis a partial agonist (JYL-1511) was used. Its partial antagonism was confirmed on vascular receptors (about 10% agonism and 70% antagonism), and its application resulted in significant tachyphylaxis, suggesting a role for desensitization rather than sustained Ca^{2+} influx in this system. In addition, although the functional response to capsaicin was transient and the arteries were completely desensitized to capsaicin, after a 40 min regeneration period, capsaicin was able to evoke vasoconstriction, suggesting resensitization of the arteries and only a partial tachyphylaxis. Taken together, these results suggest the vascular smooth muscle-located receptor and also the TRPV1 responsible for eye irritation upon capsaicin treatment *in vivo* (Figure 12) seem to have different ligand selectivity for desensitization from that of the TRPV1 expressed in CHO cells (Table 1).

It was observed that the kinetics of acute desensitization were different in the case of agonists evoking vascular constriction. With capsaicin, complete acute desensitization was observed, while for other agonists, JYL-79, MSK-195, only a partial desensitization was observed. The fact that different agonists evoked responses with different durations suggests that TRPV1 agonists may be tailored to desired duration of vascular effects.

Several mechanisms have been suggested to regulate TRPV1 sensitivity and desensitization. These include PKC- (Bhave, 2003) or PKA- (Bhave *et al.*, 2002) mediated phosphorylation and calcineurin-mediated dephosphorylation (Docherty *et al.*, 1996). As regards TRPV1 mediating skeletal muscle vasoconstriction, phosphorylation seems to be the most likely candidate. It was found that anandamide (Lizanecz *et al.*, 2006), similar to resiniferatoxin and JYL-273 (shown in this report), evokes complete tachyphylaxis on vascular TRPV1 without functional effects. However, it was also shown, that the anandamide-mediated tachyphylaxis was antagonized by a protein phosphatase 2B (calcineurin) inhibitor (Lizanecz *et al.*, 2006). Moreover, in accordance with this hypothesis, TRPV1 responses to agonists were differently modulated by inhibition of calcineurin in a CHO-TRPV1 cell line (Pearce *et al.*, 2008), suggesting ligand selectivity for phosphorylation-dependent TRPV1 sensitization/desensitization/tachyphylaxis.

Taken together, our results indicate that TRPV1 (a non-specific Ca^{2+} channel) activation leads to an increase in intracellular Ca^{2+} concentrations in isolated coronary smooth muscle cells and in the wall of isolated skeletal muscle arteries, resulting in vasoconstriction. The pharmacological profile of the vascular TRPV1 differs from that of the TRPV1 population responsible for sensory irritation. Arteriolar

TRPV1 was inhibited by a competitive TRPV1 antagonist developed as an analgesic suggesting that vascular TRPV1 activation may represent a side effect of TRPV1 antagonists when used as analgesics *in vivo*. Moreover, vascular TRPV1 may be a new therapeutic target for the regulation of tissue blood distribution.

Acknowledgements

The study was supported by the Hungarian Academy of Sciences OTKA (K68077 and K84300 to AT and T046244 to RP) and by the Hungarian Ministry of Health (ETT 377/2009 to AT); the work is supported by the TÁMOP 4.2.1./B-09/1/KONV-2010-0007 project (to AT and ZP). The project is implemented through the New Hungary Development Plan, co-financed by the European Social Fund; and by the National Innovation Office of Hungary (Baross Gábor Project, ÉletMent). Finally, AT was supported by the Bolyai János Research Scholarship of the Hungarian Academy of Sciences.

Conflicts of interest

The authors report no conflicts of interest.

References

Alexander SPH, Mathie A, Peters JA (2011). Guide to Receptors and Channels (GRAC), 5th Edition. Br J Pharmacol 164 (Suppl. 1): S1–S324.

Arunlakshana O, Schild HO (1959). Some quantitative uses of drug antagonists. Br J Pharmacol Chemother 14: 48–58.

Bhave G (2003). From the cover: protein kinase C phosphorylation sensitizes but does not activate the capsaicin receptor transient receptor potential vanilloid 1 (TRPV1). Proc Natl Acad Sci USA 100: 12480–12485.

Bhave G, Zhu W, Wang H, Brasier DJ, Oxford GS, Gereau R (2002). cAMP-dependent protein kinase regulates desensitization of the capsaicin receptor (VR1) by direct phosphorylation. Neuron 35: 721–731.

Caterina MJ, Schumacher MA, Tominaga M, Rosen TA, Levine JD, Julius D (1997). The capsaicin receptor: a heat-activated ion channel in the pain pathway. Nature 389: 816–824.

Di Marzo V, Blumberg PM, Szallasi A (2002). Endovanilloid signaling in pain. Curr Opin Neurobiol 12: 372–379.

Docherty RJ, Yeats JC, Bevan S, Boddeke HW (1996). Inhibition of calcineurin inhibits the desensitization of capsaicin-evoked currents in cultured dorsal root ganglion neurones from adult rats. Pflugers Arch 431: 828–837.

Donnerer J, Lembeck F (1982). Analysis of the effects of intravenously injected capsaicin in the rat. Naunyn Schmiedebergs Arch Pharmacol 320: 54–57.

Duckles SP (1986). Effects of capsaicin on vascular smooth muscle. Naunyn Schmiedebergs Arch Pharmacol 333: 59–64.

Dux M, Santha P, Jancso G (2003). Capsaicin-sensitive neurogenic sensory vasodilatation in the dura mater of the rat. J Physiol 552: 859–867.

Edvinsson L, Jansen I, Kingman TA, McCulloch J (1990). Cerebrovascular responses to capsaicin *in vitro* and *in situ*. Br J Pharmacol 100: 312–318.

Gavva NR, Tamir R, Qu Y, Klionsky L, Zhang TJ, Immke D *et al.* (2005). AMG 9810 [(E)-3-(4-t-butylphenyl)-N-(2,3-dihydrobenzo[b][1,4] dioxin-6-yl)acrylamide], a novel vanilloid receptor 1 (TRPV1) antagonist with antihyperalgesic properties. J Pharmacol Exp Ther 313: 474–484.

Gavva NR, Bannon AW, Surapaneni S, Hovland DN Jr, Lehto SG, Gore A *et al.* (2007). The vanilloid receptor TRPV1 is tonically activated *in vivo* and involved in body temperature regulation. J Neurosci 27: 3366–3374.

Gavva NR, Treanor JJ, Garami A, Fang L, Surapaneni S, Akrami A *et al.* (2008). Pharmacological blockade of the vanilloid receptor TRPV1 elicits marked hyperthermia in humans. Pain 136: 202–210.

Gunthorpe MJ, Szallasi A (2008). Peripheral TRPV1 receptors as targets for drug development: new molecules and mechanisms. Curr Pharm Des 14: 32–41.

Jakab B, Helyes Z, Varga A, Bolcskei K, Szabo A, Sandor K *et al.* (2005). Pharmacological characterization of the TRPV1 receptor antagonist JYL1421 (SC0030) *in vitro* and *in vivo* in the rat. Eur J Pharmacol 517: 35–44.

Jeffry JA, Yu SQ, Sikand P, Parihar A, Evans MS, Premkumar LS (2009). Selective targeting of TRPV1 expressing sensory nerve terminals in the spinal cord for long lasting analgesia. PLoS ONE 4: e7021.

Kark T, Bagi Z, Lizanecz E, Pasztor ET, Erdei N, Czikora A *et al.* (2008). Tissue-specific regulation of microvascular diameter: opposite functional roles of neuronal and smooth muscle located vanilloid receptor-1. Mol Pharmacol 73: 1405–1412.

Keeble JE, Brain SD (2006). Capsaicin-induced vasoconstriction in the mouse knee joint: a study using TRPV1 knockout mice. Neurosci Lett 401: 55–58.

Khairatkar-Joshi N, Szallasi A (2009). TRPV1 antagonists: the challenges for therapeutic targeting. Trends Mol Med 15: 14–22.

Lee J, Lee J, Kim J, Kim SY, Chun MW, Cho H *et al.* (2001). N-(3-Acyloxy-2-benzylpropyl)-N′-(4-hydroxy-3-methoxybenzyl) thiourea derivatives as potent vanilloid receptor agonists and analgesics. Bioorg Med Chem 9: 19–32.

Lee J, Lee J, Kang MS, Kim KP, Chung SJ, Blumberg PM *et al.* (2002). Phenolic modification as an approach to improve the pharmacology of the 3-acyloxy-2-benzylpropyl homovanillic amides and thioureas, a promising class of vanilloid receptor agonists and analgesics. Bioorg Med Chem 10: 1171–1179.

Lizanecz E, Bagi Z, Pasztor ET, Papp Z, Edes I, Kedei N *et al.* (2006). Phosphorylation-dependent desensitization by anandamide of vanilloid receptor-1 (TRPV1) function in rat skeletal muscle arterioles and in Chinese hamster ovary cells expressing TRPV1. Mol Pharmacol 69: 1015–1023.

Molnar J, Gyorgy L (1967). Pulmonary hypertensive and other haemodynamic effects of capsaicin in the cat. Eur J Pharmacol 1: 86–92.

Pearce LV, Toth A, Ryu H, Kang DW, Choi HK, Jin MK *et al.* (2008). Differential modulation of agonist and antagonist structure activity relations for rat TRPV1 by cyclosporin A and other protein phosphatase inhibitors. Naunyn Schmiedebergs Arch Pharmacol 377: 149–157.

Porszasz R, Porkolab A, Ferencz A, Pataki T, Szilvassy Z, Szolcsanyi J (2002). Capsaicin-induced nonneural vasoconstriction in canine mesenteric arteries. Eur J Pharmacol 441: 173–175.

Ross RA (2003). Anandamide and vanilloid TRPV1 receptors. Br J Pharmacol 140: 790–801.

Scotland RS, Chauhan S, Davis C, De Felipe C, Hunt S, Kabir J *et al.* (2004). Vanilloid receptor TRPV1, sensory C-fibers, and vascular autoregulation: a novel mechanism involved in myogenic constriction. Circ Res 95: 1027–1034.

Steiner AA, Turek VF, Almeida MC, Burmeister JJ, Oliveira DL, Roberts JL *et al.* (2007). Nonthermal activation of transient receptor potential vanilloid-1 channels in abdominal viscera tonically inhibits autonomic cold-defense effectors. J Neurosci 27: 7459–7468.

Szallasi A, Blumberg PM (1999). Vanilloid (capsaicin) receptors and mechanisms. Pharmacol Rev 51: 159–212.

Szallasi A, Cortright DN, Blum CA, Eid SR (2007). The vanilloid receptor TRPV1: 10 years from channel cloning to antagonist proof-of-concept. Nat Rev Drug Discov 6: 357–372.

Szolcsanyi J, Szallasi A, Szallasi Z, Joo F, Blumberg PM (1990). Resiniferatoxin: an ultrapotent selective modulator of capsaicin-sensitive primary afferent neurons. J Pharmacol Exp Ther 255: 923–928.

Szolcsanyi J, Oroszi G, Nemeth J, Szilvassy Z, Blasig IE, Tosaki A (2001). Functional and biochemical evidence for capsaicin-induced neural endothelin release in isolated working rat heart. Eur J Pharmacol 419: 215–221.

Toda N, Usui H, Nishino N, Fujiwara M (1972). Cardiovascular effects of capsaicin in dogs and rabbits. J Pharmacol Exp Ther 181: 512–521.

Toth A, Boczan J, Kedei N, Lizanecz E, Bagi Z, Papp Z *et al.* (2005a). Expression and distribution of vanilloid receptor 1 (TRPV1) in the adult rat brain. Brain Res Mol Brain Res 135: 162–168.

Toth A, Wang Y, Kedei N, Tran R, Pearce LV, Kang SU *et al.* (2005b). Different vanilloid agonists cause different patterns of calcium response in CHO cells heterologously expressing rat TRPV1. Life Sci 76: 2921–2932.

Wang Y, Toth A, Tran R, Szabo T, Welter JD, Blumberg PM *et al.* (2003). High-affinity partial agonists of the vanilloid receptor. Mol Pharmacol 64: 325–333.

Zygmunt PM, Petersson J, Andersson DA, Chuang H, Sorgard M, Di Marzo V *et al.* (1999). Vanilloid receptors on sensory nerves mediate the vasodilator action of anandamide. Nature 400: 452–457.

Life Sciences 90 (2012) 407–415

Contents lists available at SciVerse ScienceDirect

Life Sciences

journal homepage: www.elsevier.com/locate/lifescie

Vascular metabolism of anandamide to arachidonic acid affects myogenic constriction in response to intraluminal pressure elevation

Ágnes Czikora [a], Erzsébet Lizanecz [a], Judit Boczán [b], Andrea Daragó [a], Zoltán Papp [a,c], István Édes [a,c], Attila Tóth [a,c,*]

[a] Institute of Cardiology, Division of Clinical Physiology, University of Debrecen, Medical and Health Science Center, Debrecen, Hungary
[b] Department of Neurology, University of Debrecen, Medical and Health Science Center, Debrecen, Hungary
[c] Research Center for Molecular Medicine, University of Debrecen, Medical and Health Science Center, Debrecen, Hungary

ARTICLE INFO

Article history:
Received 19 November 2010
Accepted 17 December 2011

Keywords:
Anandamide
Arachidonic acid
Vasodilation
Resistance artery
Myogenic response
Vascular autoregulation
Cannabinoid receptor
Vanilloid receptor (TRPV1)

ABSTRACT

Aims: We hypothesized that arachidonic acid produced by anandamide breakdown contributes to the vascular effects of anandamide.
Main methods: Isolated, pressurized rat skeletal muscle arteries, which possess spontaneous myogenic tone, were treated with anandamide, arachidonic acid, capsaicin (vanilloid receptor agonist), WIN 55-212-2 (cannabinoid receptor agonist), URB-597 (FAAH inhibitor), baicalein (lipoxygenase inhibitor), PPOH (cytochrome P450 inhibitor), and indomethacin (cyclooxygenase inhibitor). Changes in the arteriolar diameter in response to the various treatments were measured. To assess the effect of anandamide metabolism, anandamide was applied for 20 min followed by washout for 40 min. This protocol was used to eliminate other, more direct effects of anandamide in order to reveal how anandamide metabolism may influence vasodilation.
Key findings: Anandamide at a low dose (1 μM) evoked a loss of myogenic tone, while a high dose (30 μM) not only attenuated the myogenic response but also evoked acute dilation. Both of these effects were inhibited by the FAAH inhibitor URB-597 and were mimicked by arachidonic acid. The CB1 and CB2 agonist R-WIN 55-212-2 and the vanilloid receptor agonist capsaicin were without effect on the myogenic response. The inhibition of the myogenic response by anandamide was blocked by indomethacin and PPOH, but not by baicalein or removal of the endothelium. FAAH expression in the smooth muscle cells of the blood vessels was confirmed by immunohistochemistry.
Significance: Anandamide activates the arachidonic acid pathway in the microvasculature, affecting vascular autoregulation (myogenic response) and local perfusion.

Introduction

Anandamide (N-arachidonoylethanolamine) was identified as a brain constituent which binds to cannabinoid receptors (Devane, et al., 1992). It has since been shown that anandamide is not only an endogenous ligand for cannabinoid receptors (CB1 and CB2) but may also affect vanilloid receptor 1 (Zygmunt, et al., 1999) and additional other, recently identified targets (Alexander and Kendall, 2007).

Anandamide is synthesized in the periphery by activated macrophages (Di Marzo, et al., 1996; Wagner, et al., 1997) and primary sensory neurons (Ahluwalia, et al., 2003). It is important to note that anandamide, in contrast to classical neurotransmitters, is not stored in the cells. Instead, it is synthesized upon receptor stimulation and immediately released (Di Marzo, et al., 1994). The effects of anandamide are readily terminated by intracellular hydrolysis (Di Marzo, et al., 1994), which is catalyzed by fatty acid amide hydrolase (FAAH) (Cravatt, et al., 1996) as well as by other, less characterized enzymes (Alexander and Kendall, 2007).

Anandamide evokes vasodilation in various arteriolar beds of different species (Ellis et al., 1995; Randall and Kendall, 1997; Pratt et al., 1998; Jarai et al., 1999; Wagner et al., 1997; O'Sullivan et al., 2004). Its effectiveness ranges from robust (Zygmunt, et al., 1999; Herradon, et al., 2007) to slight (Lopez-Miranda, et al., 2004; Mukhopadhyay, et al., 2002; O'Sullivan, et al., 2004, 2005) to evoke relaxation in conduit arteries. Although stimulation of cannabinoid and vanilloid receptors can evoke vasodilatation, in many cases anandamide mediated vasodilatation was found to be independent of these receptors (Herradon, et al., 2007; O'Sullivan, et al., 2004, 2005; Jarai, et al., 1999).

Blood vessels respond to intraluminal pressure elevation with constriction and to pressure reduction with dilatation; this behavior

* Corresponding author at: 22 Móricz Zs krt., 4032, Debrecen, Hungary. Tel.: +36 52 411717x56274; fax: +36 52 255978.
E-mail address: atitoth@dote.hu (A. Tóth).

0024-3205/$ – see front matter © 2012 Elsevier Inc. All rights reserved.
doi:10.1016/j.lfs.2011.12.016

is termed the "myogenic response". The myogenic response is most pronounced in resistance arteries like those of skeletal muscle. Moreover, the myogenic response in these arteries is mediated at least in part by arachidonic acid metabolites, such as 20-HETE (Frisbee, et al., 2001).

There are two distinct mechanisms for inducing dilatation in the case of cannulated, skeletal muscle arterioles possessing spontaneous myogenic tone. These are (i) activation of pathways of dilatation unrelated to the mechanisms responsible for the myogenic response or (ii) inhibition of spontaneous vasoconstrictive mechanisms responsible for the myogenic response.

Here, we report that altered myogenic response may contribute to anandamide mediated vasodilatation under *in vivo* conditions when intraluminal pressure is not held constant. This effect is mediated by activation of the arachidonic acid pathway by anandamide breakdown and is not mimicked by cannabinoid or vanilloid receptor activation. Our data suggest that anandamide is a transmitter molecule trans-activating arachidonic acid sensitive intracellular signaling in cells expressing FAAH.

Materials and methods

Preparation of cannulated skeletal muscle arterioles

Preparation of arteries was similar to that described earlier (Lizanecz, et al., 2006). Briefly, male Wistar rats (116 rats) obtained from Charles River (Isaszeg, Hungary) were fed with CRLT/N chow (Szinbad Kft, Godollo, Hungary). The rats (200–300 g) were anesthetized with an intraperitoneal injection of pentobarbital sodium (50 mg kg^{-1}). A segment of the gracilis muscle arteriole (~0.5 mm in length) was isolated and transferred into an organ chamber filled with a physiological salt solution (PSS) composed of (in mM) 110 NaCl, 5.0 KCl, 2.5 $CaCl_2$, 1.0 $MgSO_4$, 1.0 KH_2PO_4, 5.0 glucose and 24.0 $NaHCO_3$ equilibrated with a gas mixture of 10% O_2, 5% CO_2, 85% N_2, at pH 7.4. Arteries were then cannulated and the intraluminal pressure was set to 80 mm Hg (no flow conditions) and the organ bath was kept at 37 °C. The internal arteriolar diameter at the midpoint of the arteriolar segment was measured by videomicroscopy. Animal experiments were approved by the appropriate governmental organizations and were in accordance with the standards established by the National Institutes of Health.

Experimental protocol

Arteriolar functions were tested with acetylcholine (10 μM, induces endothelium dependent dilatation) and norepinephrine (10 μM, stimulates smooth muscle contraction) after the development of spontaneous myogenic tone (usually 40–60 min after cannulation) and before the beginning of the experimental treatments. Experiments were carried out at 80 mm Hg intraluminal pressure (except for determinations of myogenic response). In some cases arteriolar responses were studied after endothelium denudation. The endothelium of the arterioles was removed by perfusion of the vessels with air. Endothelium denudation was confirmed by the loss of dilation in response to acetylcholine and by the maintenance of dilation in the presence of the NO donor sodium nitroprusside.

Acute effects of anandamide (0.1–30 μM), arachidonic acid (1 μM), capsaicin (1 μM, vanilloid receptor 1 agonist, Lizanecz, et al., 2006) and WIN55-212-2 (1 μM, cannabinoid receptor agonist, Kim, et al., 2008) on arteriolar diameter were tested for 20 min with arteriolar diameter being measured every 10 s (Fig. 1A). In some cases, arteries were pretreated (5 min) with baicalein (1 μM, Machha, et al., 2007), indomethacin (10 μM, Xiang, et al., 2008), PPOH (20 μM, Xiang, et al., 2008) or URB-597 (1 μM, Piomelli, et al., 2006) before the addition of anandamide (1 or 30 μM). Concentrations of the drugs were selected according to the manufacturer's suggestions to achieve selective activation/inhibition of the desired targets.

After arteries were treated for 20 min as described above, they were then incubated with PSS alone for 40 min (washout of the original stimulus and a time-dependent action of its metabolites followed for 40 min, referred to as "regeneration" in the text). Arteriolar diameter was determined before addition of the drugs, after 20 min treatment, and finally, after the 40 min regeneration period.

Effects of the treatments on the myogenic response were also determined. Intraluminal pressure was set to 20–120 mm Hg in 20 mm Hg increments and arteriolar diameter was measured after 4 min incubations at each intraluminal pressure. These measurements were performed in PSS to assess the active myogenic response before the treatments and after the 40 min regeneration period. Passive diameter was determined in Ca^{2+} free PSS at the end of the experiments.

Immunohistochemical procedures

Tissue sections were prepared as detailed earlier (Kark, et al., 2008). Briefly, rat skeletal muscle (gracilis muscle) was dissected from Wistar rats and embedded in Tissue-Tek O.C.T compound (Electron Microscopy Sciences, Hatfield, PA, USA). Cryostat sections (thickness 10 μm) were placed on adhesive slides and fixed in acetone for 10 min. FAAH immunostaining was performed as described earlier (Cristino, et al., 2008). The slices were blocked with normal goat sera (1.5% in PBS, Sigma, St. Louis, MO, USA) for 20 min and stained with anti-FAAH (Cayman Chemical, Ann Arbor, MI, USA, dilution: 1:50) and with anti-smooth muscle actin antibodies (Sigma, St. Louis, MO, USA, dilution: 1:100) dissolved in the blocking buffer. The slices were then incubated with biotinylated anti-rabbit (Jackson, Suffolk, England, 1:300) and FITC conjugated anti-mouse antibodies (Jackson, Suffolk, England, 1:100). Biotinylated antibody was detected by Cy3 conjugated streptavidin (Jackson, Suffolk, England, 1:500). The pictures were captured by a digital camera (Scion, Frederick, MD, USA) attached to a Nikon Eclipse 80i fluorescent microscope and further processed by ImageJ software (freeware from www.nih.gov) software.

Data analysis and statistical procedures

Arteriolar diameter was determined by measuring the distances between the luminal sides of the arteriolar wall (internal diameter). Data are shown as average diameter ± SEM. Statistical analysis was made by GraphPad 5.0 using analysis of variance (repeated measures ANOVA) with Dunnett's *post hoc* test to detect significant differences from control values. P-values <0.05 were considered to be significant.

Drugs

Anandamide (N-arachidonoylethanolamine, Tocris, Ellisville, MO, USA) arachidonic acid (Sigma, St. Louis, MO, USA), capsaicin (8-methyl-N-vanillyl-*trans*-6-nonenamide, Sigma, St. Louis, MO, USA), baicalein (5, 6, 7- trihydroxyflavone, Tocris, Ellisville, MO, USA), indomethacin (1-(4-chlorobenzoyl)-5-methoxy-2-methyl-3-indoleacetic acid, Sigma, St. Louis, MO, USA), PPOH (6-(2-propargyloxyphenyl)hexanoic acid, Sigma, St. Louis, MO, USA), URB-597 ([3-(3-carbamoylphenyl)phenyl] N-cyclohexylcarbamate, Cayman Chemicals, Ann Arbor, MI, USA), WIN55-212-2 ((R)-(+)-[2,3-dihydro-5-methyl-3-(4-morpholinylmethyl) pyrrolo[1,2,3-de]-1,4-benzoxazin-6-yl]-1-naphthalenylmethanone mesylate, Tocris, Ellisville, MO, USA).

Results

Anandamide mediated effects were tested on isolated skeletal muscle resistance arteries from the rat. Anandamide (0.1 μM) was without effect upon 20 min treatment or after 40 min regeneration

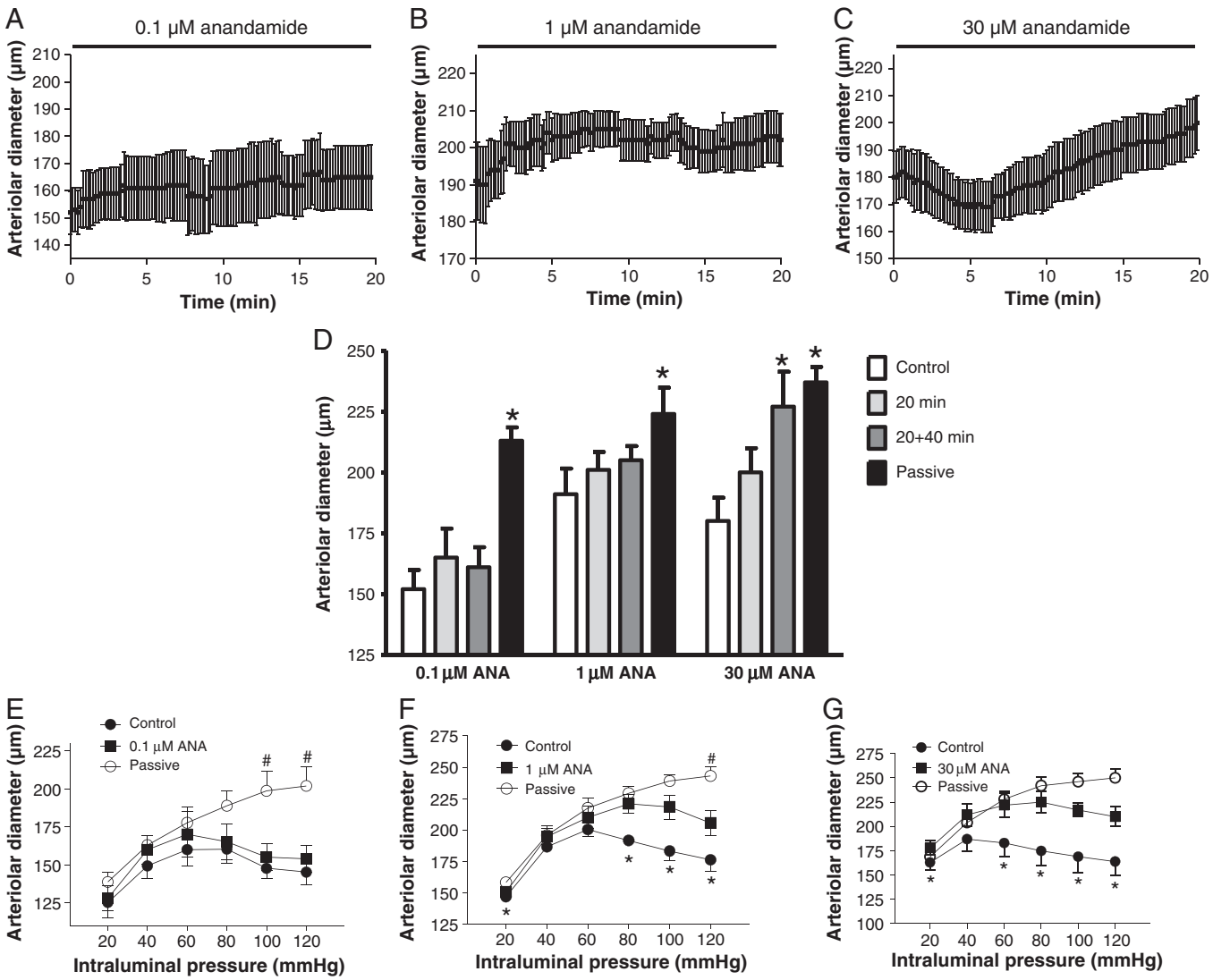

Fig. 1. Anandamide evoked effects on skeletal muscle resistance arterioles.Isolated arterioles were treated with anandamide (0.1, 1, 30 μM, n = 4, 5, 10, Graphs A–C, respectively) for 20 min. Arteriolar diameter was measured every 10 s during the 20 min continuous treatments and symbols represent average ± SEM (Graphs A–C). Fig. 1D summarizes changes in arteriolar diameter upon the above mentioned treatments. Open bars represent the control diameter before the addition of anandamide, light gray bars represent the diameter at the end of the 20 min continuous application of anandamide, dark gray bars represent the arteriolar diameter after regeneration (washing then 40 min incubation in physiological buffer after the treatments), and black bars represent the maximal diameter of the arteries determined by the application of 10 μM acetylcholine. Bars show the average ± SEM (number of independent experiments = 4–10); significant differences (paired Student's *t*-test, $P<0.05$) from the control are represented by asterisks. Finally, the effect of anandamide treatments (0.1, 1 and 30 μM, n = 4, 5, 10, Graphs E–G, respectively) was determined on the myogenic response of the arterioles. Arteriolar diameter was measured at 20–120 mm Hg intraluminal pressures before anandamide treatments (Control, ●), after 20 min anandamide treatment with the indicated concentration followed by 40 min regeneration (■) and finally in the absence of extracellular Ca^{2+}(Passive, ○). Symbols are mean ± SEM. Significant deviations (repeated measures ANOVA with Dunnett's post hoc test, $P<0.05$) of vascular diameter upon treatments from active diameter (*) or from passive diameter (#) of the same arteries are labeled.

(Fig. 1A), while higher doses showed vasoactivity. In particular, 1 μM anandamide evoked a transient dilation (Fig. 1B); 30 μM evoked a transient constriction followed by dilation at the end of the incubation (20 min, Fig. 1C and D) and this dilation was further increased over the 40 min regeneration period (incubation in PSS alone, Fig. 1D). The arteries used in this study possessed a spontaneous myogenic tone (constriction upon elevated intraluminal pressure). We hypothesized that the dilations observed under our *in vivo* conditions, where intraluminal pressure is not constant, may be related to a blunted myogenic response. To test this hypothesis in detail, the myogenic response of these arterioles was determined at the beginning of the experiments (control), at the end of the 20 min treatment + 40 min regeneration in the presence of extracellular Ca^{2+} (active diameter), and in the absence of extracellular Ca^{2+} (passive diameter). 0.1 μM anandamide was without effect on the myogenic response (Fig. 1E), while higher doses of anandamide (1 and 30 μM, Fig. 1F and G, respectively) effectively antagonized the myogenic response.

These findings suggested the existence of an anandamide sensitive pathway which may evoke dilation mediated by the synthesis and release of dilative agents, or alternatively, may impair the vascular myogenic response. In general, the major source of dilative substances is the endothelium while the myogenic response is inherent to smooth muscle cells. We therefore examined the behavior of endothelium denuded arterioles. First, the effect of denudation was tested by the application of acetylcholine (Fig. 2A). Acetylcholine responses were blunted after denudation (increase in arteriolar diameter from 180 ± 8 to 242 ± 11 μm in the case of control, $P<0.05$, compared to no change (173 ± 14 to 188 ± 10 μm) in the case of endothelium denuded arterioles, n = 5). In contrast, smooth muscle function was not altered significantly by the procedure as shown by sodium

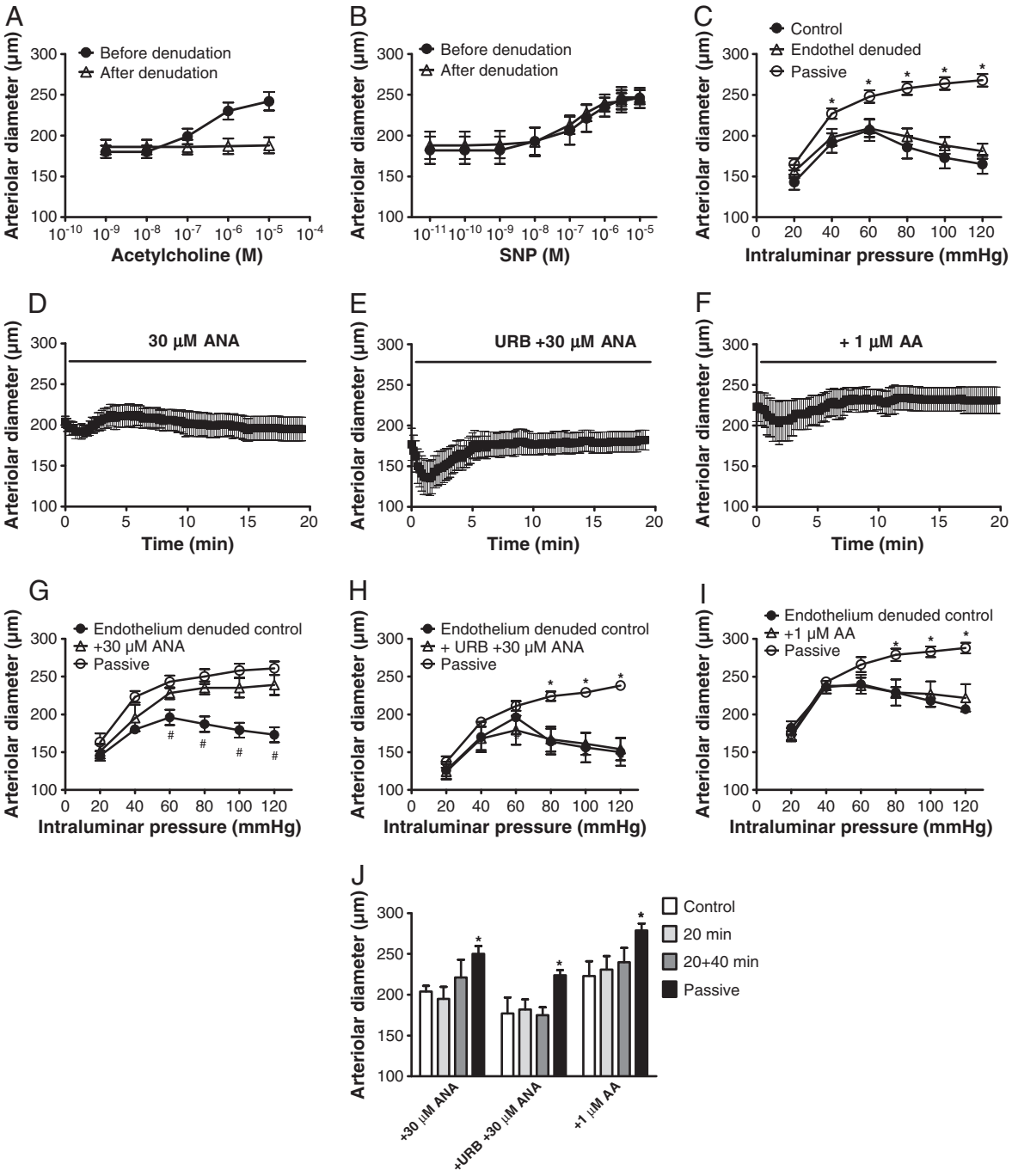

Fig. 2. Effects of endothelium denudation on the functional responses to anandamide.Denudation of the arteries was performed as described in methods. The effectivity of denudation was reflected in blunting of the acetylcholine responsiveness (Graph A, n = 5). The potential toxic effects of denudation on smooth muscle cell function were also tested. First, the endothelium-independent dilator sodium nitroprusside was administered (SNP, Graph B, n = 5). Next, arteriolar diameter was plotted (Graph C) at 20–120 mm Hg intraluminal pressures before (●) and after denudation (Δ) along with the arteriolar diameters in the absence of extracellular Ca^{2+} (Passive, ○). Arteriolar myogenic response was also tested after anandamide treatment (30 μM, 20 min followed by 40 min regeneration, Graph G, n = 5) and arachidonic acid treatment (1 μM, 20 min followed by 40 min regeneration, Graph I, n = 4). Anandamide mediated effects were also tested in the absence of the FAAH inhibitor URB-957 (1 μM, 15 min pretreatment before anandamide application, Graph H, n = 5). Acute effects of the treatments on the diameter of the endothelium denuded arterioles were measured every 10 s during the 20 min continuous treatments (Graph D–F). After the 20 min treatment followed by washing and 40 min regeneration, the effects were determined on the myogenic response of the arterioles. Values were summarized in the bar graph (Graph J). Symbols are mean ± SEM. Significant deviations (repeated measures ANOVA with Dunnett's post hoc test, $P<0.05$) from the initial diameter are labeled by asterisks on the bar graph (Graph J). Significant deviations from the passive (#) or control (*) arteriolar diameter are also shown (Graph C and G–I).

nitroprusside mediated dilation (Fig. 2B, n = 5) or by the unaltered myogenic response of the arteries (Fig. 2C, n = 11). Having confirmed that we were able to successfully denude the arterioles, we compared the effects of 30 μM anandamide on the denuded arterioles and on those with an intact endothelium. Although anandamide mediated effects were biphasic in both cases (intact endothelium, Fig. 1C and D, versus endothelium denuded arteries, Fig. 2D and J), sustained dilation upon anandamide treatment was not present in endothelium denuded arteries. Nonetheless, a similar impairment of myogenic response was noted in the endothelium denuded arteries (Fig. 2G)

as it was observed for intact arteries (Fig. 1G). Inhibition of the metabolism of anandamide to arachidonic acid (1 μM URB-597, fatty amide hydrolase inhibitor) completely prevented the effects of 30 μM anandamide on the myogenic response (Fig. 2H), although it did not affect the acute responses to anandamide, under constant pressure (Fig. 2E and J). Application of 1 μM arachidonic acid evoked a vasoconstriction similarly to the previous treatments but was without any apparent additional effects on endothelium denuded arterioles (Fig. 2F, I and J).

Next, an effort was made to identify the anandamide receptors involved in the dilation of these resistance arterioles. The TRPV1 agonist capsaicin (1 μM, Figs. 3A and 4) evoked a transient vasoconstriction during the 20 min treatment, similar to the results we had reported earlier (Lizanecz, et al., 2006) but was without effect on the arteriolar diameter at the end of the treatment (20 min) or after the regeneration period. The CB1 and CB2 receptor agonist WIN55-212-2 (1 μM, Figs. 3B and 4) was without significant effects. These observations suggested a TRPV1 and cannabinoid receptor independent pathway in the acute dilation evoked by anandamide.

To identify this pathway, the dilation evoked by 30 μM anandamide (the dose which effectively dilated the arteries in 20 min, Figs. 3C and 4) was further investigated. Inhibition of the metabolism of anandamide to arachidonic acid (1 μM URB-597, Figs. 3D and 4) completely prevented anandamide mediated dilation. Arachidonic acid treatment (1 μM, Figs. 3E and 4) resulted in dilation similar to that for anandamide in the presence of endothelium. The effects of these treatments on vascular diameter after 40 min regeneration were also tested (Fig. 4). Again, no dilative effect of TRPV1 or CB1 and CB2 activation was found, while anandamide mediated dilation was lost upon the inhibition of the anandamide metabolizing enzyme FAAH (URB + ANA, Fig. 4) and was mimicked by arachidonic acid (Fig. 4).

Effects on the myogenic response were also studied in detail (Fig. 5). Stimulation of TRPV1 by capsaicin (1 μM, Fig. 5A) and of cannabinoid receptors by WIN55-212-2 (1 μM, Fig. 5B) were without effects on the myogenic response. On the contrary, 30 μM anandamide evoked a loss of myogenic response (Fig. 5C) which was completely

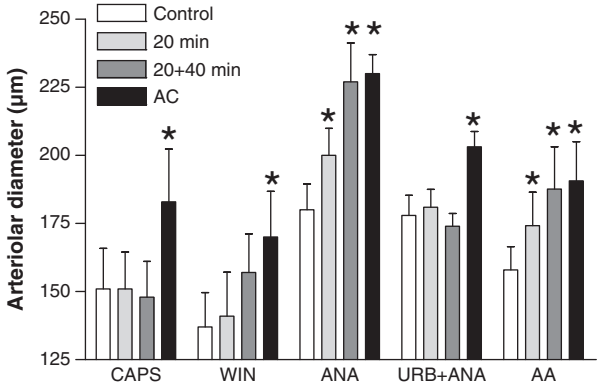

Fig. 4. Identification of the mechanisms of anandamide mediated effects: metabolic effects.Arteriolar diameter was measured before treatment (Control, white bars), after 20 min treatment (20 min, light gray bars) and after 40 min regeneration (20 + 40 min, dark gray bars). Maximal dilatative capacity of the arteries was determined at the beginning of the experiments (AC, diameter in the presence of 10 μM acetylcholine) and shown by black bars. Arteries were treated with capsaicin (CAPS, 1 μM, n = 9), WIN55-212-2 (WIN, 1 μM, n = 4), anandamide (ANA, 30 μM, n = 10) or arachidonic acid (AA, 1 μM, n = 5). Effects of FAAH inhibition (URB957, 1 μM, 5 min pre-treatment) on the anandamide (30 μM) response (URB + ANA, n = 7) were also tested. Bars are mean ± SEM. Significant differences (repeated measures ANOVA with Dunnett's post hoc test, $P<0.05$) from the control are represented by asterisks.

prevented by the FAAH inhibitor URB-597 (1 μM, Fig. 5D), similar to that in the absence of endothelium (Fig. 2G and H). Arachidonic acid (1 μM, Fig. 5E) evoked a loss of myogenic response similar to that by 30 μM anandamide in the presence of endothelium.

Based on these data, we hypothesized that the vascular dilation induced by anandamide was at least partly mediated by arachidonic acid resulting from its hydrolysis by FAAH and reflected the loss of myogenic response caused by this arachidonic acid. To test this hypothesis, 1 μM anandamide (the lowest dose found to be effective at antagonizing the myogenic response (Figs. 1 and 6A, E and F)) was

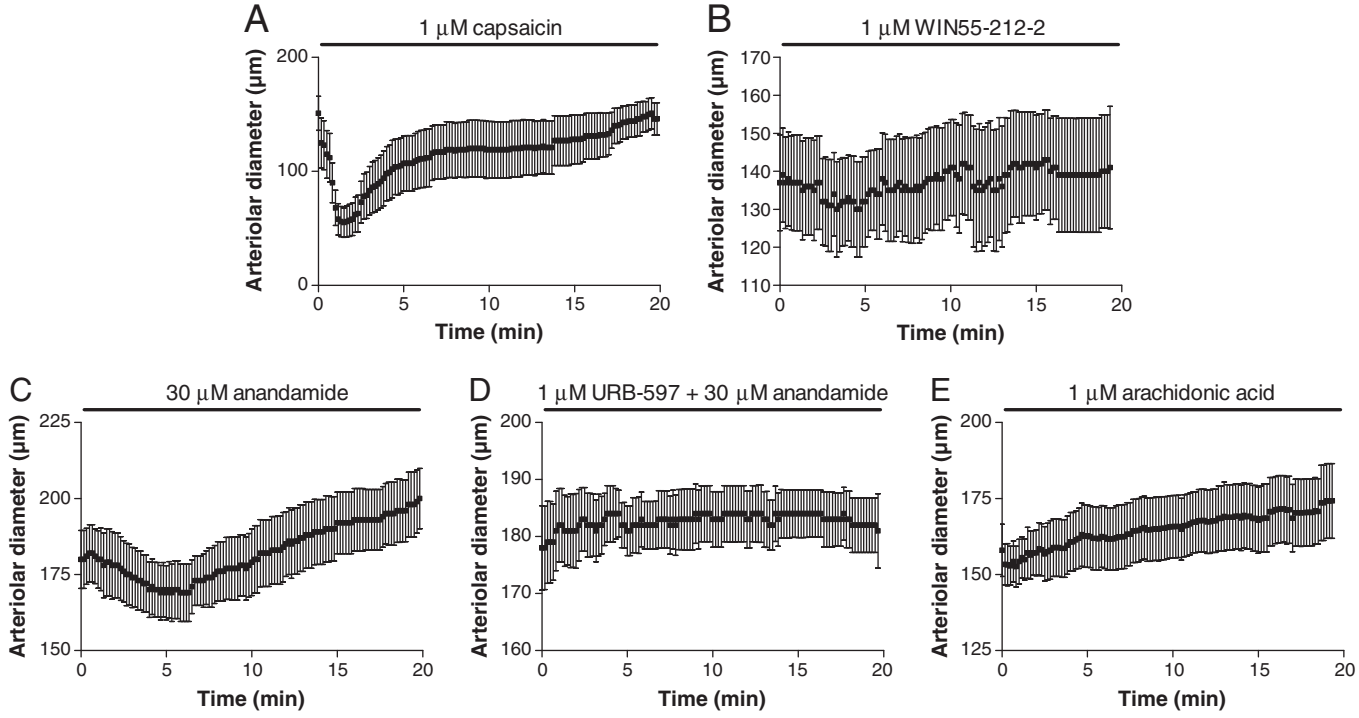

Fig. 3. Identification of the mechanisms of anandamide mediated effects: acute effects.Isolated arteries were treated with the TRPV1 agonist capsaicin (1 μM, n = 9, Graph A), the cannabinoid receptor agonist WIN 55-212-2 (1 μM, n = 4, Graph B), anandamide (30 μM, n = 10, Graph C) or arachidonic acid (1 μM, n = 5, Graph E) and arteriolar diameter was measured every 10 s during the 20 min incubation. In some cases, arteries were pre-treated for 5 min with the FAAH inhibitor URB-957 (1 μM) prior to anandamide (30 μM) addition (n = 7, Graph D). Symbols are mean ± SEM.

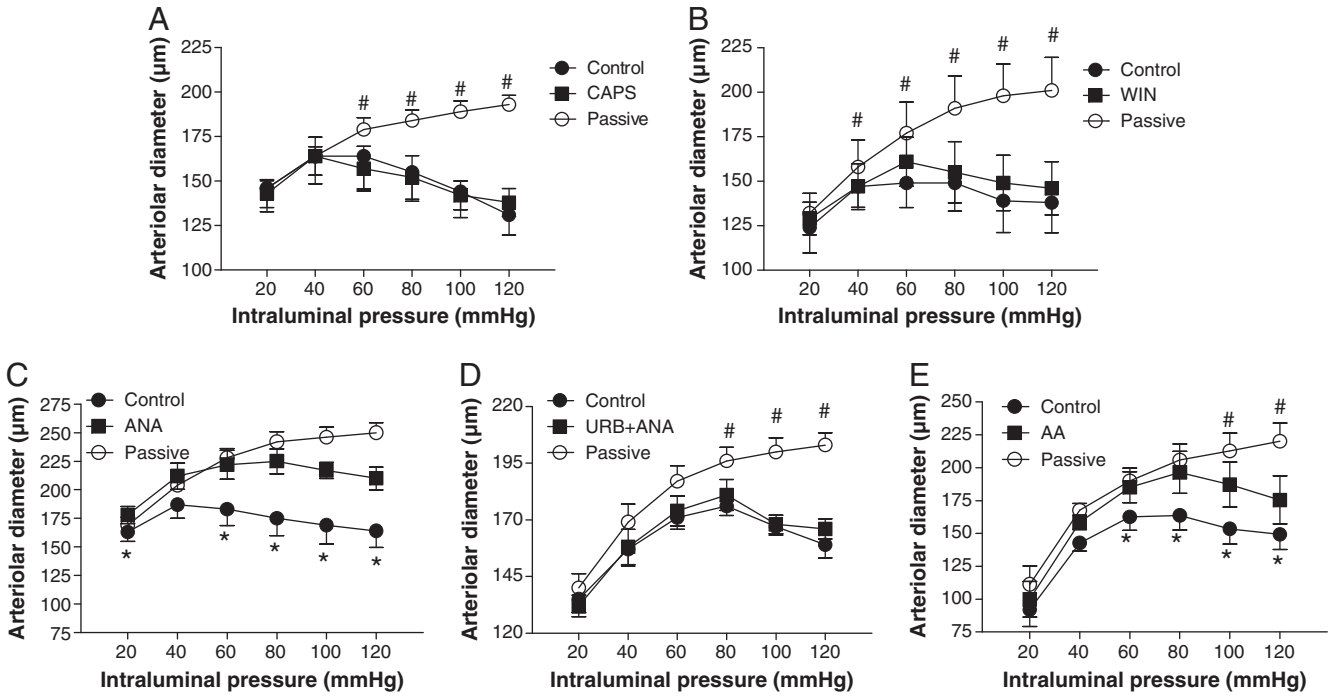

Fig. 5. Identification of the mechanisms of anandamide mediated effects: myogenic response.Arteriolar diameter was measured at intraluminal pressures of 20–120 mm Hg before (Control, ●) and after treatments (20 min treatment followed by 40 min regeneration, ■) in PSS. Passive diameter of the arteries was determined at the end of the experiments in the absence of extracellular Ca^{2+} (Passive, ○). Arteries were treated with capsaicin (CAPS, 1 μM, n = 9), WIN55-212-2 (WIN, 1 μM, n = 4), anandamide (ANA, 30 μM, n = 10) or arachidonic acid (AA, 1 μM, n = 5). Effects of FAAH inhibition (URB957, 1 μM, 5 min pre-treatment) on the anandamide (30 μM) response (URB + ANA, n = 7) were also tested. Symbols are mean ± SEM. Significant differences (repeated measures ANOVA with Dunnett's post hoc test, $P<0.05$) of vascular diameter upon treatments compared to the active diameter (*) or to the passive diameter (#) of the same arteries are labeled.

used and the main pathways responsible for the synthesis of vasoactive agents derived from arachidonic acid were selectively inhibited. 1 μM anandamide evoked a transient constriction if the lipoxygenase pathway (baicalein, 1 μM, Fig. 6B) or cytochrome P450 (PPOH, 20 μM, Fig. 6C) was inhibited. This vasoconstriction was similar to that found in the case of higher doses of anandamide (30 μM, Fig. 1C). Nonetheless, vascular diameter was generally not significantly different at the end of the treatments (Fig. 6A, B and C), nor were there any vascular effects after 40 min regeneration (Fig. 6E), except in the case of inhibition of cyclooxygenase by indomethacin (10 μM), which unmasked a fast and robust dilation evoked by 1 μM anandamide (Fig. 6D and E).

An effort was also made to identify the pathways involved in the mediation of anandamide evoked loss of the myogenic response. Baicalein did not abolish anandamide mediated loss of the myogenic response (Fig. 6G). In contrast, inhibition of cytochrome P450 by PPOH (20 μM) or of cyclooxygenase by indomethacin (10 μM) completely prevented the anandamide mediated loss of the myogenic response (Fig. 6H and I, respectively).

Finally, the vascular localization of the anandamide metabolizing enzyme FAAH was studied. FAAH expression was detected by immunhistochemistry in the smooth muscle layer of the same arteries which were isolated for the physiological measurements (Fig. 7).

Discussion

The aim of the study was to investigate the mechanism of anandamide evoked vasodilation in skeletal muscle resistance arteries of the rat. Our main results are: (1) anandamide effects were mediated by its FAAH mediated breakdown (catabolism) to arachidonic acid in these arterioles; (2) this pathway was related for the first time to the altered myogenic response; (3) effects of anandamide on the myogenic response were independent of endothelium; (4) the anandamide mediated loss of the myogenic response was mediated by the cytochrome P450 and cyclooxygenase pathways; and (5) anandamide mediated dilation under isobaric conditions appears to be dependent on the breakdown of anandamide by FAAH and the presence of functional endothelium. It is important to note that intraluminal pressure is not held constant under our *in vivo* conditions, so the contribution of anandamide metabolism and the blunted myogenic response to physiological dilation (resulting from endothelium dependent acute dilation and from endothelium independent blunted myogenic constriction) may be relevant.

The importance of anandamide catabolism *in vivo* has recently been recognized in different systems, highlighted by the fact that the anandamide level is 15 fold higher in FAAH knockout mice, accompanied with decreased nociception (Cravatt, et al., 1996), but no obvious hemodynamic differences compared to wild type littermates (Pacher, et al., 2005). It should be noted, however, that detailed examination of *in vivo* myogenic reactivity and autoregulatory ability is yet to be performed. A similar effect was observed by inhibition of FAAH by URB-597 (the same inhibitor which was used here), which evoked decreased inflammatory responses (Holt, et al., 2005; Jayamanne, et al., 2006; Jhaveri, et al., 2006). In these inflammatory pain models, the analgesic effects of FAAH inhibition were related to the elevated level of anandamide and presumably to higher stimulation of the analgesic cannabinoid receptors.

Anandamide was found to be rapidly metabolized in vascular preparations and it was suggested that its metabolism may limit anandamide effectiveness on vascular cannabinoid receptors (Ho and Randall, 2007). Moreover, vascular effects of anandamide breakdown products were published more than a decade ago, suggesting significant metabolism of anandamide to arachidonic acid and to prostaglandin E2 in cerebral arterioles, contributing to indomethacin (a cyclooxygenase inhibitor) dependent dilatations (Ellis, et al., 1995). These findings were confirmed in bovine coronary artery rings by experiments showing that inhibition of anandamide conversion

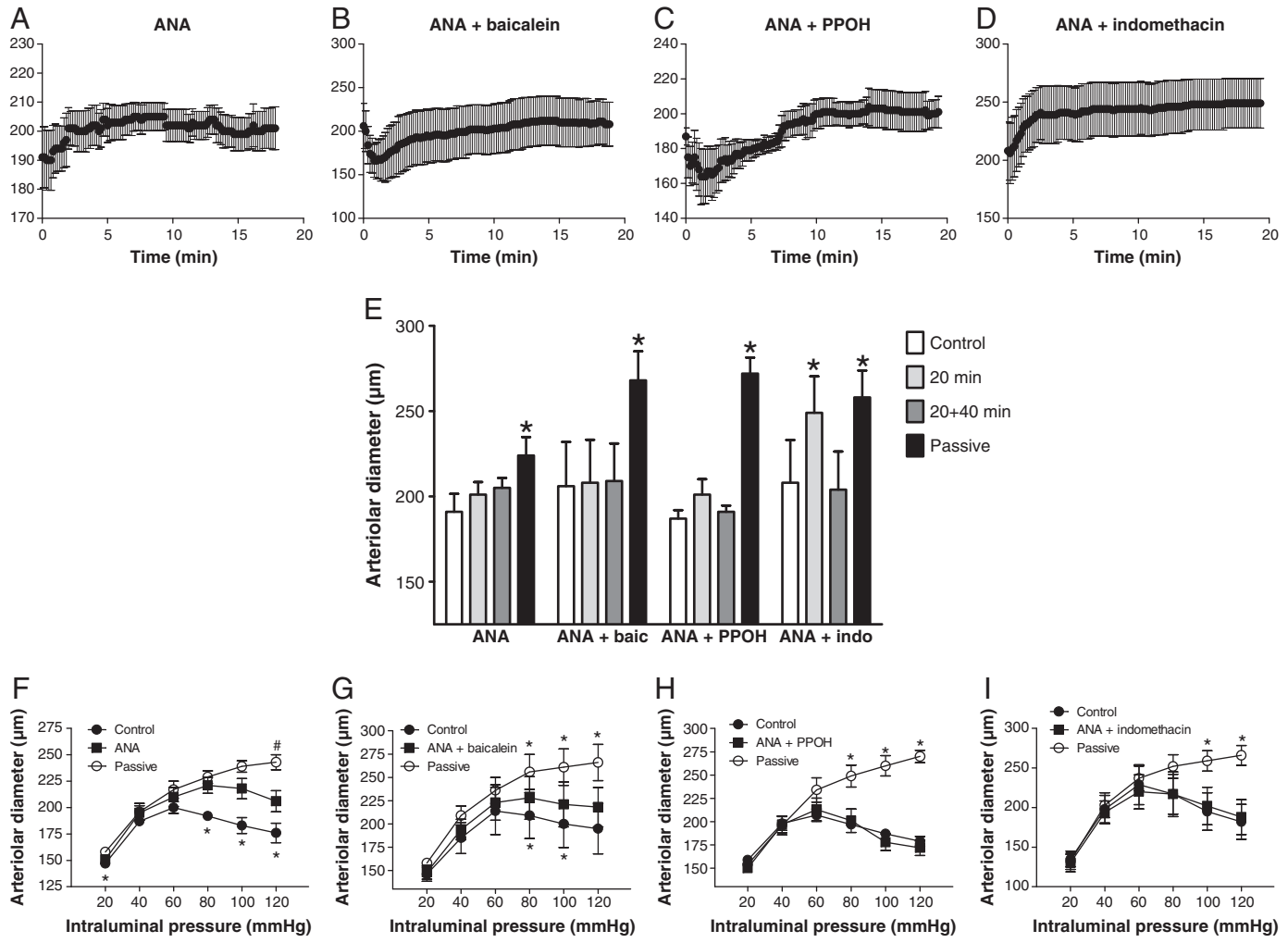

Fig. 6. Anandamide derived arachidonic acid metabolism.Arteries were pre-treated (5 min) with physiological buffer (control, ANA, Graphs A, E and F, n = 5), lipoxygenase inhibitor (baicalein, 1 μM, Graphs B, E and G, n = 5), cytochrome P450 inhibitor (PPOH, 20 μM, Graphs C, E and H, n = 5) or cyclooxygenase inhibitor (indomethacin, 10 μM, Graphs D, E and I, n = 5). Then, changes in arteriolar diameter were recorded for 20 min in the presence of 1 μM anandamide (Graphs A–D). Changes in arteriolar diameters were summarized in Graph E. Arteriolar diameter was measured before the experiments (Control, open bars), after 20 min continuous treatment with anandamide (20 min, light gray bars), and after the 40 min regeneration (20 + 40 min, dark gray bars). In addition, arteriolar diameter was measured in the presence of 10 μM acetylcholine to determine the maximum diameter (Passive, black bars). Bars show the average ± SEM, significant differences (repeated measures ANOVA with Dunnett's post hoc test, $P<0.05$) from the control (untreated arteries in the presence of Ca^{2+} containing PSS) are represented by asterisks. An effort was made to determine the effects of the above mentioned treatments on the myogenic response after the regeneration (Graphs F–I). In these cases arteriolar diameter was measured at intraluminal pressures of 20–120 mm Hg before (Control, ●) and after treatments (20 min treatment followed by 40 min regeneration, ■) in physiological buffer. Passive diameter of the arteries was determined at the end of the experiments in the absence of Ca^{2+} (Passive, ○). Symbols are mean ± SEM. Significant deviations (repeated measures ANOVA with Dunnett's post hoc test, $P<0.05$) of vascular diameter upon treatments from active diameter (*) or from passive diameter (#) of the same arteries are labeled.

prevented anandamide mediated relaxation and the relaxation was not affected by cannabinoid receptor inhibition (Pratt, et al., 1998). On coronary (porcine and rabbit) and carotid (rabbit) arteries, anandamide mediated dilatation was found to be dependent on diclofenac (another cyclooxygenase inhibitor) (Fleming, et al., 1999). In sheep coronary arteries, dilatation induced by anandamide was independent of cannabinoid and vanilloid receptors but was again inhibited by FAAH inhibition or by indomethacin (Grainger and Boachie-Ansah, 2001).

Our data confirm these observations in small arteries isolated from rat skeletal muscle (gracilis muscle). First of all, anandamide evoked vasodilation was inhibited by FAAH inhibition and was mimicked by arachidonic acid, suggesting the prominent role of anandamide metabolism to arachidonic acid in arteries with functional endothelium. Nonetheless, inhibition of cyclooxygenase by indomethacin unmasked a robust dilative effect of anandamide, which was maintained throughout the 20 min incubation but disappeared during the 40 min regeneration (Fig. 5D and E). This finding suggests a complex interplay between CB1, TRPV1 and arachidonic acid metabolites. In particular, cyclooxygenase inhibition may shift the local arachidonic acid metabolism toward the cytochrome P450 epoxygenase pathway, which may evoke dilatation.

A significant novelty of the present study is to relate the effects of anandamide to the myogenic response of resistance arterioles. Cannulated resistance arterioles develop a myogenic constriction upon elevated intraluminal pressures (myogenic response), a process which has a prominent role in the regulation of blood distribution *in vivo*. The effect of anandamide and its breakdown on the spontaneous myogenic response was addressed for the first time. To this end, the effects of anandamide were evaluated after a 20 min application followed by a 40 min washout in order to observe the long-term effects of metabolism. This protocol may eliminate other more direct effects of anandamide which could complicate analysis, revealing its vasodilatative actions via metabolism.

Our data showed that anandamide antagonized the myogenic response (Figs. 1F, G and 2 G), which was mediated by its FAAH dependent breakdown (Fig. 5D), independently of endothelium (Fig. 2H).

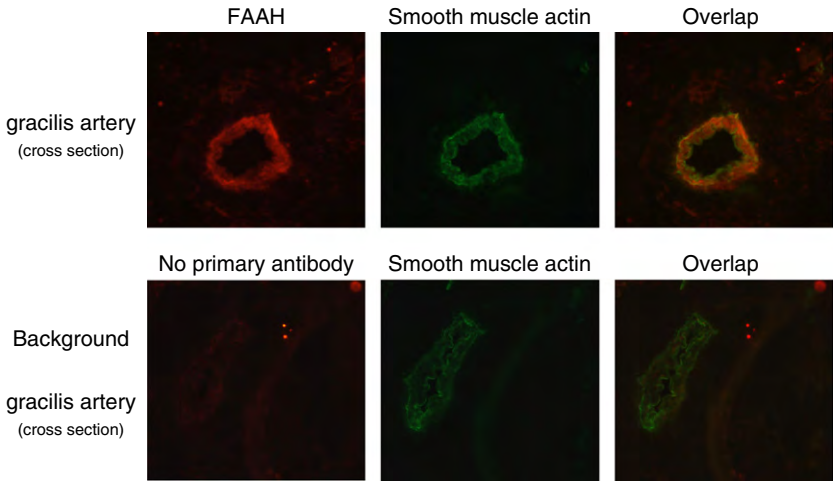

Fig. 7. Expression of fatty acid amide hydrolase (FAAH) in skeletal muscle arterioles.10 μm thick tissue slices of the gracilis muscle were stained with anti-FAAH and with anti-smooth muscle actin antibodies. In the case of control (Background) no FAAH specific (primary) antibody was used. Binding of the primary antibodies was visualized with FITC (green) and Cy3 (red) conjugated secondary antibodies.

This finding was further investigated regarding the potential mechanisms. Arachidonic acid had effects similar to anandamide on the myogenic response in arterioles with intact endothelium (Fig. 5E). Functional data suggested that the metabolism of anandamide to arachidonic acid, which was responsible for the myogenic response, was smooth muscle specific. Correspondingly, expression of FAAH (the metabolizing enzyme which was inhibited by URB) was localized to the smooth muscle cell layer of the gracilis arteries (Fig. 7). Furthermore, stimulation of the known anandamide receptors (vanilloid and cannabinoid receptors) was without effect on the myogenic response.

It needs to be noted that it is not easy to differentiate between specific effects on a myogenic signaling pathway (such as pressure induced constriction, examined here) and the opposing effects of a dilator pathway. It is especially complicated when a substance (such as anandamide, Fig. 1C) appears to evoke dilation almost immediately after application. Nonetheless, this dilation is apparently mediated by endothelium in this case, because it was missing in endothelium denuded arteries (Fig. 2D), while the effects on the myogenic response were preserved (Fig. 1G versus Fig. 2G). Finally, the myogenic response was determined here by measuring its re-development. This fact may be particularly important in the case of endothelium denuded arteries. In these experiments anandamide did not evoke dilation suggesting no production of dilatative substances and a maintained myogenic response. However, when this apparently maintained myogenic response was eliminated by decreasing the intraluminal pressure to 20 mm Hg, it was not able to re-develop during the 4 min incubation period which was used to test the response after anandamide treatment, suggesting a direct effect of anandamide on this parameter.

The finding that 1 μM arachidonic acid had different effects on the myogenic response in intact (Fig. 5E) and endothelium denuded arterioles (Fig. 2I) is potentially intriguing. One may speculate that arachidonic acid mediated antagonism of the myogenic response may be dose dependent in arteries without functional endothelium, because 30 μM anandamide antagonized the myogenic response (Fig. 2G) and this effect was missing when its metabolism to arachidonic acid was inhibited (Fig. 2H). Moreover, it may also be considered that the arachidonic acid synthesized by anandamide metabolism resulting from the subcellular localization of FAAH may have different effects than that of arachidonic acid diffusing through the plasma membrane.

The exact pathway downstream of anandamide derived arachidonic acid leading to dilation remained elusive. A prominent role of cytochrome P450 epoxygenase and cyclooxygenase enzymes were found, suggesting a complex interplay between these systems. It is conceivable that both epoxyeicosatrienoic acids produced by cytochrome P450 epoxygenase and prostacyclins produced by cyclooxygenase may attenuate the myogenic response. In summary, it is not clear which anandamide metabolites modulate the myogenic response. This cannot be assessed under the present conditions as the effect of anandamide on the pressure–diameter relationships could probably be mimicked by many vasodilators.

Nonetheless, the myogenic response is an important determinant of local tissue perfusion (Davis and Hill, 1999), suggesting a functional role for anandamide synthesized upon activation of neurons and macrophages (Devane, et al., 1992; Di Marzo, et al., 1996; Wagner, et al., 1997; Ahluwalia, et al., 2003) in the regulation of blood distribution. Regarding this possibility, anandamide antagonized the myogenic response at 1 μM concentration and physiological levels of anandamide may reach this concentration, as has been shown in the case of cultured sensory neurons (Ahluwalia, et al., 2003).

Conclusion

Taken together, these data suggest that anandamide mediated vascular effects are independent of vanilloid and cannabinoid receptors in the rat gracilis artery. We propose that anandamide is metabolized to arachidonic acid in vascular smooth muscle cells. Anandamide derived arachidonic acid synthesis may directly lead to dilation (in an endothelium dependent manner) or to a blunted myogenic response (in an endothelium independent fashion) which may also contribute to physiological vasodilatation. Furthermore, these findings also suggest that anandamide synthesized in cells like neurons or activated macrophages may diffuse to the adjacent vascular beds and trans-activate the arachidonic acid pathway in the vascular wall by its FAAH mediated breakdown. This transactivation of the arachidonic acid pathway may result in an impaired vascular autoregulation and in a consequent vasodilatation (proposed mechanism is shown in Fig. 8) affecting tissue blood distribution. Moreover, the concentration-dependent effects of anandamide observed here through differential mechanisms may suggest a significant role not only in local blood flow/distribution but also in certain vascular pathophysiological states, such as hypotension, associated with inflammation.

Conflict of interest statement

The authors declare that there are no conflicts of interest.

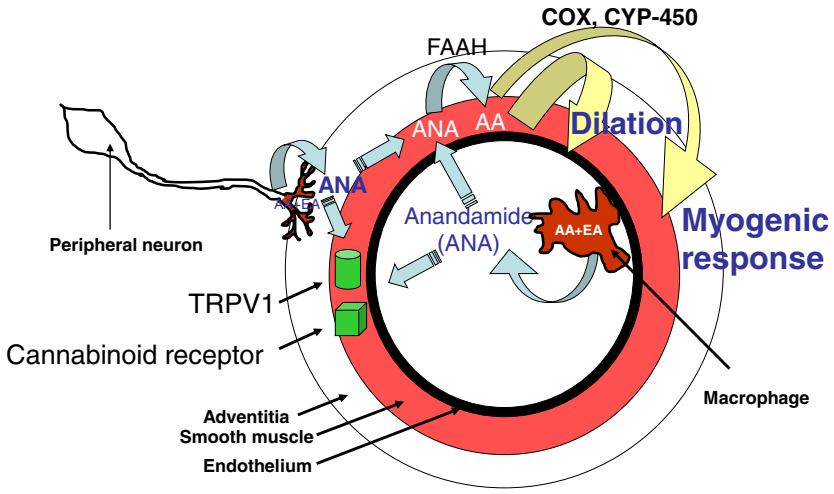

Fig. 8. Transactivation of the arachidonic acid pathway by anandamide contributes to vascular autoregulation.Anandamide (ANA) may be synthesized in perivascular neurons or by macrophages. After synthesis, anandamide is released and diffuses to the vascular wall. It is metabolized to arachidonic acid (AA) and ethanolamide by fatty acid amide hydrolase (FAAH) in vascular smooth muscle cells. The intracellularly released arachidonic acid in turn activates arachidonic acid pathways in smooth muscle cells, leading to cyclooxygenase (COX) and cytochrome P-450 (CYP-450) mediated dilation and to impaired myogenic autoregulation.

Acknowledgments

The work is supported by the TÁMOP 4.2.1./B-09/1/KONV-2010-0007 and TÁMOP 4.2.2/B-10/1-2010-0024 projects (to ZP and AT). These projects are implemented through the New Hungary Development Plan, co-financed by the European Social Fund. In addition, the study was supported by the Hungarian Academy of Sciences OTKA (K68077 to AT) and Bolyai János Research Fellowship (to AT), by the Hungarian Ministry of Health (ETT 430/2006 to AT) and by Baross Gábor ÉletMent grant by the National Office for Research and Technology, Hungary. We thank Peter M. Blumberg for reading the manuscript.

References

Ahluwalia J, Yaqoob M, Urban L, Bevan S, Nagy I. Activation of capsaicin-sensitive primary sensory neurones induces anandamide production and release. J Neurochem 2003;84(3):585–91.
Alexander SP, Kendall DA. The complications of promiscuity: endocannabinoid action and metabolism. Br J Pharmacol 2007;152(5):602–23.
Cravatt BF, Giang DK, Mayfield SP, Boger DL, Lerner RA, Gilula NB. Molecular characterization of an enzyme that degrades neuromodulatory fatty-acid amides. Nature 1996;384(6604):83–7.
Cristino L, Starowicz K, De Petrocellis L, Morishita J, Ueda N, Guglielmotti V, et al. Immunohistochemical localization of anabolic and catabolic enzymes for anandamide and other putative endovanilloids in the hippocampus and cerebellar cortex of the mouse brain. Neuroscience 2008;151(4):955–68.
Davis MJ, Hill MA. Signaling mechanisms underlying the vascular myogenic response. Physiol Rev 1999;79(2):387–423.
Devane WA, Hanus L, Breuer A, Pertwee RG, Stevenson LA, Griffin G, et al. Isolation and structure of a brain constituent that binds to the cannabinoid receptor. Science 1992;258(5090):1946–9.
Di Marzo V, Fontana A, Cadas H, Schinelli S, Cimino G, Schwartz JC, et al. Formation and inactivation of endogenous cannabinoid anandamide in central neurons. Nature 1994;372(6507):686–91.
Di Marzo V, De Petrocellis L, Sepe N, Buono A. Biosynthesis of anandamide and related acylethanolamides in mouse J774 macrophages and N18 neuroblastoma cells. Biochem J 1996;316(Pt 3):977–84.
Ellis EF, Moore SF, Willoughby KA. Anandamide and delta 9-THC dilation of cerebral arterioles is blocked by indomethacin. Am J Physiol 1995;269(6 Pt 2):H1859–64.
Fleming I, Schermer B, Popp R, Busse R. Inhibition of the production of endothelium-derived hyperpolarizing factor by cannabinoid receptor agonists. Br J Pharmacol 1999;126(4):949–60.
Frisbee JC, Roman RJ, Falck JR, Krishna UM, Lombard JH. 20-HETE contributes to myogenic activation of skeletal muscle resistance arteries in Brown Norway and Sprague–Dawley rats. Microcirculation 2001;8(1):45–55.
Grainger J, Boachie-Ansah G. Anandamide-induced relaxation of sheep coronary arteries: the role of the vascular endothelium, arachidonic acid metabolites and potassium channels. Br J Pharmacol 2001;134(5):1003–12.
Herradon E, Martin MI, Lopez-Miranda V. Characterization of the vasorelaxant mechanisms of the endocannabinoid anandamide in rat aorta. Br J Pharmacol 2007;152(5):699–708.
Ho WS, Randall MD. Endothelium-dependent metabolism by endocannabinoid hydrolases and cyclooxygenases limits vasorelaxation to anandamide and 2-arachidonoylglycerol. Br J Pharmacol 2007;150(5):641–51.
Holt S, Comelli F, Costa B, Fowler CJ. Inhibitors of fatty acid amide hydrolase reduce carrageenan-induced hind paw inflammation in pentobarbital-treated mice: comparison with indomethacin and possible involvement of cannabinoid receptors. Br J Pharmacol 2005;146(3):467–76.
Jarai Z, Wagner JA, Varga K, Lake KD, Compton DR, Martin BR, et al. Cannabinoid-induced mesenteric vasodilation through an endothelial site distinct from CB1 or CB2 receptors. Proc Natl Acad Sci U S A 1999;96(24):14136–41.
Jayamanne A, Greenwood R, Mitchell VA, Aslan S, Piomelli D, Vaughan CW. Actions of the FAAH inhibitor URB597 in neuropathic and inflammatory chronic pain models. Br J Pharmacol 2006;147(3):281–8.
Jhaveri MD, Richardson D, Kendall DA, Barrett DA, Chapman V. Analgesic effects of fatty acid amide hydrolase inhibition in a rat model of neuropathic pain. J Neurosci 2006;26(51):13318–27.
Kark T, Bagi Z, Lizanecz E, Pasztor ET, Erdei N, Czikora A, et al. Tissue specific regulation of microvascular diameter: opposite functional roles of neuronal and smooth muscle located vanilloid receptor-1 (TRPV1). Mol Pharmacol 2008:1405–12.
Kim SR, Bok E, Chung YC, Chung ES, Jin BK. Interactions between CB(1) receptors and TRPV1 channels mediated by 12-HPETE are cytotoxic to mesencephalic dopaminergic neurons. Br J Pharmacol 2008;155(2):253–64.
Lizanecz E, Bagi Z, Pasztor ET, Papp Z, Edes I, Kedei N, et al. Phosphorylation-dependent desensitization by anandamide of vanilloid receptor-1 (TRPV1) function in rat skeletal muscle arterioles and in Chinese hamster ovary cells expressing TRPV1. Mol Pharmacol 2006;69(3):1015–23.
Lopez-Miranda V, Herradon E, Dannert MT, Alsasua A, Martin MI. Anandamide vehicles: a comparative study. Eur J Pharmacol 2004;505(1–3):151–61.
Machha A, Achike FI, Mohd MA, Mustafa MR. Baicalein impairs vascular tone in normal rat aortas: role of superoxide anions. Eur J Pharmacol 2007;565(1–3):144–50.
Mukhopadhyay S, Chapnick BM, Howlett AC. Anandamide-induced vasorelaxation in rabbit aortic rings has two components: G protein dependent and independent. Am J Physiol Heart Circ Physiol 2002;282(6):H2046–54.
O'Sullivan SE, Kendall DA, Randall MD. Heterogeneity in the mechanisms of vasorelaxation to anandamide in resistance and conduit rat mesenteric arteries. Br J Pharmacol 2004;142(3):435–42.
O'Sullivan SE, Kendall DA, Randall MD. Vascular effects of delta 9-tetrahydrocannabinol (THC), anandamide and N-arachidonoyldopamine (NADA) in the rat isolated aorta. Eur J Pharmacol 2005;507(1–3):211–21.
Pacher P, Batkai S, Osei-Hyiaman D, Offertaler L, Liu J, Harvey-White J, et al. Hemodynamic profile, responsiveness to anandamide, and baroreflex sensitivity of mice lacking fatty acid amide hydrolase. Am J Physiol Heart Circ Physiol 2005;289(2):H533–41.
Piomelli D, Tarzia G, Duranti A, Tontini A, Mor M, Compton TR, et al. Pharmacological profile of the selective FAAH inhibitor KDS-4103 (URB597). CNS Drug Rev 2006;12(1):21–38.
Pratt PF, Hillard CJ, Edgemond WS, Campbell WB. N-arachidonylethanolamide relaxation of bovine coronary artery is not mediated by CB1 cannabinoid receptor. Am J Physiol 1998;274(1 Pt 2):H375–81.
Randall MD, Kendall DA. Involvement of a cannabinoid in endothelium-derived hyperpolarizing factor-mediated coronary vasorelaxation. Eur J Pharmacol 1997;335(2–3):205–9.
Wagner JA, Varga K, Ellis EF, Rzigalinski BA, Martin BR, Kunos G. Activation of peripheral CB1 cannabinoid receptors in haemorrhagic shock. Nature 1997;390(6659):518–21.
Xiang L, Naik JS, Hester RL. Functional vasodilation in the rat spinotrapezius muscle: role of nitric oxide, prostanoids and epoxyeicosatrienoic acids. Clin Exp Pharmacol Physiol 2008;35(5–6):617–24.
Zygmunt PM, Petersson J, Andersson DA, Chuang H, Sorgard M, Di MV, et al. Vanilloid receptors on sensory nerves mediate the vasodilator action of anandamide. Nature 1999;400(6743):452–7.